(12) INTERNATIONAL APPLICATION PUBLISHED UNDER THE PATENT COOPERATION TREATY (PCT)

(19) World Intellectual Property Organization
International Bureau

(43) International Publication Date
18 June 2020 (18.06.2020)

WIPO | PCT

(10) International Publication Number
WO 2020/123613 A1

(51) International Patent Classification:
C07F 9/36 (2006.01)

(21) International Application Number:
PCT/US2019/065657

(22) International Filing Date:
11 December 2019 (11.12.2019)

(25) Filing Language: English

(26) Publication Language: English

(30) Priority Data:
62/779,679 14 December 2018 (14.12.2018) US
62/910,001 03 October 2019 (03.10.2019) US

(71) Applicant: **TEXAS TECH UNIVERSITY SYSTEM** [US/US]; Office of Research Commercialization, P.O. Box 42007, Lubbock, TX 79409-2007 (US).

(72) Inventor: **GUIGEN, Li**; 1204 Boston Avenue, Lubbock, TX 79409 (US).

(74) Agent: **CHALKER, Daniel, J.** et al.; Chalker Flores, LLP, 14951 North Dallas Parkway, Suite 400, Dallas, TX 75254 (US).

(81) Designated States *(unless otherwise indicated, for every kind of national protection available)*: AE, AG, AL, AM, AO, AT, AU, AZ, BA, BB, BG, BH, BN, BR, BW, BY, BZ, CA, CH, CL, CN, CO, CR, CU, CZ, DE, DJ, DK, DM, DO, DZ, EC, EE, EG, ES, FI, GB, GD, GE, GH, GM, GT, HN, HR, HU, ID, IL, IN, IR, IS, JO, JP, KE, KG, KH, KN, KP, KR, KW, KZ, LA, LC, LK, LR, LS, LU, LY, MA, MD, ME, MG, MK, MN, MW, MX, MY, MZ, NA, NG, NI, NO, NZ, OM, PA, PE, PG, PH, PL, PT, QA, RO, RS, RU, RW, SA, SC, SD, SE, SG, SK, SL, SM, ST, SV, SY, TH, TJ, TM, TN, TR, TT, TZ, UA, UG, US, UZ, VC, VN, ZA, ZM, ZW.

(84) Designated States *(unless otherwise indicated, for every kind of regional protection available)*: ARIPO (BW, GH, GM, KE, LR, LS, MW, MZ, NA, RW, SD, SL, ST, SZ, TZ, UG, ZM, ZW), Eurasian (AM, AZ, BY, KG, KZ, RU, TJ, TM), European (AL, AT, BE, BG, CH, CY, CZ, DE, DK, EE, ES, FI, FR, GB, GR, HR, HU, IE, IS, IT, LT, LU, LV, MC, MK, MT, NL, NO, PL, PT, RO, RS, SE, SI, SK, SM, TR), OAPI (BF, BJ, CF, CG, CI, CM, GA, GN, GQ, GW, KM, ML, MR, NE, SN, TD, TG).

Published:
— *with international search report (Art. 21(3))*

(54) Title: CHIRAL ORGANIC SANDWICH AND MULTI-LAYER CHIRALITY OF MOLECULES AND ACHIRAL DERIVATIVES

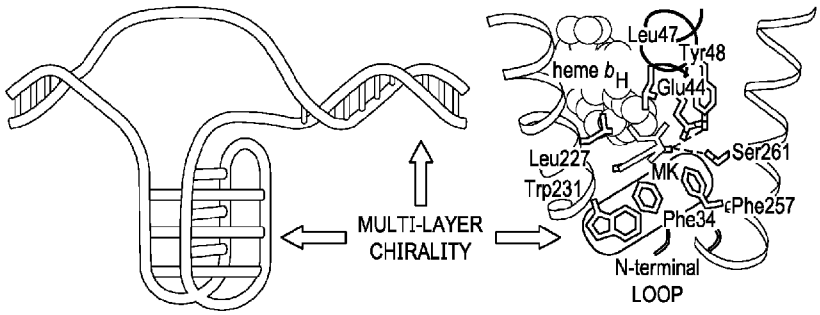


FIG. 1A
(PRIOR ART)

(57) Abstract: The present invention includes a multi-layer 3D material, a method of making, and a catalyst comprising: a first, a second, and a third layer, wherein each of the layers are arranged in a nearly parallel fashion with chirality along a center plane.

WO 2020/123613 A1

CHIRAL ORGANIC SANDWICH AND MULTI-LAYER CHIRALITY OF MOLECULES AND ACHIRAL DERIVATIVES

CROSS-REFERENCE TO RELATED APPLICATIONS

[0001] None.

TECHNICAL FIELD OF THE INVENTION

[0002] The present invention relates in general to the field of organic polymers forming an organic sandwich having a controlled chirality and methods of making the same.

STATEMENT OF FEDERALLY FUNDED RESEARCH

[0003] None.

BACKGROUND OF THE INVENTION

[0004] Without limiting the scope of the invention, its background is described in connection with organic polymers.

[0005] Chirality in biomolecules includes examples such as nucleic acids, proteins and carbohydrates, which are involved in the biological mechanism in human beings, animals and plants (*1-6*). Chirality has also become increasingly important in pharmaceutical science and industry on the design, discovery and development of drugs for enhancing their potency and selectivity (*5,6*). In this regard, asymmetric and catalytic synthesis of chiral compounds have been actively pursued for more than half a century to meet the needs of chemical and biomedical research (*7-20*). Among the numerous chiral biomolecules and their complexes, DNA has attracted special attention in the chemical community because it shows multi-layer paired chirality along with their double- or single-strand and i-Motif backbones (Fig. 1A) (*21-23*). Proteins also show multi-layer chirality in their folding structures (*24*).

[0006] Even though multi-layer chirality has existed in nature, a strategy to mimic this functionality chemically has not been established. So far, planar chirality has only been focused on two-layer arrangement, which has been applied to a series of asymmetric reactions (Fig. 1B-**a-c**)(*25-30*). For example, based on Wilkinson's ferrocene, the Fu group has established planar-chiral Lewis bases of π-complexes with transition metals, and has successfully utilized them for asymmetric catalytic reactions, such as allylic alkylations (*31*), [4+1] cycloadditions (*32*), and carboiodination (*33*) (Fig. 1B-**a**). Several other groups have made great progress on planar chiral Lewis acids of Ti, Zr and Dy, which showed effectiveness on polymer chemistry and molecular magnetic hysteresis (*34-37*). Very recently, Aponick's group has developed a two-layer chirality of imidazoline-based biaryl *P,N*-ligands for asymmetric alkyne conjugate addition and alkynylation reactions

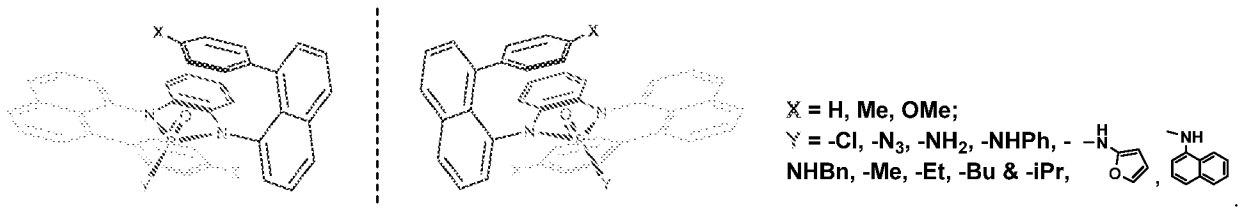
with excellent asymmetric induction (Fig. 1B-**c**) (*38*). In the meanwhile, chiral two-layer helicenes have also attracted much attention in material sciences (*39,40*).

[0007] In case of Fig. 1B-**a**, a transition metal is needed to anchor two planes; and in case of Fig. 1B-**b**, two covalent bridges are necessitated to assemble two-layer chirality from which (*R*)- [2,2]phanephos ligands has applied to asymmetric catalysis (*41*). In the latest case of Fig. 1B-**c**, the aromatic interaction between fully fluorinated electron-deficient phenyl ring and electron- efficient naphthyl ring plays a crucial role in stabilizing chiral planar stacking (*38*).

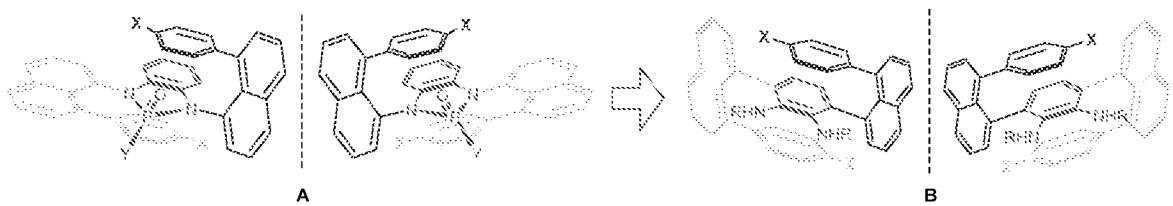
[0008] Thus, a need remains for new materials having new structures, characteristics, and uses for three dimensional chiral structures.

SUMMARY OF THE INVENTION

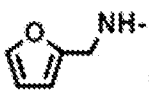
[0009] In one embodiment, the present invention includes a multi-layer 3D material comprising: a first, a second, and a third layer, wherein each of the layers are arranged in a nearly parallel fashion with chirality along a center plane. In one aspect, each of the first, second, and third layers are parallel. In another aspect, the multi-layer 3D material has a right-hand chirality, a left-hand chirality, or both a left- and a right-handed chirality. In another aspect, each of the first, second, and third layers are at least one of: *anti, syn,* or both *anti* and *syn* isomers. In another aspect, each of the first, second, and third layers are *N,N*-phosphornyl amides. In another aspect, each of the first, second, and third layers comprise chiral or achiral *N*-phosphonyl- or *N*-phosphinyl groups. In another aspect, each of the first, second, and third layers comprise a Multi-Layer Organic Framework (M-LOF) of single organic molecules with pseudo C_2-chiral characteristics. In another aspect, each of the first, second, and third layers comprises:



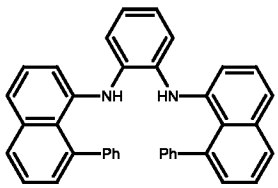
[0010] In another aspect, the each of the first, second, and third layers comprises:



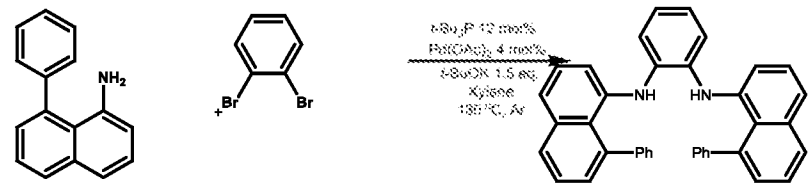
[0011] wherein

X = H, Me; Y = -Cl, -N_3, -NH_2, -NHPh, -NHBn, -Me, -Et, -Bu, -iPr, -NH-Naph, , 

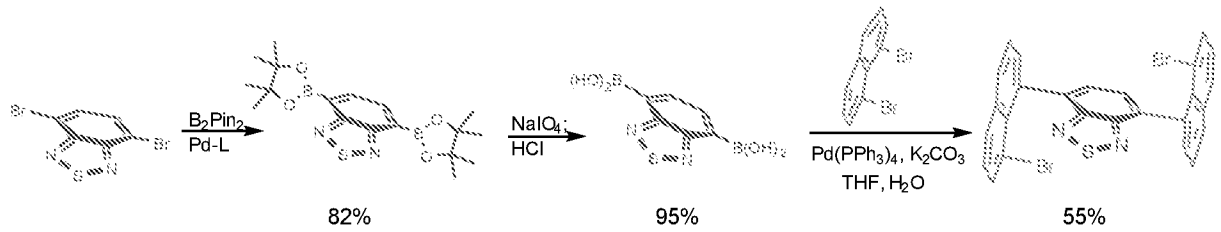
[0012] In another aspect, the one or more of the first, second, or third layers are made by:



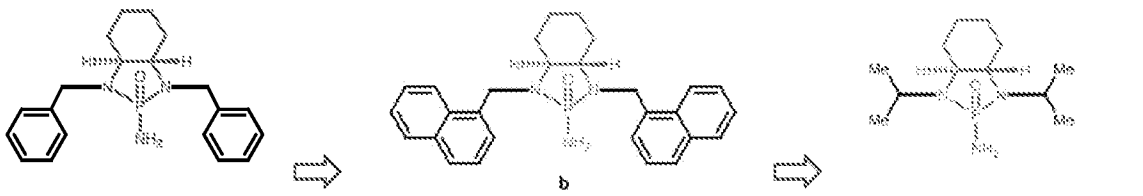
[0013] is produced by the following:



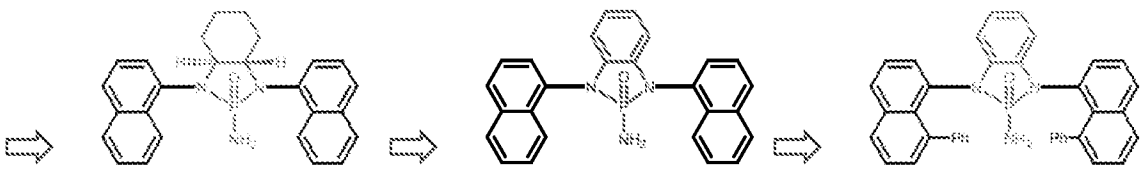
[0014] . In another aspect, the one or more of the first, second, or third layers are made by:



[0015] In another aspect, a monomeric precursors of the multi-layer 3D material is selected from at least one of:

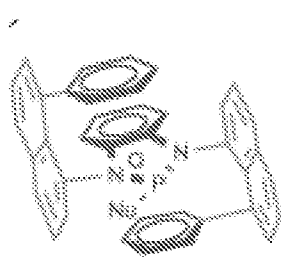


a; b; c;

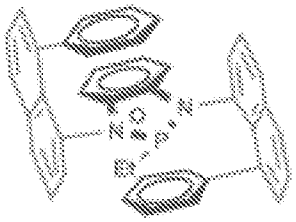


d; e; or f.

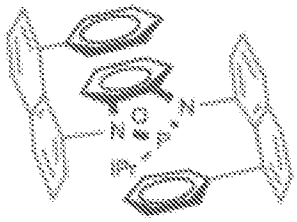
[0016] In another aspect, the multi-layer 3D material is selected from at least one of:



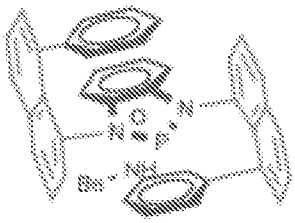
;



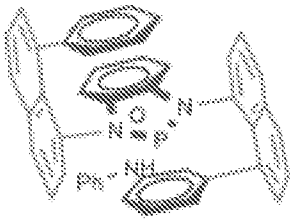
20 ;



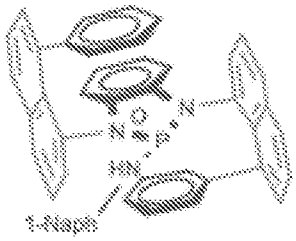
21 ;



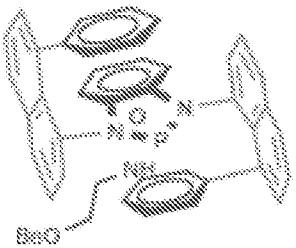
22 ;



23 ;

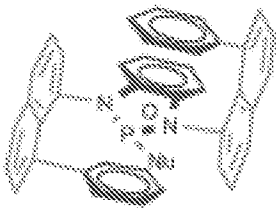


24 ; or



25 .

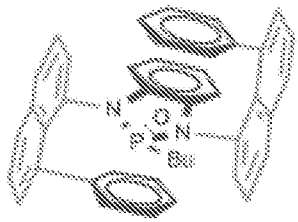
[0017] In another aspect, the multi-layer 3D material is selected from at least one of:



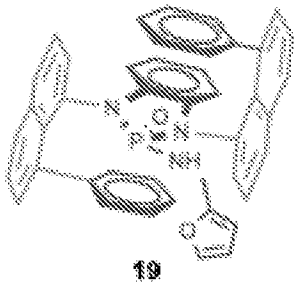
;



17 ;



18 ; or



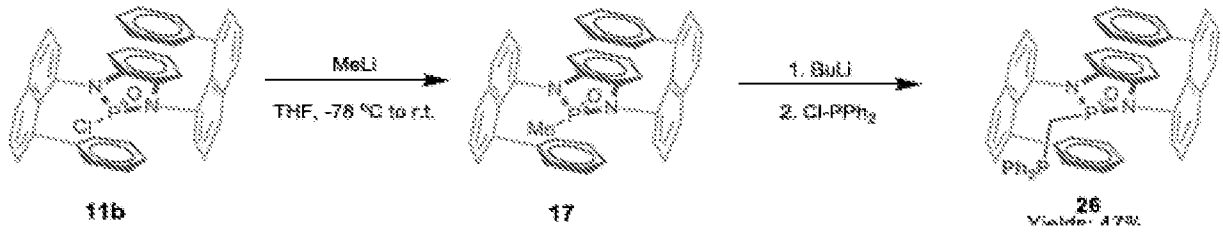
19 .

[0018] In another aspect, the product of formula:



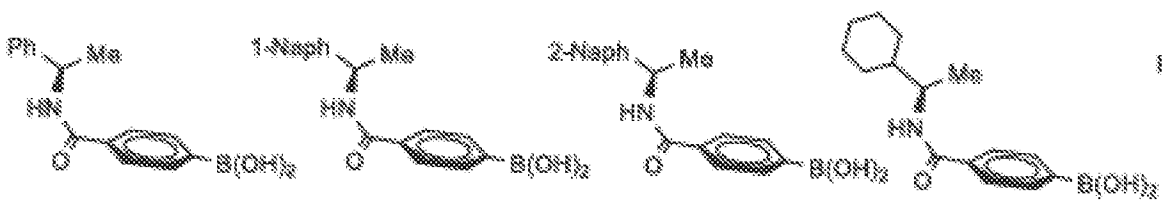
26

[0019] is made by a method comprising:

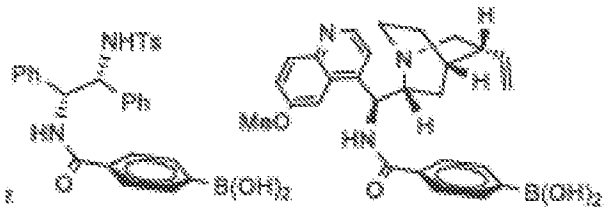


11b 17 26 .

[0020] In another aspect, the product of at least one compound of formula 2a to 2f:

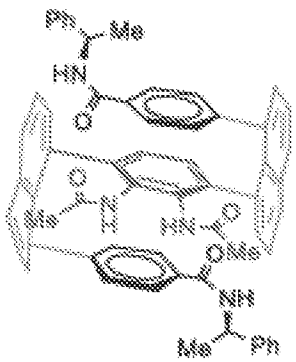


2a 2b 2c 2d

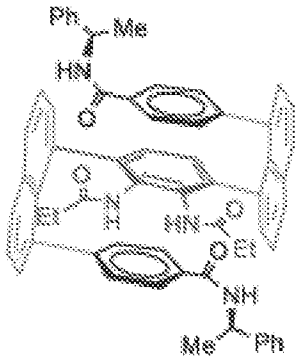


2e 2f

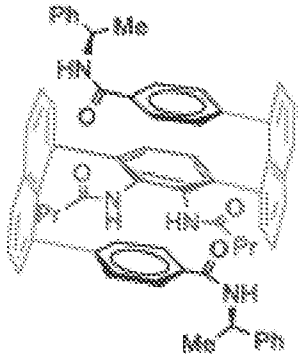
[0021] In another aspect, the product of at least one compound of formula:



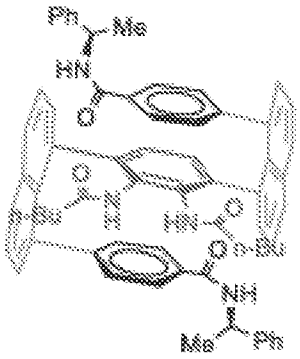
yield 56%
8a



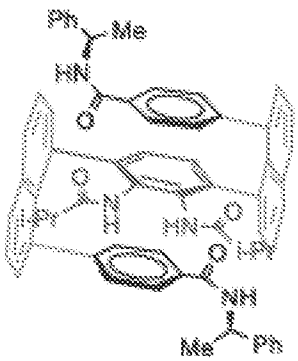
yield 39%
8b



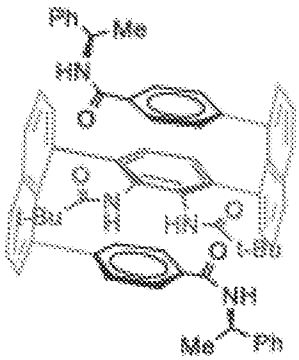
yield 42%
8c



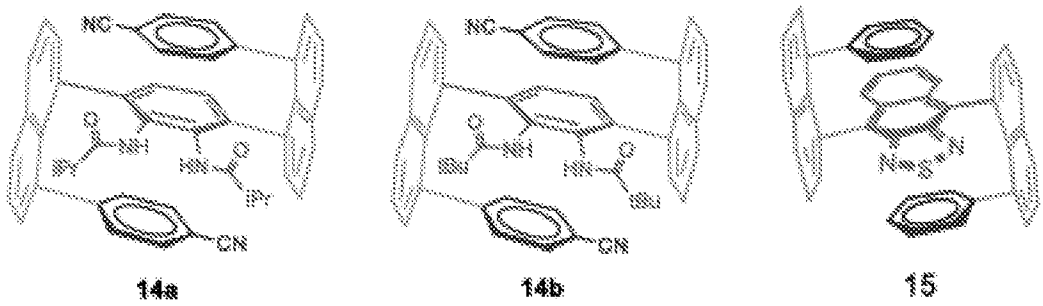
yield 47%
8d



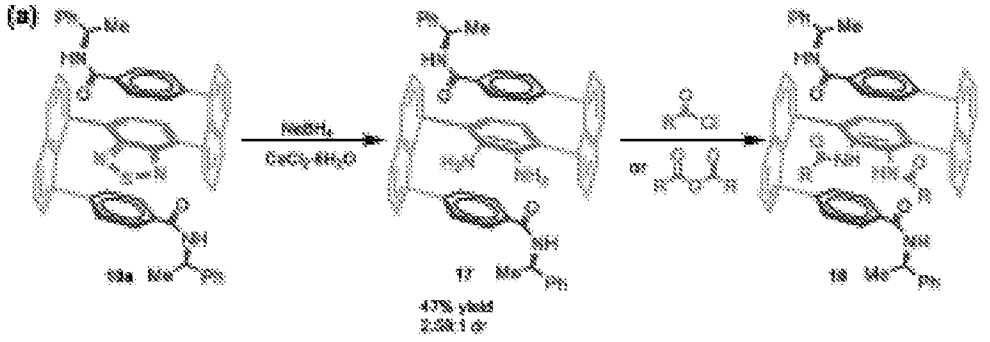
yield 36%, $[\alpha]_D^{25} = 92°$
8e

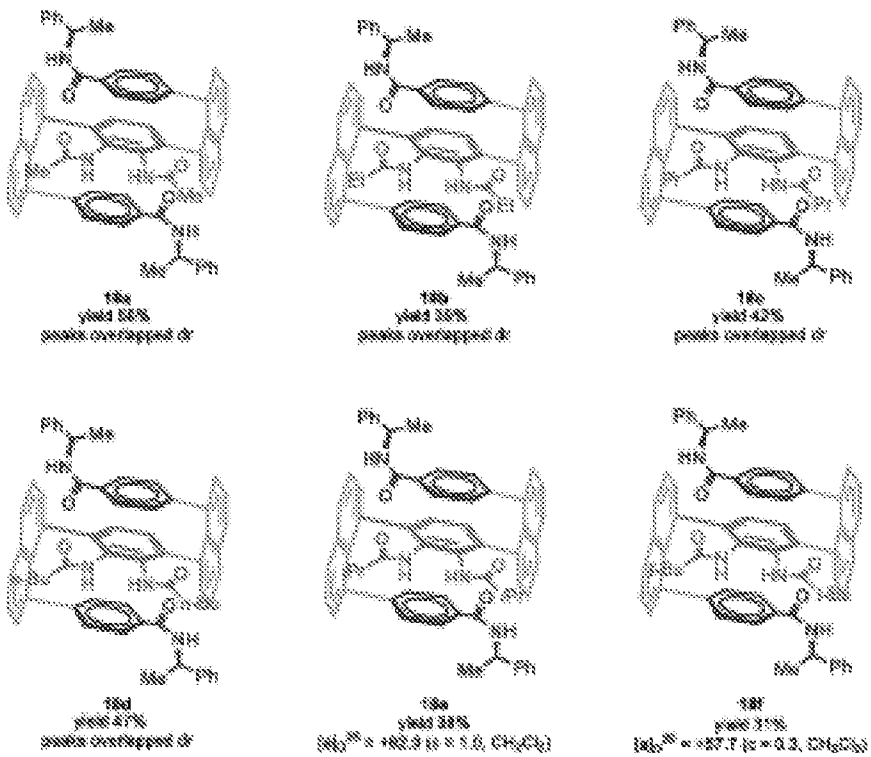


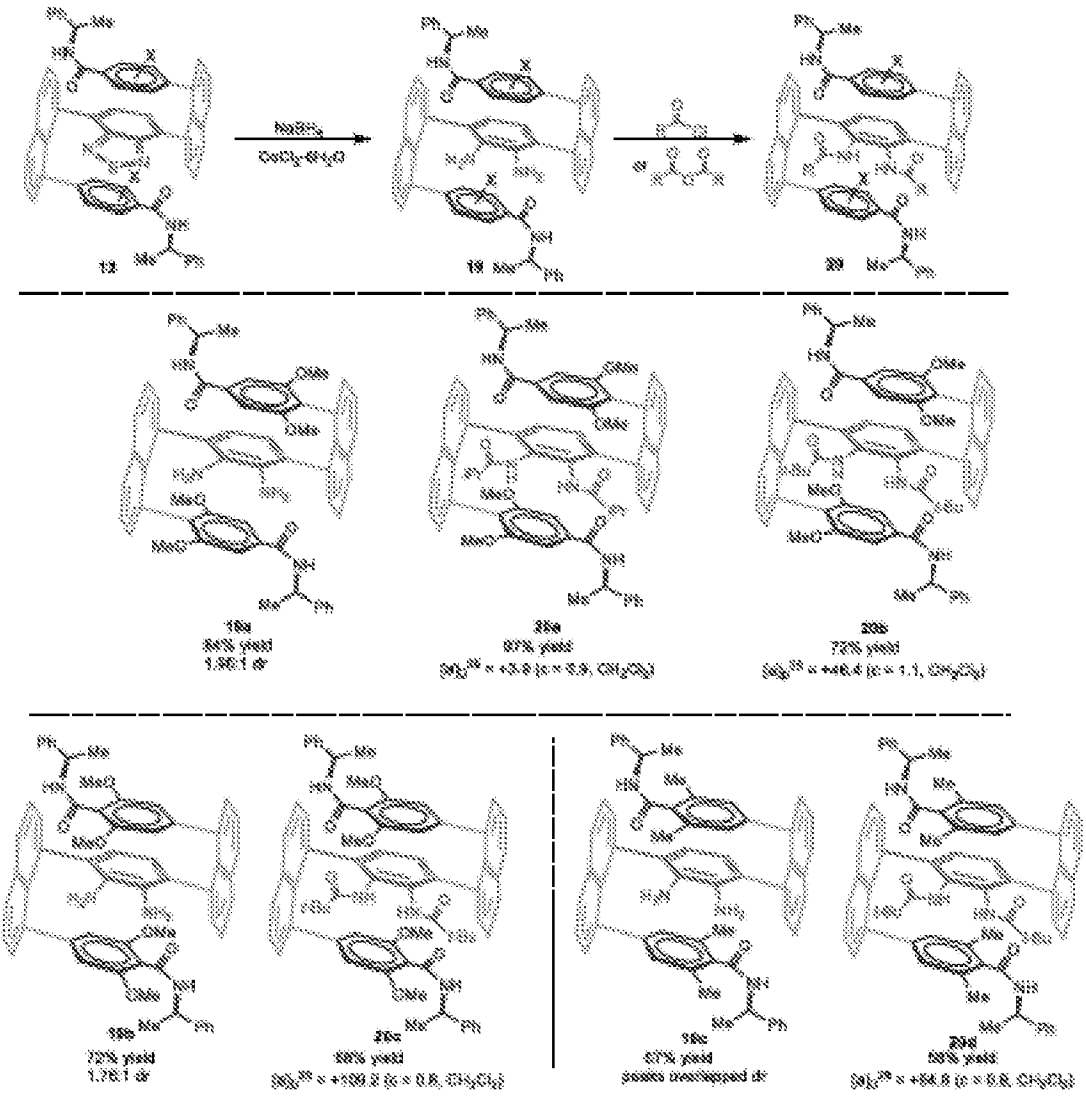
yield 31%, $[\alpha]_D^{25} = 58°$
8f

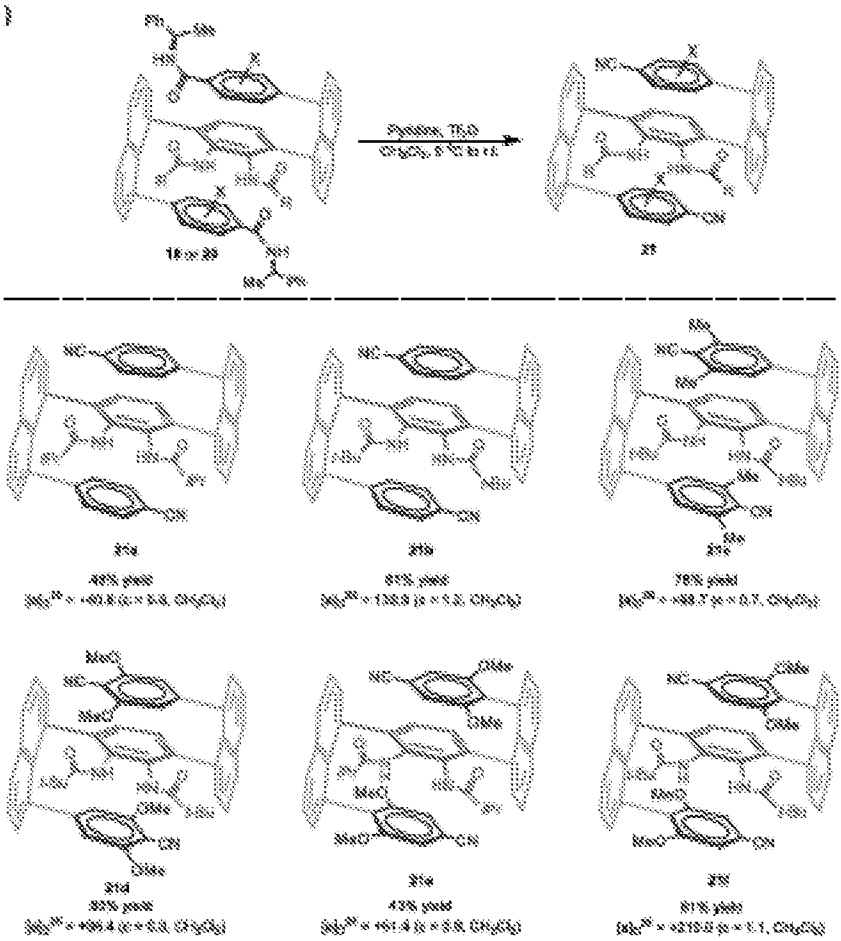


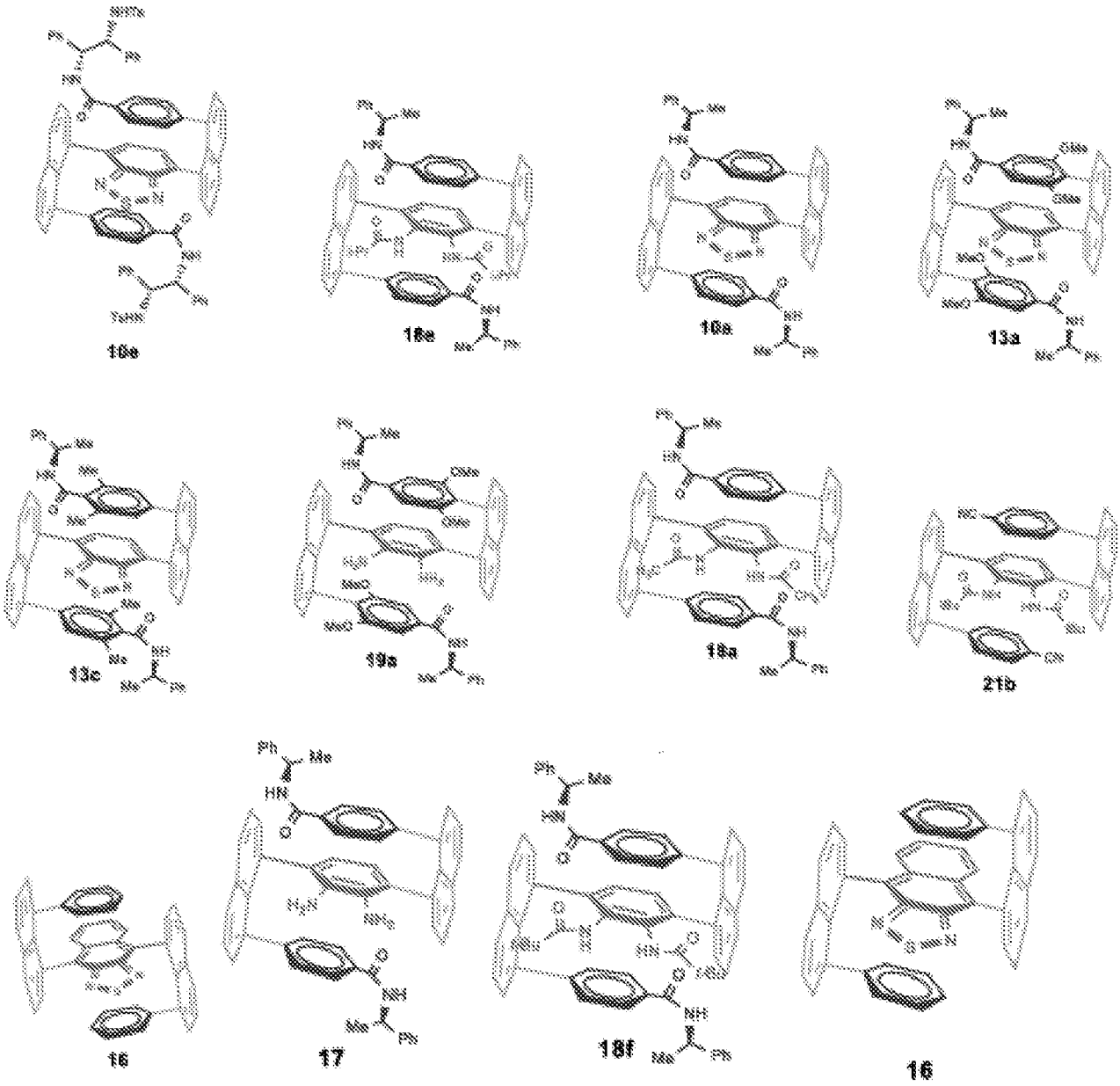
14a 14b 15



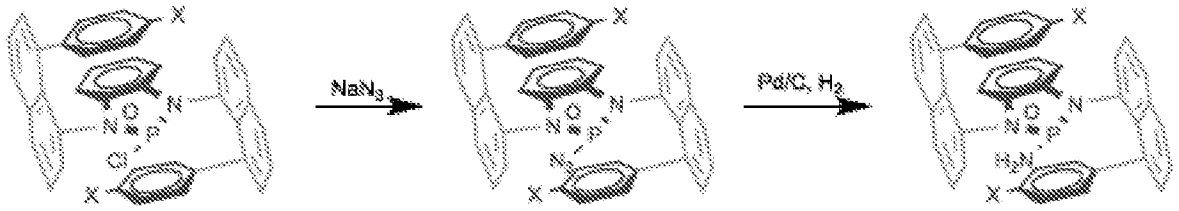








[0022] In another embodiment, the present invention includes a method of making a multi-layer 3D material comprising: a first, a second, and a third layer, wherein each of the layers are arranged in a nearly parallel fashion with chirality along a center plane comprising:

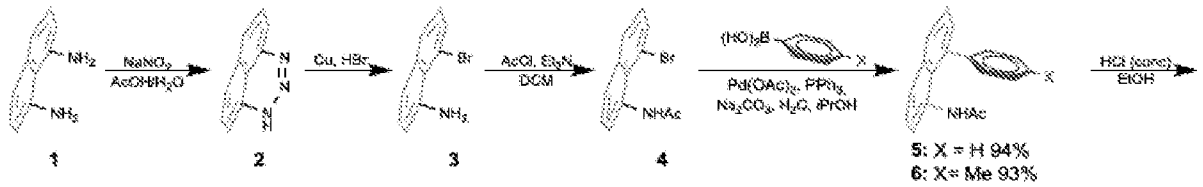


11a: X = H
12a: X= Me

13a: X = H
14a: X= Me

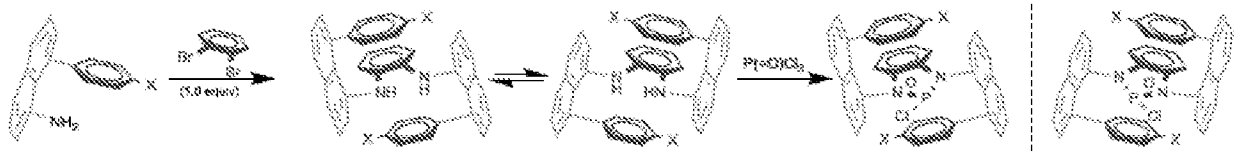
15a: X = H 81%
16a: X= Me 78%

; or



1 2 3 4

5: X = H 94%
6: X= Me 93%

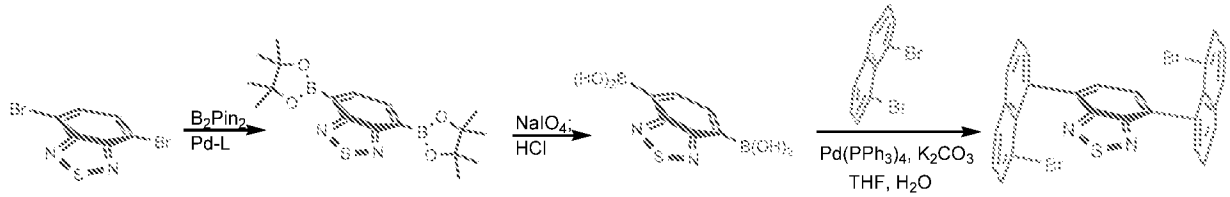


7: X = H 98%
8: X= Me 96%

9: X = H 27%
10: X= Me 24%

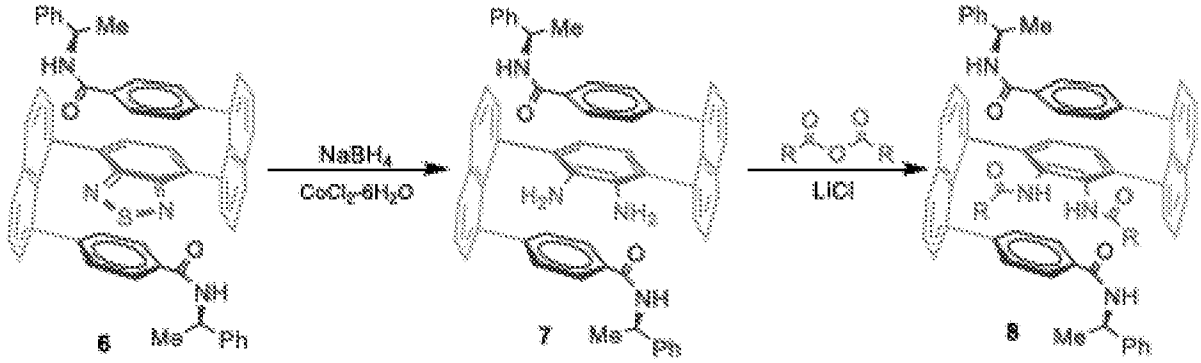
a **11: X = H 39%** b
12: X= Me 45%

;



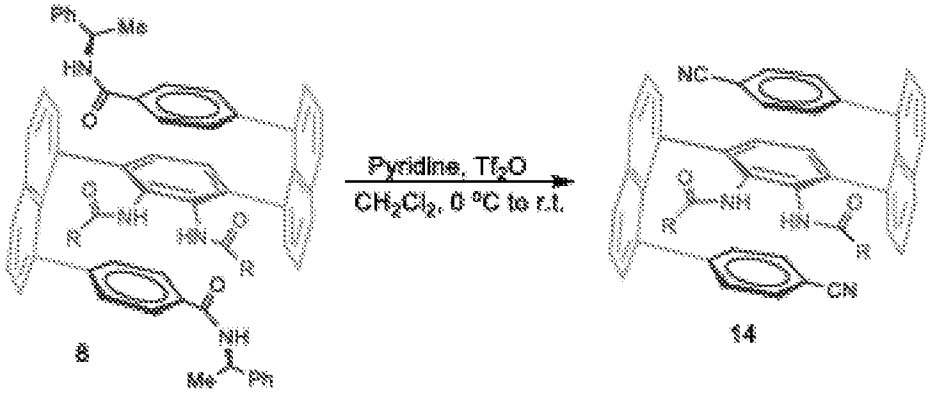
82% 95% 55%

;



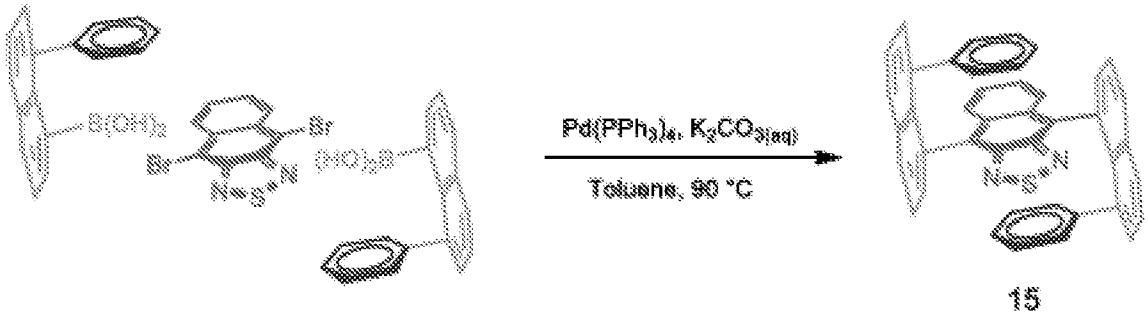
6 7 8

;



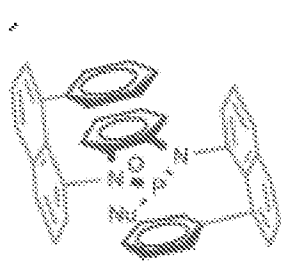
8 14

; or

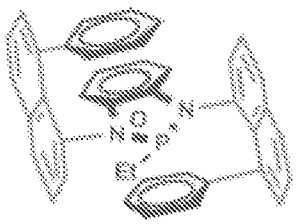


15

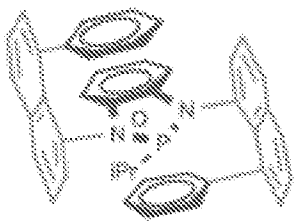
[0023] In one aspect, the multi-layer 3D material is a 2-amino-1,3-bis(8-phenylnaphthalen-1-yl)-1,3-dihydrobenzo[d][1,3,2]diazaphosphole 2-oxide **(15a)**. In another aspect, the multi-layer 3D material is selected from at least one of:



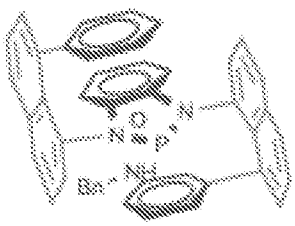
;



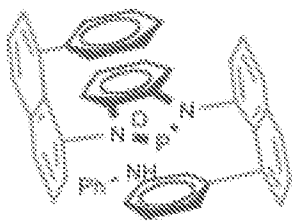
20 ;



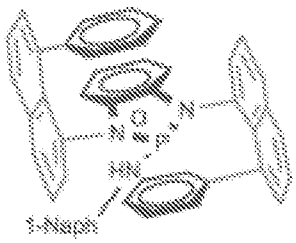
21 ;



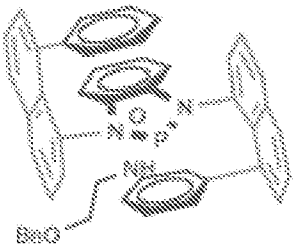
22 ;



23 ;

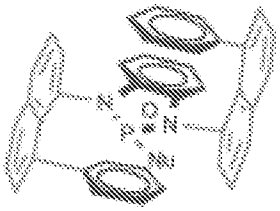


24 ; or



25 .

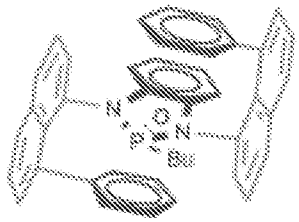
[0024] In another aspect, the multi-layer 3D material is selected from at least one of:



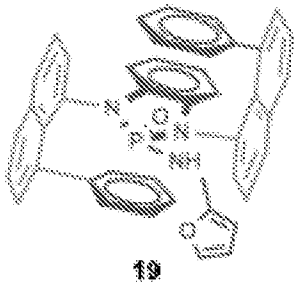
;



17 ;



18 ; or

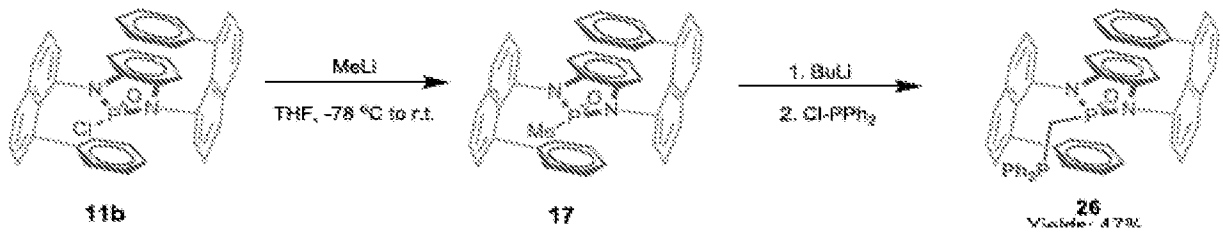


19 . In another aspect, the product of formula comprises:



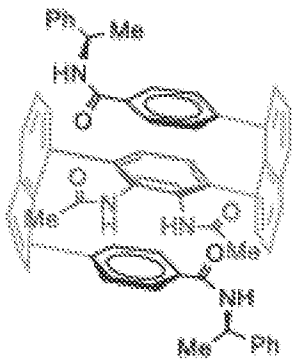
26

is made by a method comprising:



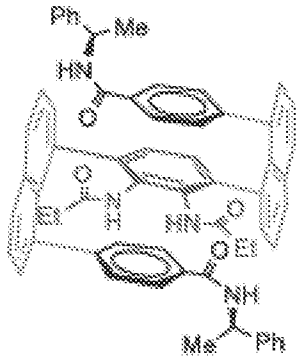
11b 17 26 .

[0025] In another aspect, the product of formula comprises:



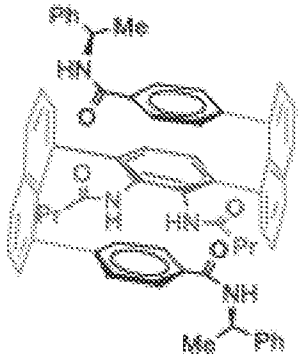
yield 56%

8a



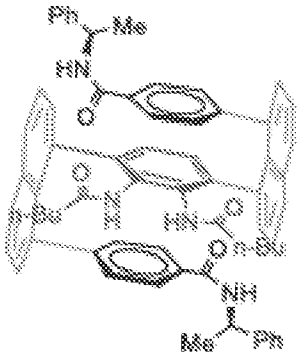
yield 39%

8b



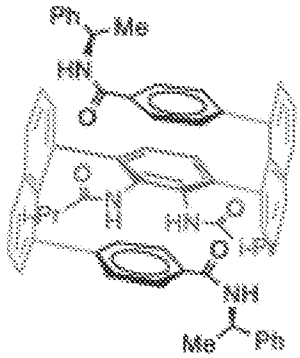
yield 42%

8c



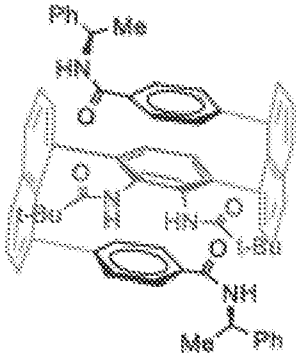
yield 47%

8d



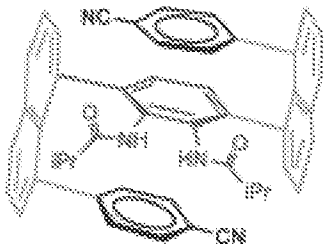
yield 38%, $[\alpha]_D^{25}$ = 92°

8e

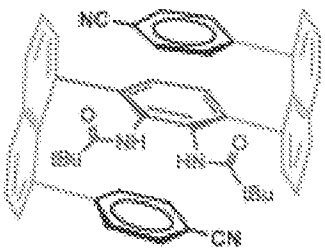


yield 31%, $[\alpha]_D^{25}$ = 58°

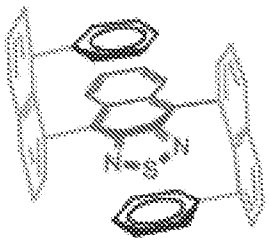
8f



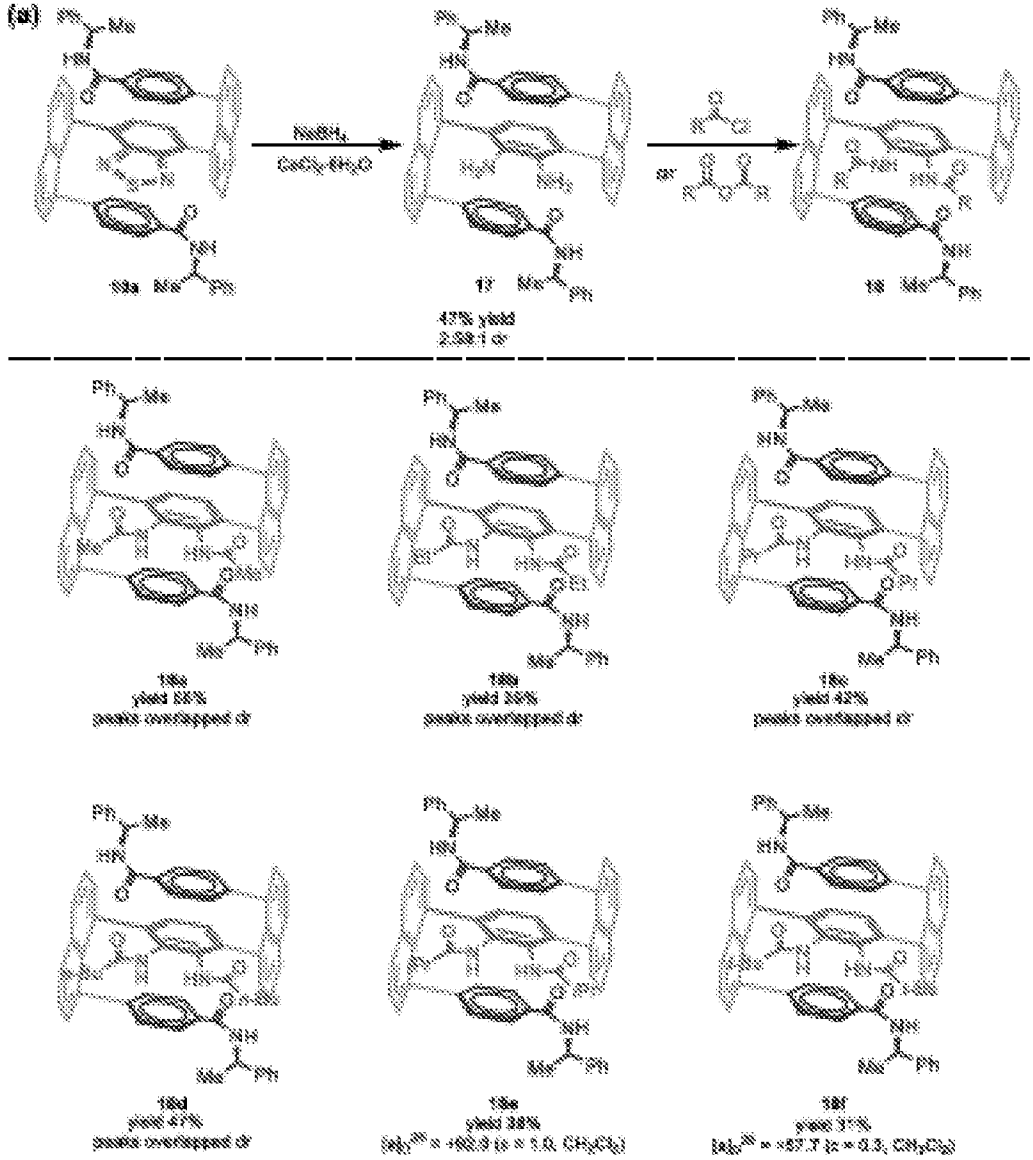
14a

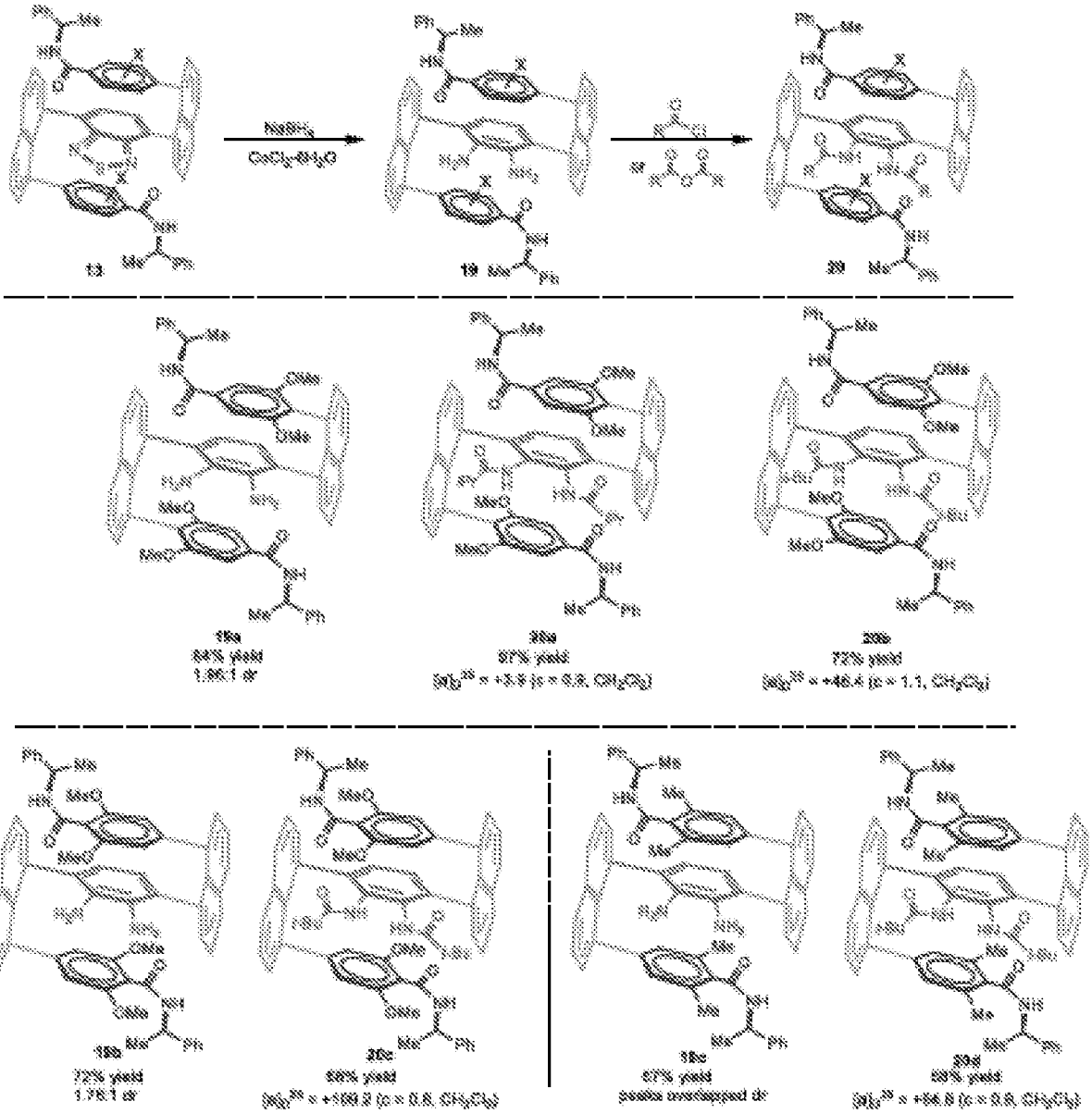


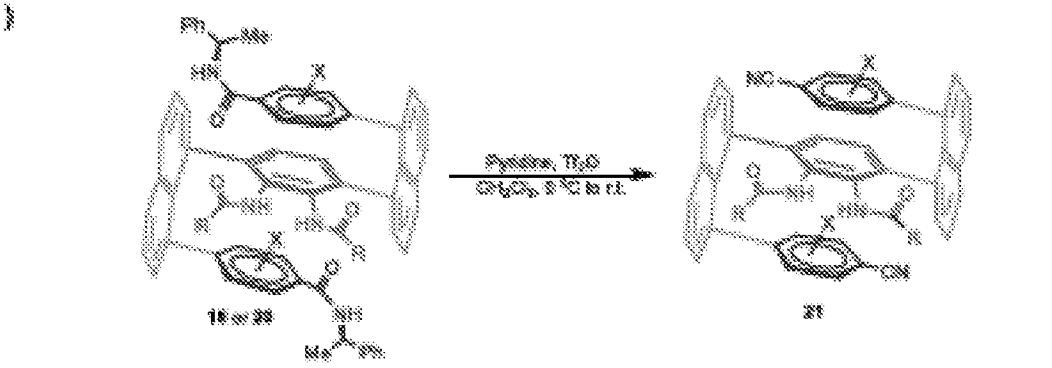
14b

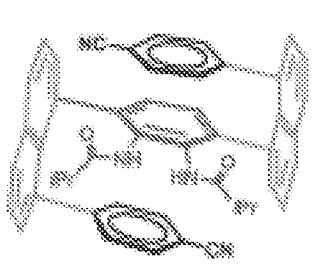


15





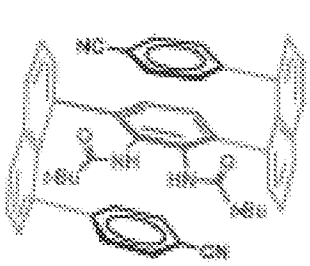




21a

49% yield

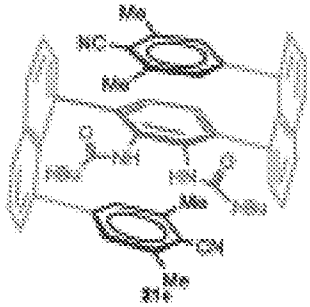
$[\alpha]_D^{20}$ = +60.6 (c = 0.8, CH_2Cl_2)



21b

81% yield

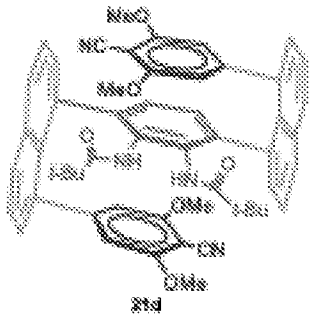
$[\alpha]_D^{20}$ = 133.3 (c = 1.2, CH_2Cl_2)



21c

76% yield

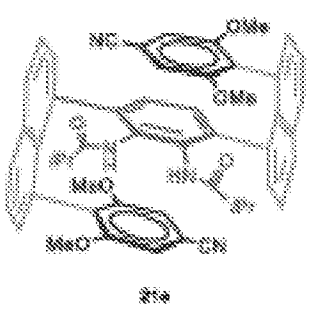
$[\alpha]_D^{20}$ = +68.7 (c = 0.7, CH_2Cl_2)



21d

82% yield

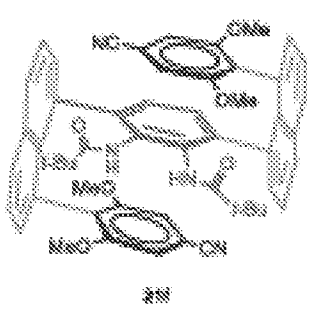
$[\alpha]_D^{20}$ = +90.4 (c = 0.3, CH_2Cl_2)



21e

43% yield

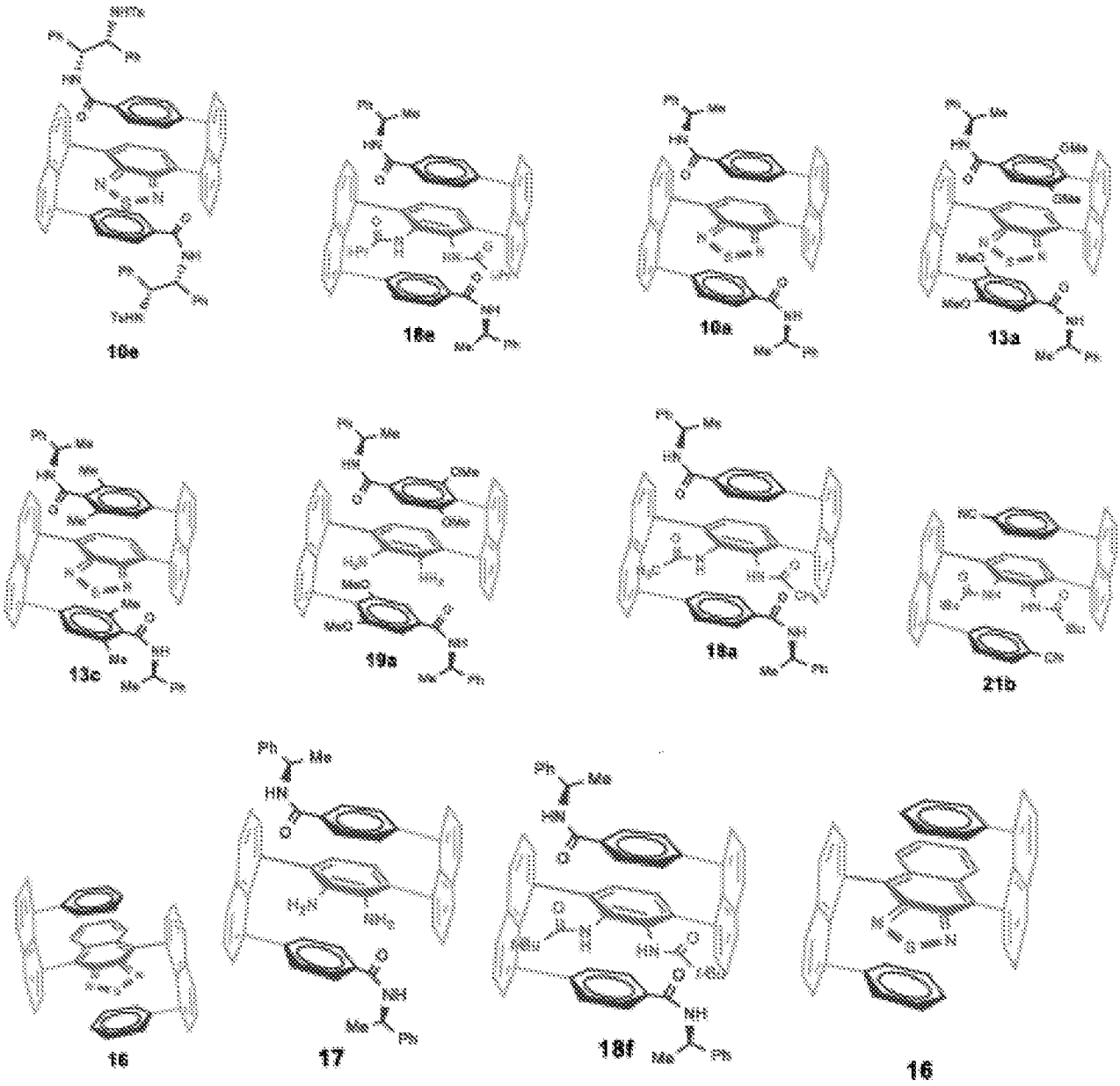
$[\alpha]_D^{20}$ = +61.4 (c = 0.8, CH_2Cl_2)



21f

81% yield

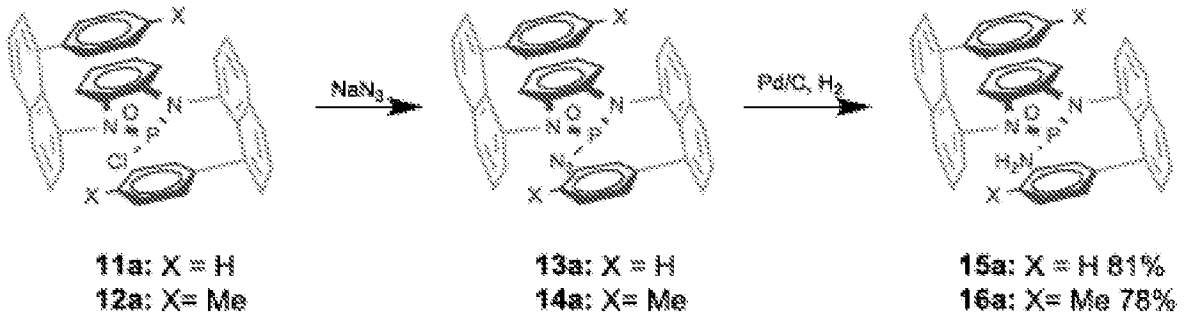
$[\alpha]_D^{20}$ = +215.0 (c = 1.1, CH_2Cl_2)



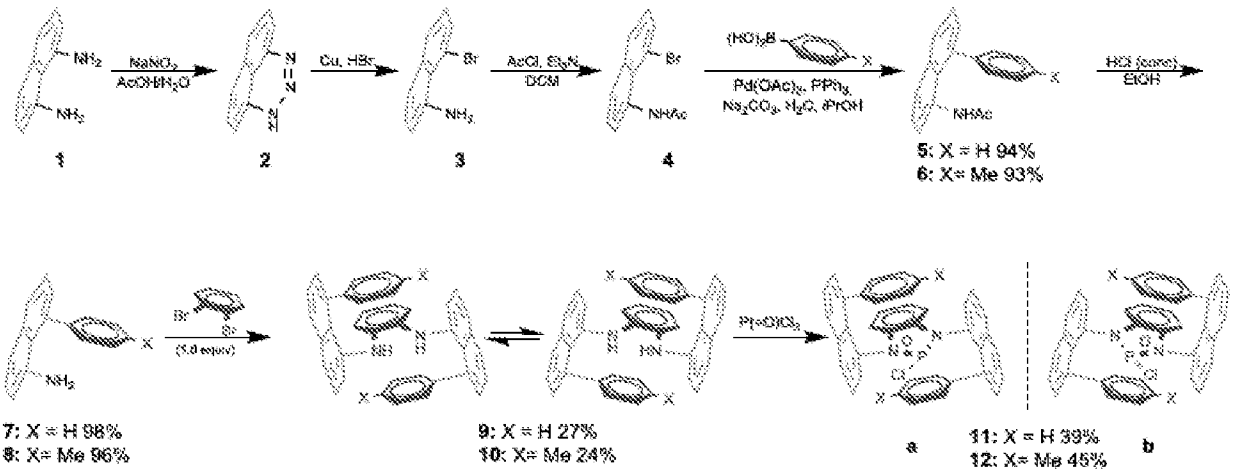
[0026] In another aspect, the first, the second, and the third layers have: a right-hand chirality, a left-hand chirality, or both the left- and the right-handed chirality. In another aspect, the first, the second, and the third layers each comprise a plane, and wherein: (a) one of the three planes is replaced by carbon-carbon triple bond (alkyne bridges and arms); (b) further comprising two additional layers having a right-hand chirality, a left-hand chirality, or both the left- and the right-handed chirality. In another aspect, the additional layers comprise at least one of: 4,4'-(2,7-dimethoxynaphthalene-1,8-diyl)bis(3-methoxybenzonitrile); N,N'-(1,8-bis(2-methoxyphenyl)naphthalene-2,7-diyl)bis(4-methylbenzenesulfonamide); 8,8"-dibromo-2,2",7,7"-tetramethoxy-1,1':8',1"-ternaphthalene; (1'R)-8,8"-dibromo-2',7'-dimethoxy-1,1':8',1"-ternaphthalene; wherein, Br can be H, aliphatics, aromatics; MeO can be NHAc, NHTs, NH-protection groups, aromatics, alkylyl, alkenyls; N-(1-((8-([1,1'-biphenyl]-4-yl)naphthalen-1-yl)ethynyl)naphthalen-2-yl)-4-

methylbenzenesulfonamide (Ts can be Ac, Ns, Fmoc, t-Boc, CBZ, etc., para Ph can be a halo, alkyl, Aryl, CN, N3, or NHAc. In another aspect, the multi-layer 3D material is a polymer and the first, the second, and the third layers can have a right-hand chirality, a left-hand chirality, or both the left- and the right-handed chirality. In another aspect, monomers are formed into one or more additional layers or polymers are above, below, or both above and below the first, the second, and the third layers.

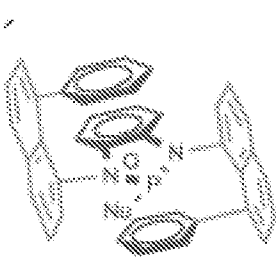
[0027] In yet another embodiment, the present invention includes a Group-Assisted Purification (GAP) catalyst comprising: a multi-layer 3D material comprising: a first, a second, and a third layer, wherein each of the layers are arranged in a nearly parallel fashion with chirality along a center plane comprising the GAP-catalyst anchored by *N,N*-phosphonyl groups. In one aspect, the multi-layer 3D material comprises a first, a second, and a third layer, wherein each of the layers are arranged in a nearly parallel fashion with chirality along a center plane comprising:



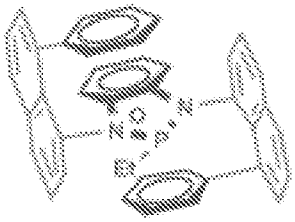
; or



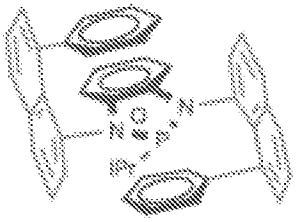
[0028] In another aspect, the multi-layer 3D material is a 2-amino-1,3-bis(8-phenylnaphthalen-1-yl)-1,3-dihydrobenzo[d][1,3,2]diazaphosphole 2-oxide (**15a**). In another aspect, the multi-layer 3D material is selected from at least one of:



;



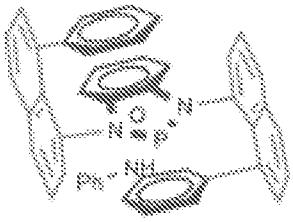
20 ;



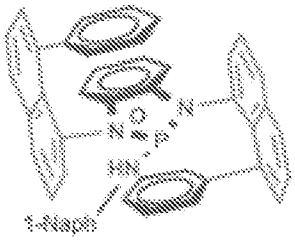
21 ;



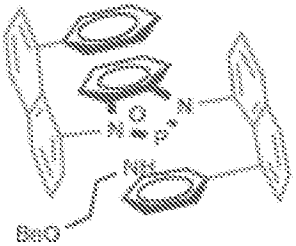
22 ;



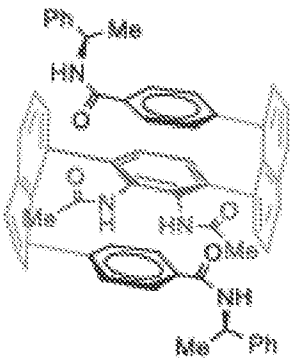
23 ;



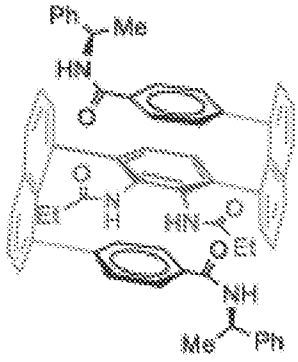
24 ; or



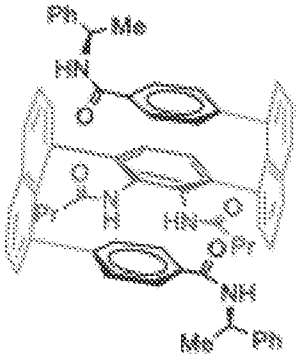
25



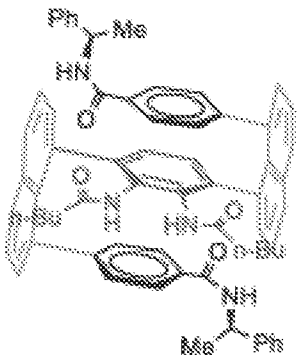
yield 56%
8a



yield 39%
8b

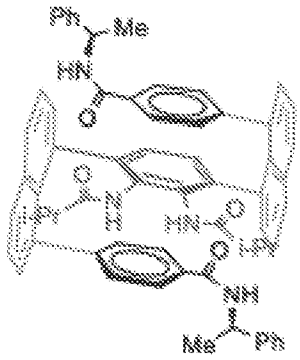


yield 42%
8c



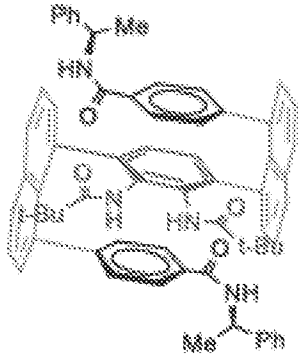
yield 47%

8d



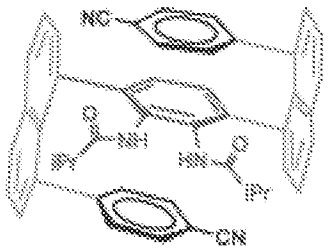
yield 38%, $[\alpha]_D^{25}$ = 92°

8e

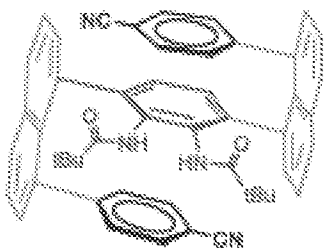


yield 31%, $[\alpha]_D^{25}$ = 58°

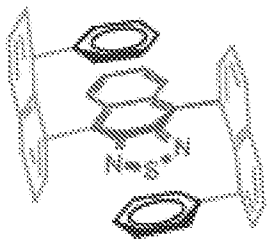
8f



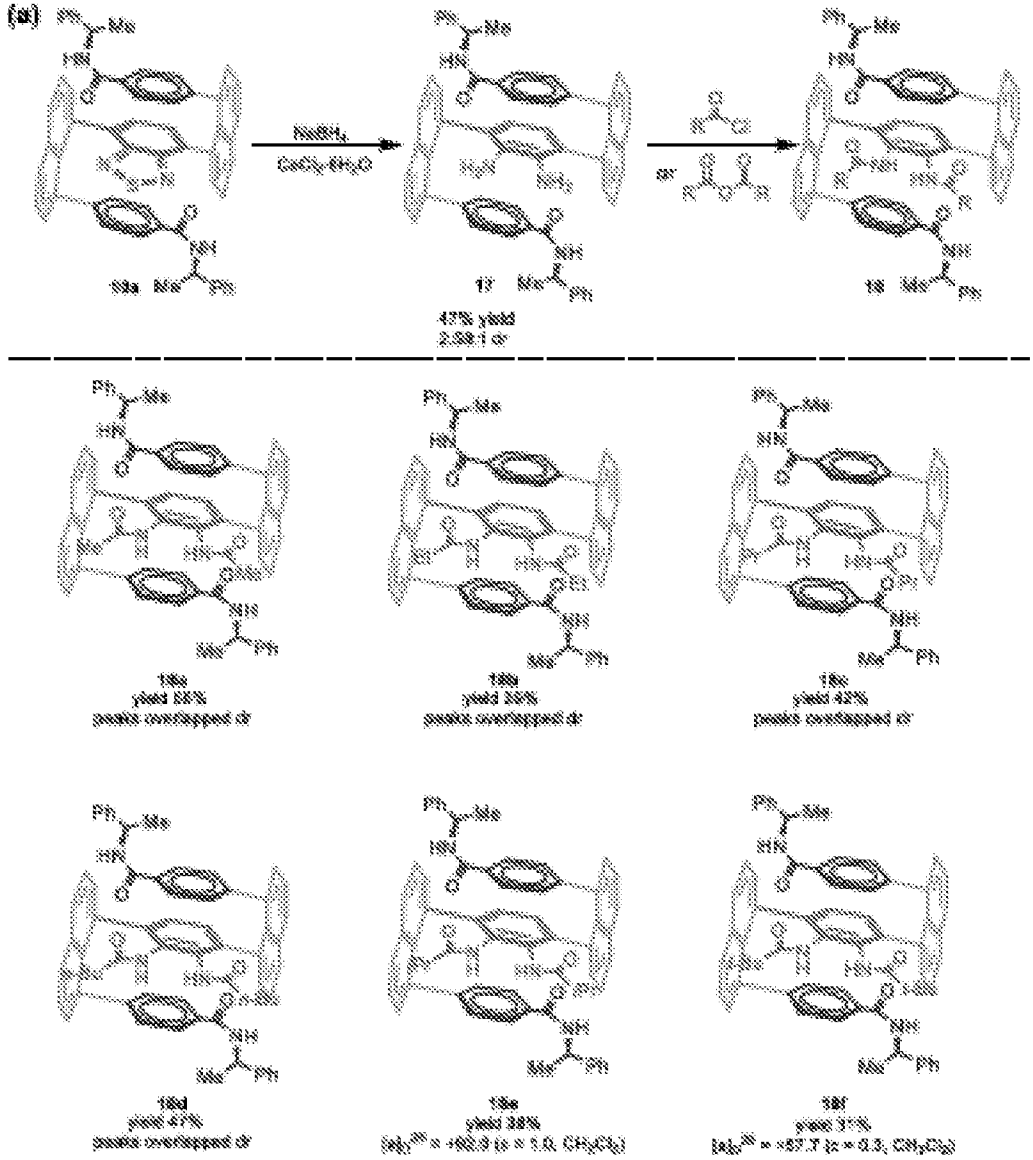
14a

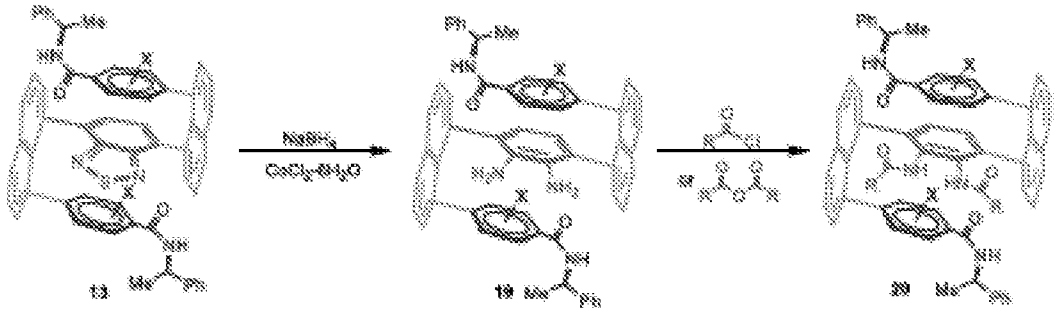


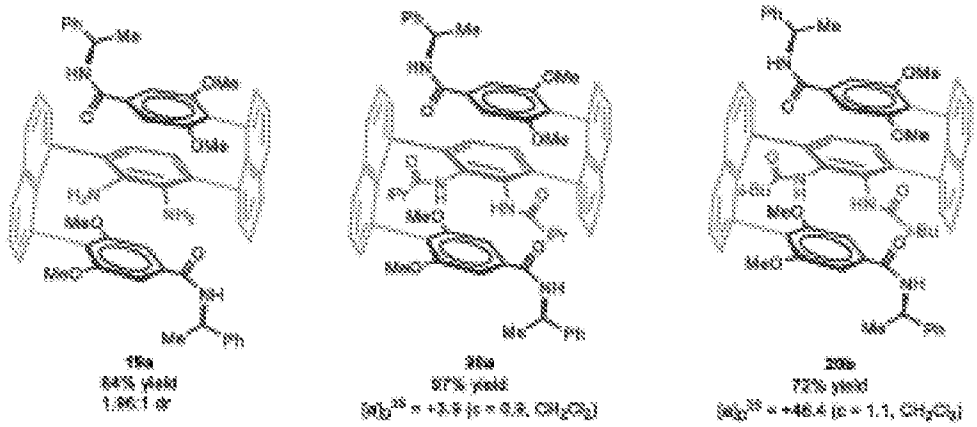
14b

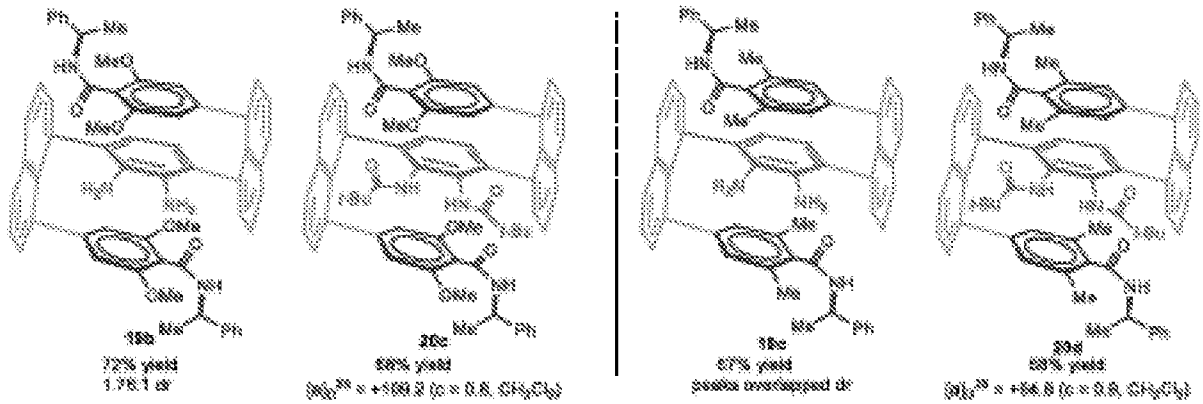


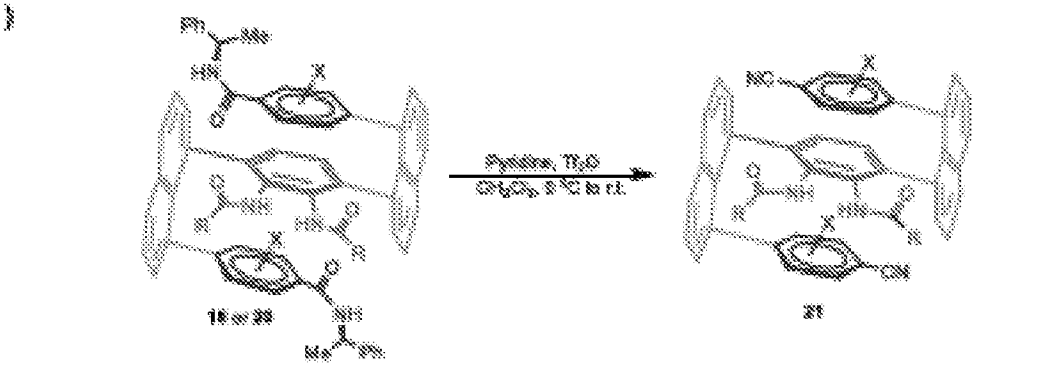
15

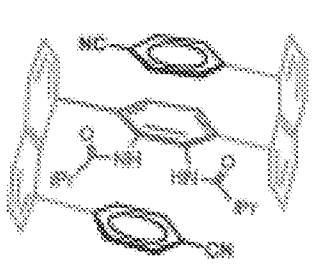








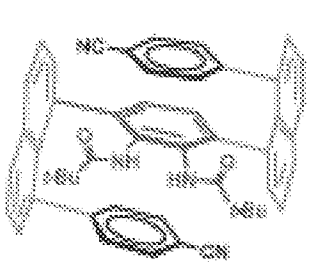




21a

49% yield

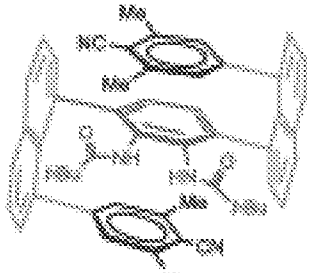
$[\alpha]_D^{20}$ = +60.8 (c = 0.8, CH_2Cl_2)



21b

81% yield

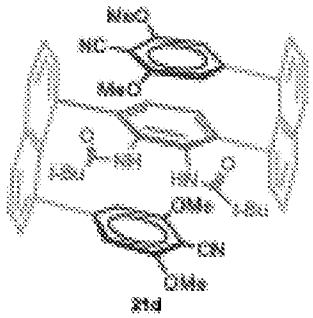
$[\alpha]_D^{20}$ = 133.3 (c = 1.2, CH_2Cl_2)



21c

76% yield

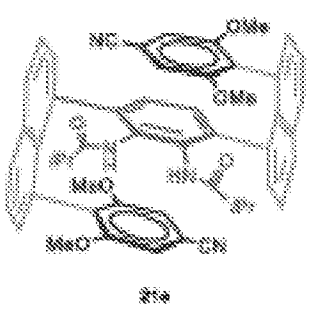
$[\alpha]_D^{20}$ = +68.7 (c = 0.7, CH_2Cl_2)



21d

82% yield

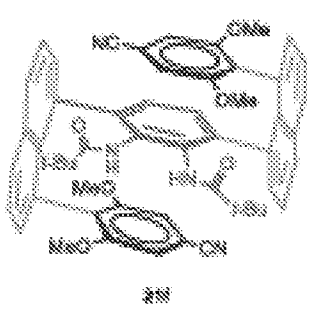
$[\alpha]_D^{20}$ = +90.4 (c = 0.3, CH_2Cl_2)



21e

43% yield

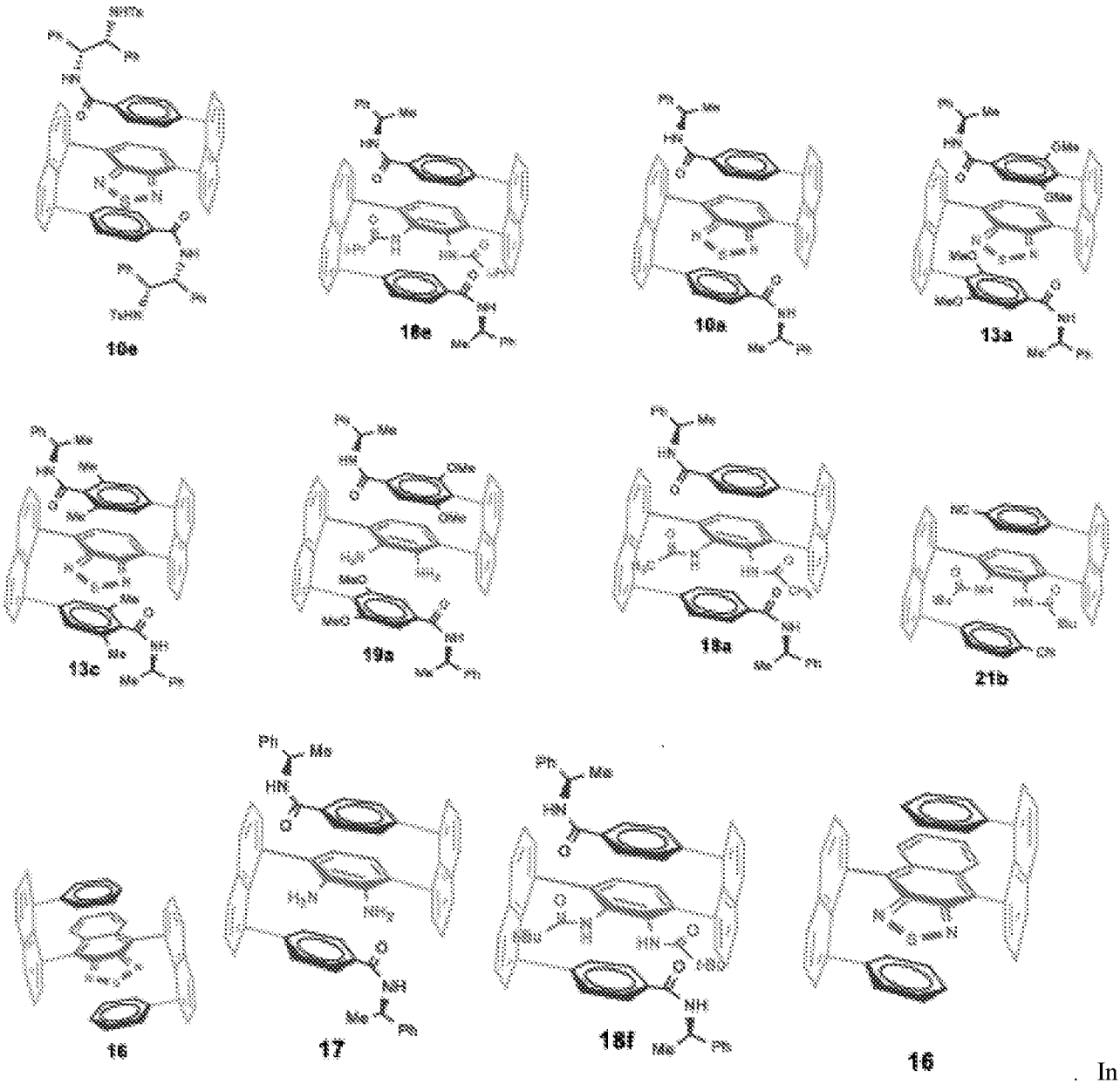
$[\alpha]_D^{20}$ = +61.4 (c = 0.8, CH_2Cl_2)



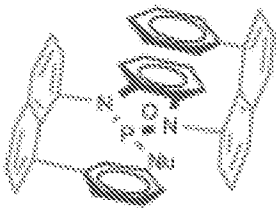
21f

81% yield

$[\alpha]_D^{20}$ = +215.0 (c = 1.1, CH_2Cl_2)



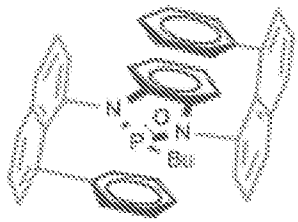
. In another aspect, the multi-layer 3D material is selected from at least one of:



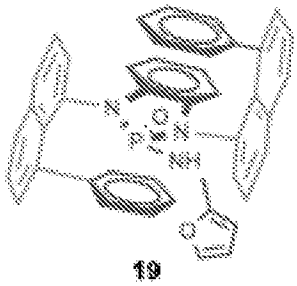
;



17 ;



18 ; or

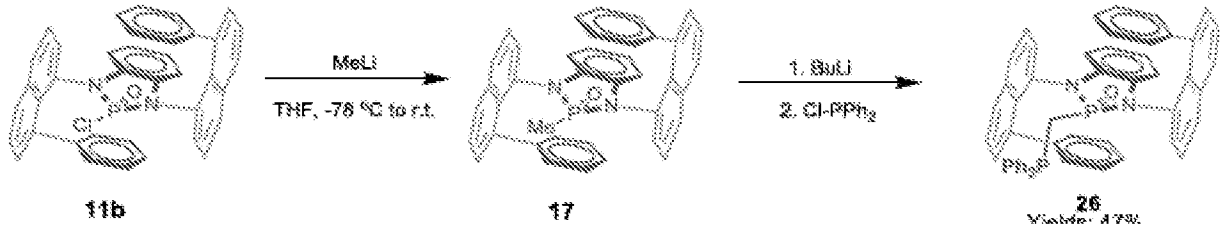


19 . In another aspect, the product of formula:



26

[0029] is made by a method comprising:



11b 17 26 .

[0030] In another embodiment, the present invention also includes a method of conducting a synthetic reaction comprising: providing a Group-Assisted Purification (GAP) catalyst comprising a multi-layer 3D material comprising: a first, a second, and a third layer, wherein each of the layers are arranged in a nearly parallel fashion with chirality along a center plane comprising the GAP-catalyst anchored by *N,N*-phosphonyl groups; and catalyzing a reaction in the presence of the GAP-catalyst. In one aspect, the multi-layer 3D material has a right-hand chirality, a left-hand chirality, or both a left- and a right-handed chirality. In another aspect, each of the first, second, and third layers are at least one of: *anti, syn,* or both *anti* and *syn* isomers. In another aspect, each of the first, second, and third layers are *N,N*-phosphornyl amides. In another aspect, each of the first, second, and third layers comprise chiral or achiral *N*-phosphonyl- or *N*-phosphinyl groups. In

another aspect, each of the first, second, and third layers comprise a Multi-Layer Organic Framework (M-LOF) of single organic molecules with pseudo C_2-chiral characteristics. In another aspect, the first, the second, and the third layers have: a right-hand chirality, a left-hand chirality, or both the left- and the right-handed chirality. In another aspect, the first, the second, and the third layers each comprise a plane, and wherein: (a) one of the three planes is replaced by carbon-carbon triple bond (alkyne bridges and arms); (b) further comprising two additional layers having a right-hand chirality, a left-hand chirality, or both the left- and the right-handed chirality. In another aspect, the additional layers comprise at least one of: 4,4'-(2,7-dimethoxynaphthalene-1,8-diyl)bis(3-methoxybenzonitrile); N,N'-(1,8-bis(2-methoxyphenyl)naphthalene-2,7-diyl)bis(4-methylbenzenesulfonamide); 8,8"-dibromo-2,2",7,7"-tetramethoxy-1,1':8',1"-ternaphthalene; (1'R)-8,8"-dibromo-2',7'-dimethoxy-1,1':8',1"-ternaphthalene; wherein, Br can be H, aliphatics, aromatics; MeO can be NHAc, NHTs, NH-protection groups, aromatics, alkylyl, alkenyls; N-(1-((8-([1,1'-biphenyl]-4-yl)naphthalen-1-yl)ethynyl)naphthalen-2-yl)-4-methylbenzenesulfonamide (Ts can be Ac, Ns, Fmoc, t-Boc, CBZ, etc., para Ph can be a halo, alkyl, Aryl, CN, N3, or NHAc. In another aspect, the multi-layer 3D material is a polymer and the first, the second, and the third layers can have a right-hand chirality, a left-hand chirality, or both the left- and the right-handed chirality. In another aspect, monomers are formed into one or more additional layers or polymers are above, below, or both above and below the first, the second, and the third layers.

BRIEF DESCRIPTION OF THE DRAWINGS

[0031] For a more complete understanding of the features and advantages of the present invention, reference is now made to the detailed description of the invention along with the accompanying figures and in which:

[0032] FIGS. 1A to 1C show various examples of planar chirality. FIG. 1A shows the DNA i-motif and mycobacterial proteins of the prior art. FIG. 1B shows a two-layer planar chirality of the prior art. By contrast, FIG. 1C shows the mirror models and structures of multi-layer 3D molecules of the present invention. FIG. 1D shows the design of a fully C-C bond-anchored chiral multi-layer *3D* frameworks.

[0033] FIGS. 2A and 2B show the design and synthesis of the multi-layer 3D. FIG. 2A shows more efficient GAP groups. FIG. 2B shows the synthesis of N,N-Diaryl benzene-1,2-diamines. FIG. 2C shows the Scheme for Synthesis of 4,7-bis(8-bromonaphthalen-1-yl)benzo[c][1,2,5]thiadiazole.

[0034] FIGS. 3A to 3D shows the physical characteristics of diamino products. FIGS. 3A, 3B, 3C shows the physical appearance of N,N-bis(8-phenylnaphthalen-1-yl)benzene-1,2-diamine. FIG. 3D shows a Hornet' nest pattern of product 21.

[0035] FIGS. 4A and 4B shows the synthetic routes. FIG. 4A shows the synthesis of 8-phenylnaphthalen-1-amine precursors and N,N-phosphonyl chlorides. FIG. 4B shows the synthesis of N,N-phosphonyl azides and amides.

[0036] FIG. 5 shows the substitution reactions of enantioners of N,N-phosphonyl chloride.

[0037] FIG. 6. Conversion of one isomer of N,N-phosphonyl chloride to phosphine.

[0038] FIGS. 7A to 7C show Retro-Synthetic Analysis (RSA) of fully C-C bond-anchored multi-layer 3D targets.

[0039] FIGS. 8A to 8C show: 8A Synthesis of 4,7-bis(8-bromonaphthalen-1-yl)benzo[c][1,2,5]thiadiazole. 8B Synthesis of chiral 1-arylethylamine or alkylethylamine-attached boronic acids. 8C Synthesis of chiral 1-arylethylamine-derived boronic acids. [a]combined yields of two diastereoisomers [b]determined by proton NMR.

[0040] FIGS. 9A to 9D show: 9A Synthetic results of chiral multi-layer 3D amides. 9B Alternative approaches to chiral multi-layer 3D amides. 9C Synthetic results of chiral multi-layer 3D amides by using branched boronic acids. 9D Synthesis of 4,9-bis(8-phenylnaphthalen-1-yl)naphtho[2,3-c][1,2,5]thiadiazole. [a]combined yields of two diastereoisomers [b]determined by proton NMR.

[0041] FIGS. 10A to 10C show: 10A and 10B show the results of free diamines and N-carbonyl-protected multi-layer 3D chiral compounds. (10C shows converting diastereomeric isomers into enantiomers under mild conditions.

[0042] FIG. 11 shows the macrochirality phenomenon of 10e: image under natural light with black background (A1); image under UV light (365 nm) (B1); image under natural light after rotavapor evaporation (C1). Spiro textile-type of macrochirality of 18e formed inside NMR tube (A2 and B2); luminescence of samples under UV light (365 nm): A3-A8 without UV irradiation, B3-B8 with UV irradiation; fluorescence images of 16 under different physical conditions (A9, appearance under natural lights; B9, UV irradiation in natural background; C2, UV irradiation in dark background).

[0043] FIG. 12 shows the luminescence of CDCl3 solutions of samples 17, 18e and 18f in NMR tubes, [c] (mg/ml): A, left =6.7 right = 2.2; B, left (18e) and right (18f) = 8. AIE displays of multi-layer 3D molecules: 10a; 18f and 16 in THF/water systems; (M).

DETAILED DESCRIPTION OF THE INVENTION

[0044] While the making and using of various embodiments of the present invention are discussed in detail below, it should be appreciated that the present invention provides many applicable inventive concepts that can be embodied in a wide variety of specific contexts. The specific embodiments discussed herein are merely illustrative of specific ways to make and use the invention and do not delimit the scope of the invention.

[0045] To facilitate the understanding of this invention, a number of terms are defined below. Terms defined herein have meanings as commonly understood by a person of ordinary skill in the areas relevant to the present invention. Terms such as “a”, “an” and “the” are not intended to refer to only a singular entity, but include the general class of which a specific example may be used for illustration. The terminology herein is used to describe specific embodiments of the invention, but their usage does not limit the invention, except as outlined in the claims.

[0046] In this work, the inventors present the discovery of an unprecedented chirality of multi-layer and three dimensions. This chirality belongs to a type of Multi-Layer Organic Framework (*M*-LOF) of single organic molecules with *pseudo* C2-chiral characteristics. The key element of this chirality is characterized by three layers of planes that are arranged nearly in parallel fashion with one on top and another one down from planar center as presented in FIG. 1C (molecular models & chemical structures). FIG. 1D shows the design of a fully C-C bond-anchored chiral multi-layer *3D* frameworks.

[0047] This discovery resulted from the use of the present inventor's Group-Assisted Purification (GAP) chemistry by taking advantage of *N*-phosphonyl imine reagents and their usages for asymmetric reactions (Fig. 2A, **a-c**). In this example, it was found that chiral and achiral *N*-phosphonyl- or *N*-phosphinyl groups avoided the formation of oily and sticky products; instead, they afforded special crystalline solids that can be purified simply by washing crude products with common petroleum solvents without the use of column chromatography and recrystallization. It was also found that these GAP groups can increase chemical yields, particularly for peptide synthesis, which is defined as Group-Assisted Synthesis (GASyn). GASyn chemistry has resulted in nearly quantitative yields for each step of polypeptide synthesis. In addition, GAP and GASyn chemistry has made it possible for the Fmoc-based peptide synthesis to be performed in solution phase synthesis for the first time. In pharmaceutical industry, the synthesis of 1 kg of peptide and oligonucleotide drugs (10-15 mer products), 3000-15000 kg of wastes are generated mostly from purification. The GAP chemistry thus provides a unique environmentally friendly tool by taking advantages of both solution-phase and solid-phase syntheses (*50-52*) without much of their shortcomings. Indeed, GAP chemistry is the only chemical methodology that combines four aspects into one: reagent, reaction, separation and purification; it requires the consideration of both reactants and products on their chemical and physical factors in regard to reactivity, selectivity, stability and solubility. For asymmetric synthesis and catalysis, diastereo-, enantio- and chemoselectivity have to be taken into account concurrently.

[0048] Typical GAP functionality is represented by *N,N*-phosphonyl amides with their development process described in FIG. 2A. Continuing the search for more efficient GAP functionality has been a main goal has been pursued by the present inventors to provide more environmentally friendly and greener syntheses, particularly, asymmetric synthesis. In one example, the strategy was to replace *N,N*-dialkyl motifs of GAP functionality with their naphthyl counterparts, which improves GAP synthesis (FIG. 2A-**d**). This novel chemistry allows, for the first time, to create new chirality if the chiral centers on vicinal cyclohexyl diamine framework is removed, from which two individual enantiomers of *N,N*-phosphonyl GAP amides are generated.

[0049] As shown in FIG. 2A, the synthesis of naphthyl-based GAP functionality was started with the Buchwald-Hartwig cross coupling of 1-bromo-8-phenylnaphthalene with (*1S,2S*)-cyclohexane-1,2- diamine or vicinal benzene diamine under a slightly modified condition consisting of Pd(OAc)2 and butylphosphine as catalysts and potassium *tert*-butoxide as base additive. The reactions proceeded smoothly to give the

corresponding coupling products in over 80% chemical yields (FIG. 2A-**d** & **e**). The following steps included cyclization of resulting *N,N*-protected diamines with phosphoryl trichloride in pyridine, displacement with sodium azide in DMF, and Pd/C-catalyzed hydrogenation to give *N,N*-phosphornyl amides in overall over 65% yields. While the product of FIG. 2A-**d** showed the arrangement of di-1-nathphyl rings in *anti* configuration; however, product of FIG. 2A-**e** were formed as a mixture of *anti* and *syn* isomers, which can be separated via column chromatography. Increasing temperature of this mixture in dichloromethane to 50 °C for over 5 hours, these two isomers reached equilibrium with two paired of enantiomeric peaks as 25% for each as revealed by chiral HPLC analysis.

[0050] Next, the *N,N*-phosphonyl GAP functionality was changed by introducing a phenyl group onto 1-bromonaphthalene on its position 8 to restrict the axial flexibility so as to control *anti* isomerism of *N,N*-di-1-nathphyls predominantly. The synthesis was started with the Buchwald-Hartwig cross coupling (*53,54*) between vicinal benzene diamine and 1-bromo-8-phenylnaphthalene. Surprisingly, the coupling reaction resulted in a complex mixture with nearly no formation of N,N-protected diamino product under the same condition as the above (FIG. 2B, equation **a**). Other similar modifications on catalytic conditions all failed to result in any promising outcomes. The strategy was thus changed to use 1,2-dibromobezene for the reaction with 1-amino-8-phenylnaphthalene under $Pd(OAc)_2$-based catalytic systems. Among three common phosphines (Bu_3P, *t*-Bu_3P and Ph_3P), only *t*-Bu_3P gave promising results when reaction was performed by refluxing in toluene for three days. The use of $Pd(OAc)_2$ and *t*-Bu_3P in 4 mol% and 10 mol%, respectively, afforded the coupling product, *N,N*-bis(8-phenylnaphthalen-1-yl)benzene-1,2-diamine in a chemical yield of 15%. Replacing toluene with xylenes as solvents under the similar condition increased the formation of desired product to 27% yield (FIG. 2B, equation **b**); the reaction was run at 130°C for 16 hours to completion. Although the yield of this step is still much lower than that of normal cross coupling reactions, it enabled the following steps to be continued to achieve *N,N*-phosphonyl GAP amides (FIG. 4). FIG. 2C shows the Scheme for Synthesis of 4,7-bis(8-bromonaphthalen-1-yl)benzo[c][1,2,5]thiadiazole.

[0051] While performing the C-N coupling reactions, *N,N*-bis(8-phenylnaphthalen-1-yl)benzene-1,2-diamine (**9**) was found to be show green colored shining under irradiation under UV light (FIG. 3A). A major unknown side product also shines with purple color under UV irradiation. This product was formed as various long bars of firm solids with up to a length of a few centimeters (FIG. 3B); When they are evaporated in a relatively smaller flask, a nest-work of firm solid was formed, which filled the majority flask space (FIG. 3C). Single crystals of this product were obtained from co-solvent of EtOAc/hexane during a period of two weeks; the X-ray structural analysis revealed that each phenyl ring is nearly parallel to the naphthylene ring of their neighboring 8-phenylnaphthalen-1-yl group (not shown). There was no hydrogen bonding formation existing between two amino groups; and there is no intermolecular hydrogen bonding observed either. Interestingly, the intermolecular packing of *N,N*-bis(8-phenylnaphthalen-1-yl)benzene-1,2-diamine shows a helix type of structural arrangement (not shown).

[0052] The total synthesis (FIG. 4) of this new chirality was started from oxidative cyclization by reacting naphthalene-1,8-diamine with sodium nitrite in aqueous media containing acetic acid to give 1H-naphtho[1,8-de][1,2,3]triazine (**2**). Ring-opening of this triazine was performed by treating with metal copper in hydrogen bromide. The resulting 8-bromonaphthalen-1-amine (**3**) was converted to *N*-(8-bromonaphthalen-1-yl)acetamide (**4**), followed by Suzuki coupling to afford *N*-acetyl 8-phenylnaphthalen-1-amine (**5**). 8-Phenylnaphthalen-1-amine (**7**), was generated by acidic hydrolysis with concentrated aqueous HCl, which is subjected to the Buchwald-Hartwig C-N double cross couplings.

[0053] The *N,N*-diamino cross coupling product was anticipated to exist in the form of two major enantiomeric conformers (**9**), which are not distinguishable by chiral HPLC. However, after they are cyclized into 2-chloro-1,3-bis(8-phenylnaphthalen-1-yl)-1,3-dihydrobenzo[d][1,3,2]diazaphosphole 2-oxide (**11**), two individual enantiomers can be analyzed and separated through analytical and preparative chiral HPLC columns, respectively. At this cyclization step, previous conditions for forming amides by treating diamines with in triethyl amines or pyridine failed to give any cyclization product for case Fig. 2A-**f**, although they worked well for cases of Fig. 2A-**a** to Fig. 2A-**e**. The cyclization reaction was successfully conducted by deprotonating *N,N*-bis(8-phenylnaphthalen-1-yl)benzene-1,2-diamines (**9**) with *n*- butyl lithium followed by treating with trichlorophosphine oxide at -78°C in dried THF. This cyclization difficulty is probably due to the large steric effect from the phenyl group on position 8 of naphthalene ring, this would also be responsible for the incomplete conversion of this reaction. A yield of 39% was obtained at this step while the remained 1,2-diamine starting material was recovered for re-use *via* column chromatography in 48% yield.

[0054] Attempts were made to obtain single crystals of individual enantiomers of 2-chloro-1,3-bis(8-phenylnaphthalen-1-yl)-1,3-dihydrobenzo[d][1,3,2]diazaphosphole 2-oxide (*N*-phosphonyl chloride, **11a**) without success. Pleasantly, the inventors achieved X-ray diffraction analysis of crystals of 2-amino-1,3-bis(8-phenylnaphthalen-1-yl)-1,3-dihydrobenzo[d][1,3,2]diazaphosphole 2-oxide (**15a**) (not shown), which was derived from the above *N,N*-phosphonyl chloride through the formation of corresponding azide precursor, which eventually enabled the absolute structure of the *N*-phosphonyl chloride to be determined indirectly. Also, the effort on obtaining single crystals for 2-azido-1,3-bis(8-phenylnaphthalen-1-yl)-1,3-dihydrobenzo[d][1,3,2]diazaphosphole 2-oxide (**13a**) were unsuccessful. Also unsuccessful were finding chiral analytical HPLC conditions for the azide racemic samples. Quantitative yields were obtained at the azide displacement step when the reaction was performed in acetonitrile at 90°C, the resulting *N,N*-phosphonyl azide was directly subjected to the final Pd/C catalyzed hydrogenation which showed quantitative yields as well.

[0055] After individual enantiomers of N,N-phosphonyl chlorides were generated through preparative chiral HPLC, the inventors investigated their synthetic potentials by transferring them into various building blocks. At first, methyl lithium was subjected to the nucleophilic substitution reaction with isomer (11b) of N,N-phosphonyl chloride (Fig. 5). The reaction was finished by running in dried THF at -78 oC for 30 min and then

raised to room temperature for 6 h. A yield of 64% was achieved without observation of any racemization; this was confirmed by running the same reaction using racemic N,N-phosphonyl chloride with the resulting product subjected to chiral HPLC analysis (see SI). As the inventors expected that bulky sandwich center plane can prevent the axial rotation which is necessitated for racemization. Other two nucleophiles, n-butyl lithium and furan-2-ylmethanamine, were also employed for the reaction with this enantiomer under similar conditions to give 2-butyl-1,3-bis(8-phenylnaphthalen-1-yl)-1,3- dihydrobenzo[d][1,3,2]diazaphosphole 2-oxide and 2-((furan-2-ylmethyl)amino)-1,3-bis(8- phenylnaphthalen-1-yl)-1,3-dihydrobenzo[d][1,3,2]diazaphosphole 2-oxide (19) in yields of 33% and 84%, respectively (Fig. 5).

[0056] Based on the availability of enantiomerically pure N,N-phosphonyl chlorides generated from preparative HPLC, the inventors then examined other nucleophiles for the similar reaction with the other isomer (11a). These nucleophiles include ethyl magnesium bromide, i-propyl lithium, phenylmethanamine, aniline, naphthalen-1-amine and 2-(benzyloxy)ethan-1-amine. All of these nucleophiles reacted with N,N-phosphonyl chloride isomer (11a) smoothly to give good to high yields as shown in Fig. 5. It should be noted that for amino nucleophiles, their treatment with n- butyl lithium was performed for pre-formation of lithium alkylamide or lithium arylamide prior to the nucleophilic substitution reaction. All of these products (Fig. 5, 20-25) were proven to be stable at room temperature, no decomposition was detected for more than one month without any inner gas protection.

[0057] Interestingly, during conducting i-propyl lithium-based substitution, the inventors found the resulting product of 2-isopropyl-1,3-bis(8-phenylnaphthalen-1-yl)-1,3- dihydrobenzo[d][1,3,2]diazaphosphole 2-oxide (21) was formed in flask by showing a hornet' nest pattern of white color after evaporation was operated to dryness (FIG. 3D). The hornet's nest units include an almost identical shape of various sizes. Other alkyl derivatives did not show this phenomenon, indicating that i-propyl groups can be used for controlling properties for certain materials.

[0058] To further investigate synthetic potential of this novel chirality, the inventor converted enantiomerically pure isomer (11b) of N,N-phosphonyl chloride into a chiral phosphine ligand which belongs to the most active field in asymmetric catalysis (Fig. 6, 26) (60-66). The key step was to conduct the deprotonation of 2-methyl-1,3-bis(8-phenylnaphthalen-1-yl)-1,3- dihydrobenzo[d][1,3,2]diazaphosphole 2-oxide by using n-BuLi followed by nucleophilic substitution reaction with chlorodiphenylphosphine. This two-step synthesis gave an excellent overall yield of 47%. Since this new ligand is anchored by GAP functionality, it would be anticipated to be recyclable for re-use via simple GAP purification. The work on improving yields of N,N-di-coupling reaction and applications of this new chirality are currently being investigated in our labs.

[0059] In conclusion, the inventor discovered a novel organic sandwich chirality showing multi-layer three dimensions. The absolute structure has been unambiguously confirmed by X-ray diffraction analysis of signal

crystals. The key element of this chirality is characterized by three planes that are arranged nearly in parallel fashion with one on top and one down from the center layer. The resulting 3D-multi-layer chiral products have been converted into various building blocks, particularly, anchored by N,N-phosphonyl GAP group to give new chiral phosphine ligands for asymmetric chemistry. The GAP-catalyst strategy resulted in the design, synthesis and applications of more environmentally friendly materials and catalysts for recycling and re-use. The work would be anticipated to have a great impact on chemical, pharmaceutical and material sciences in future.

[0060] Next, the inventors pursued additional structural designs by analyzing original chiral sandwich-shaped structures of multi-layer *3D* chirality. As shown in FIG. 1C, the key characteristics of this chirality are shown by three levels of planar units arranging nearly in parallel fashion with one on top and the other one down from the central layer, and by its unique *pseudo* C_2 symmetry which is made possible by differentiating moieties on phosphorous on *N*-phosphonyl ring. In the nine-step total synthesis of this chirality, the key steps involved the dual Buchwald-Hartwig C-N couplings [83-85] and diamino cyclization. At beginning, only 15%-19% and 39%-45% were achieved for these two steps, respectively. Afterwards, these yields were improved to 27%-41% and 45%-65%, respectively, by choosing more suitable substrates and by changing Buchwald-Hartwig catalytic conditions. An additional shortcoming in that work is that the free diamine products are not so stable, particularly when they are dissolved in solutions. Usually, they are utilized just after they are prepared. This situation prompted us to continue seeking new multi-layer *3D* molecules and corresponding synthetic strategies for future applications.

[0061] For the previous multi-layer *3D* chirality anchored by C-N bonds, shown above, the inventors had to obtain individual enantiomers through physical separation *via* pre-preparative chiral HPLC. The inventors envisioned that if the dual C-N bonds in the original multi-layer *3D* structures (FIG. 1C)) were moved backwards onto the central phenyl rings, this would result in fully C-C bond-anchored multi-layer *3D* chiral molecules and would generate new properties and asymmetric environments for chemical and material applications (FIG. 1D). Furthermore, it would make its asymmetric synthesis to be more convenient and practical. In this communication, the inventors would like to disclose this new design and its synthetic assembly. The present work presents the first fully C-C bond-anchored multi-layer 3D chirality and the first enantioselective assembly of multi-layer 3D chiral molecules.

[0062] In these new chiral multi-layer structures (FIGS. 1C and 1D), two smallest hydrogen atoms exist on 4- and 5-positions of the central phenyl ring, which allows the phenyl rings to freely rotate back and forth within an angle range of 180° in classical doubly-layered chiral structures. However, in this new chirality, its top and bottom layers restrict and limit each other from free rotation, i.e., this multi-layer 3D chirality would not exist if it lacks the presence of a third layer. This would fundamentally differentiate the present multi-layer 3D

chirality from the well-known planar and axial chirality documented in literature. In addition, the pseudo C_2 symmetry of previous C-N anchored chirality has become C_2 symmetry in the present structural frameworks.

[0063] Retro-Synthetic Analysis (RSA). Retro-synthetic analysis [81] revealed that there are several strategies to assemble the present multi-layer *3D* molecular framework. These strategies are mainly based on the dual Suzuki-Miyaura C-C couplings as represented by the cases of using (*R*)-(+)-1-phenylethylamine derivatives as the substrate (Fig. 7A). Since the inventors have failed several attempts on the direct coupling 2(2,3-diamino-1,4-phenylene)diboronic acid or its *N,N*-diacetyl derivatives with 1,8-dibromonaphthalene, the inventors have to turn attention to the use of benzo[c][1,2,5]thiadiazole-4,7-diyldiboronic acid as the bridge synthon for this coupling reaction. Benzo[c][1,2,5]thiadiazole-4,7- diyldiboronic acid is readily made by converting 4,7-dibromobenzo[c][1,2,5]thiadiazole into 4,7-bis(4,4,5,5-tetramethyl-1,3,2-dioxaborolan-2-yl)benzo[c][1,2,5]thiadiazole followed by HCl hydrolysis. 1,8-Dibromonaphthalene was synthesized by reacting 1,8-diaminonaphthalene with $NaNO_2$ followed by the treatment with copper (I) bromide [82].

[0064] The retro-synthetic analysis revealed the coupling of (*R*)-(8-(4-((1-phenylethyl)carbamoyl)phenyl)naphthalen-1-yl)boronic acid with 1,8-dibromonaphthalene (Fig. 7B) would be less suitable because the preparation of this boronic acids and its derivatives requires more steps and more costs for the total synthesis of nine targets than strategy FIG. 7A. Naphthalene-1,8-diyldiboronic acid was also planned as a synthon unit for the coupling with 4,7-dibromobenzo[c][1,2,5]thiadiazole (FIG. 7C). Unfortunately, during the synthesis of this precursor, the inventors found when tetramethyl naphthalene-1,8-diyldiboronate was subjected to hydrolysis, naphthalene-1,8-diyldiboronic acid cannot be generated. Instead, its dehydrated product, 1H,3H-naphtho[1,8-cd][1,2,6]oxadiborinine-1,3-diol, was formed predominantly as confirmed by X-ray structural analysis (FIG. 7C). This compound is inert to the coupling reaction under the standard and even more harsh conditions. These results also proved that it is promising to directly employ 4,7-bis(4,4,5,5-tetramethyl-1,3,2-dioxaborolan-2-yl)benzo[c][1,2,5]thiadiazole as a bridge synthon for this synthetic assembly.

[0065] Synthetic Assembly. The inventors used dual Buchwald-Hartwig C-N couplings, which played a key role in the nine-step synthesis [83-85]. Similarly, in this synthesis, the dual Suzuki-Miyaura C-C couplings [86-88] were planned to assembly two moles of 1,8-dibromonaphthalene with one mole of 1,4-di-boronic acid bridge. Therefore, the synthesis of central planar building block, 4,7-bis(8-bromonaphthalen-1-yl)benzo[c][1,2,5]thiadiazole, was started by reacting 4,7-dibromo-2,1,3-benzothiadiazole with bis(pinacolato)diboron in the presence of (1,1-bis(diphenylphosphino)ferrocene) dichloropalladium(II) as the catalyst [87]. The resulting diboronic ester was treated with sodium periodate and subsequently by hydrochloric acid, to give 2,1,3-benzothiadiazole-4,7-diboronic acid. The dual Suzuki-Miyaura C-C couplings of this diboronic acid with 1,8-dibromonaphthalene in the presence of $Pd(PPh_3)_4$ in co-solvent of THF/H_2O resulted in 4,7-bis(8-bromonaphthalen-1-yl)benzo[c][1,2,5]thiadiazole in an overall yield of 43% in three steps

(FIG. 8A) [88]. The major reason of affording a low yield at the last step is partially caused by mono- and di-debromination occurred during the Suzuki-Miyaura catalytic process.

[0066] The chiral auxiliary is attached onto the para-position on phenyl ring of 4-boronobenzoic acid which is commercially available. A literature procedure is followed for the preparation of six chiral amide-based boronic acids [89]. In this preparation, 4-carboxybenzeneboronic acid (1.0 equiv) was treated with PyBOP (2.0 equiv) in DMF stirring for a few minutes, followed by adding chiral 1-arylethylamine or alkylethylamine (2.0 equiv) into the reaction mixture. The carbonyl coupling was completed within 14 h at room temperature prior to quenching, work-up and purification *via* column chromatography to give **6a–6f** in chemical yields arranging from 47% to 83%. It is not surprising the bulkier the amine reagents, the lower the chemical yields as shown in FIG. 8B and 8C.

[0067] The dual Suzuki-Miyaura C-C couplings were conducted by following a typical procedure of mono Suzuki-Miyaura C-C coupling [86-88]. An excess amount of (*R*)-(8-(4-((1-arylethyl)carbamoyl)phenyl)naphthalen-1-yl)-, or, (*R*)-(8-(4-((1-alkylethyl)carbamoyl)phenyl)naphthalen-1-yl)-boronic acids (**6a-6f**, 2.3 equiv) was reacted with 4,7-bis(8-bromonaphthalen-1-yl)benzo[c][1,2,5]thiadiazole (**4**, 1.0 equiv) in presence of $Pd(PPh_3)_4$ (20 % mol) and potassium carbonate (6.0 equiv) in THF/H_2O (5:1, *v/v*). The limiting reagent of 4,7-bis(8-bromonaphthalen-1-yl)benzo[c][1,2,5]thiadiazole dibromide can be consumed within 12 h after being stirred at 85 ^oC. As shown in FIG. 9A that the dual coupling product of (*R*)-(8-(4-((1-phenylethyl)carbamoyl)phenyl)naphthalen-1-yl)boronic acid (**6a**) gave highest yield of 48% among the above six chiral boronic acids (**6a-6f**) which were examined. These chiral boronic acids showed similar diastereoselectivity arranging from 1.46:1 to 3.00:1 dr. The modest diastereoselectivity would be attributed to relatively high temperature of catalytic condition leading to some degrees of rotation of chiral reactants during asymmetric induction processes. Since the absolute structure of chiral boronic acid **6a**-derived major isomer of multi-layer *3D* chirality was assigned by X-ray diffraction analysis (FIG. 9A-B), and its overall outcomes (yield and diastereoselectivity) are among the best, it was thus chosen as the substrate for extension with other branched chiral amide-derived boronic acids (FIG. 9C) and for other steps of the present total synthesis (FIGS. 10A and 10B).

[0068] The inventors also enhanced yields and diastereoselectivity for the synthesis of chiral multi-layer *3D* amides by changing C-C bond connections based on the use of (*R*)-(8-(4-((1-phenylethyl)carbamoyl)phenyl)naphthalen-1-yl)boronic acid or its bromide precursor (FIG. 9B). Unfortunately, the two alternative methods did not give obvious improvements on either yield (60% and 53%, respectively) and diastereoselectivity (1.91:1 and 2.17:1, respectively). The former is to use 4,7-dibromobenzo[c][1,2,5]thiadiazole as the anchor for the reaction with (*R*)-(8-(4-((1-phenylethyl)carbamoyl)phenyl)naphthalen-1-yl)boronic acid under the standard the Suzuki-Miyaura coupling system (Fig. 9B-A). The disadvantage of this strategy is shown by lower yields for the preparation of

individual (8-(4-((1-phenylethyl)carbamoyl)aryl)naphthalen-1-yl)boronic acids. The latter is to employ benzo[c][1,2,5]thiadiazole-4,7-diyldiboronic acid as the bridge template for the reaction with (*R*)-4-(8-bromonaphthalen-1-yl)-N-(1-phenylethyl)benzamide (FIG. 9B-B). It also showed a disadvantage on the synthesis of individual 4-(8-bromonaphthalen-1-yl)-N-(1-phenylethyl)benzamide derivatives, *i.e.*, it is not as divergent as the other two assembly strategies.

[0069] It is very intriguing that the resulting chiral multi-layer *3D* amides displayed macro-chirality phenomenon which has not been reported in literature to the best of our knowledge. As shown in FIG. 11-A1 and B1 that when a solution containing diamino boronic acid-derived product **10e** was slowly evaporated by being exposed to air for a few days, *anti*-clockwise spiral loops were formed. These spiral loops shine with green color when it is irradiated under UV light at 365 nm. Unlike reported macro-chiral cases in which the chiral mappings can only be seen with the aid of microscopic devices, but the present macro-chiral mapping can be observed by eyes directly. It is similarly interesting that *anti*-clockwise spiral loops are formed when the same solution was evaporated in rotavapor (FIG. 11-(a)-C1), which is also very rarely encountered in organic synthesis.

[0070] Since two individual diastereoisomers of **10a** were extremely difficult to be separated *via* column chromatography or recrystallization, its mixture was thus directly subjected to the reductive opening by treating with an excess amount of sodium borohydride in the presence of $CoCl_2 \cdot 6H_2O$ as the catalyst [90]. The resulting vicinal diamino product **17** was purified *via* column chromatography to give isomeric mixture (**17** and its diastereoisomer) in a combined yield of 47% and 2.58:1 dr. This free diamine mixture was next protected with carbonyl anhydride in anhydrous THF solution containing an excess amount of trimethylamine (FIG. 10A). Fortunately, as indicated by proton NMR that two of these protected diamino products can be separated to give pure major individual isomers (**18e** & **18f**, FIG. 10A) while minor isomers are always contaminated with the major one. The rest of other four cases failed to give pure individual isomers *via* column chromatography.

[0071] It is also very intriguing when a capped NMR tube containing a $CDCl_3$ solution of compound **18e** was stored at r.t. for over three weeks, right-handed spiro textile-shaped solids were formed inside the NMR tube. For small chiral organic molecules, this is also an unprecedented phenomenon to the best of our knowledge, FIG. 11-(b) shows the images of chirally wired textile-type of forms of **18e** upon irradiation with UV light under natural lights (FIG. 11-(b)-A2) and dark backgrounds (FIG. 11-(b)-B2).

[0072] After the successful separation of pure major isomers of **18e** and **18f** was achieved with bulkier *N*-isobutyryl and *N*-pivaloyl groups, the inventors envisioned that similarly increasing steric effects on top and bottom aromatic rings of this series would benefit obtaining corresponding major single isomers as well. Therefore, the inventors conducted the synthesis of three bulkier chiral amide-anchored boronic acids: (*R*)-(2,6-dimethoxy-4-((1-phenylethyl)carbamoyl)phenyl)-,(*R*)-(3,5-dimethoxy-4-((1-

phenylethyl)carbamoyl)phenyl)-, and (*R*)-(3,5-dimethyl-4-((1-phenylethyl)carbamoyl)phenyl)-boronic acids (**9a**, **9b** and **9c**, FIG. 8C). Unlike the case of (*R*)-(4-((1-phenylethyl)carbamoyl)phenyl)-boronic acid in FIG. 8B where 4-boronobenzoic acid is commercially available, for latter three substrates, chiral boronic acids need to be pre-generated by starting from their 4-bromobenzoic acid precursors (FIG. 8C The first step is to perform the carbonyl coupling under standard condition[91,92] to give (*R*)-4-bromo-N-(1-arylethyl)benzamides **9a**, **9b** and **9c** in yields of 42%, 25% and 21%, respectively, which were then converted into corresponding boronic acids by treating with *n*-BuLi followed by $B(OMe)_3$ and subsequently by aqueous HCl [93]. The poor yields at this *in situ* synthesis could be caused by the presence of -NH group which may participate in nucleophilic reaction with $B(OMe)_3$ and HCl hydrolysis to form more side products. The reason to employ these symmetrically branched aromatic rings is to avoid stereochemical complexity in forming various diastereoisomers; for most of these resulting multi-layer *3D* isomers, there has not been a nomenclature system available to name their stereochemistry yet.

[0073] The above three new chiral amide-anchored boronic acids were subjected to the dual Suzuki-Miyaura C-C couplings [88] with synthetic results summarized in FIG. 9C. Surprisingly, although bulkier chiral 1-arylethylamine-derived boronic acids were utilized for this reaction, the resulting diastereoselectivity is still in a similar range to that of the non-branched assembly as shown in FIGS. 9A and 9C. In this latter assembly, **13b** was obtained with the highest diastereoselectivity of 2.36:1 dr. The yields of cases **13a** and **13b** were achieved as 70%. As indicated in FIG. 9C, the yields are much higher than those of non-branched assembly arranging from 16% to 48% (FIG. 9A), although the yield of **13c** still remained as low as 23% (FIG. 9C).

[0074] The inventors selected a few samples of this series for irradiating with ultraviolet light (365 nm), and the inventors found these solid products showed luminescence with strong fluorescence of various colors (FIG. 11B). The substituents of different electronic properties on top and bottom aromatic rings are responsible for the change of different colors. They may also impose the effects on the fluorescence activity *via* certain degrees of conformationally constrained stereochemistry.

[0075] A similar situation to above cases still exists where two individual diastereoisomers of **13a-13c** cannot be separated *via* column chromatography. The dr after column chromatography can be determined by $-CH_3$ proton NMR integration of (*R*)-1-phenylethylamino functionality as 2.17:1 and 2.36:1, for **13a** and **13b**, respectively (FIG. 9C). However, due to the overlap of the peaks in proton NMR of **13c**, the dr was not able to be measured. Therefore, these isomeric mixtures were directly subjected to the reductive opening under the literature conditions as mentioned previously [90]. It was difficult to separate the resulting free vicinal diamines **19a-19c** either *via* column chromatography or recrystallization. After purified by column chromatography, these free diamino products showed dr of 1.96:1 and 1.76:1 for **19a** and **19b**, respectively (FIG. 10B), but for case **19c**, the proton NMR signals of two diastereoisomers are seriously overlapped, making it difficult to measure its dr. Pleasantly, after these free diamine mixtures were protected by bulky

isobutyryl and pivaloyl groups by the treatment with isobutyryl anhydride and pivaloyl chloride at r.t. [91,92], the inventors were able to obtain optically pure major isomers of **20a-20d** *via* column chromatography. All of these optical isomers have been proven to be stable at room temperature as revealed by $-CH_3$ proton NMR signals of (*R*)-1-phenylethylamino functionality.

[0076] The isolation of individual diastereomeric isomers of 4,4'-((2,3-di-alkylamido-1,4-phenylene)bis(naphthalene-8,1-diyl))-bis(N-((R)-1-phenylethyl)benzamide) (**18e** & **18f**) and their symmetrically substituted derivatives (**20a-20d**) enabled us to convert them into corresponding enantiomeric isomers under mild conditions at 0 °C to r.t. [94,95]. The inventors conducted this transformation by stirring a cold anhydrous DCM solution containing the diasteromerically pure isomers above together with pyridine and Tf_2O for 30 min, and then warmed up to room temperature, kept stirring the reaction mixture for about 6-8 hours until the starting materials are consumed as monitored by TLC. As revealed by FIG. 10C that modest to good yields (43% to 81%) were achieved for six cases with their optical rotation data measured. It is interesting to note that all these six enantiomers showed positive optical rotation data, albeit these numbers vary substantially from $[\alpha]_D^{25}$ = 36.4 to 210.0. Qualitative examination of fluorescence sensitivity was conducted on randomly selected samples in NMR tubes with $CDCl_3$ as solvent. As shown in FIG. 12A that the vicinal free diamino compound **17** displayed gold color. Sample **17-A2** with a higher concentration showed stronger fluorescence activity than **17-A1** with a lower concentration, indicating its potential as aggregation-induced emission (AIE) and bioanalytical probe candidate in future [37,96-99]. The corresponding *N,N*-bis-isobutyryl and *N,N*-bis-pivaloyl protected samples **18e** and **18f** displayed the same blue color. Intriguingly, these two protection groups were able to convert the color from gold to blue, indicating there are great potentials for structure-activity-relationship (SAR) study on these compounds serving for AIE materials by changing protection groups on diamino functionality on the aromatic rings.

[0077] Finally, naphtho[2,3-c][1,2,5]thiadiazole was used as the bridge for assembling this series of fully C-C anchored *3D* chiral targets. The racemic product **16** was formed; its structure has been unambiguously confirmed by X-ray diffractional analysis (Fig. 8D). Intriguingly, even in its solid form, the product **16** showed strong fluorescence sensitivity under UV light at 365 nm (Fig. 11-(b)-C2). This racemic compound and two other chiral multi-layer *3D* products, **10a** and **18f**, displayed aggregation-induced emission (AIE) properties (FIG. 12) in which the higher fraction of water, the stronger the luminescence.

[0078] Thus, the inventors demonstrate the first enantioselective total synthesis of sandwich-shaped organic targets of multi-layer *3D* chirality. Asymmetric dual Suzuki-Miyarua couplings were proven to be a suitable tool for this *3D* assembly by taking advantage of chiral amide-derived boronic acids and other reactions. This work presents the first design of fully C-C anchored multi-layer *3D* chirality as represented by six optically pure enantiomers; each of them takes seven to ten synthetic steps. The absolute structure of this fully C-C anchored multi-layer *3D* chirality has been unambiguously confirmed by X-ray diffractional analysis. Unlike

well-known planar or axial chirality in literature, the present chirality would not exist if it lacks a third layer either above or below the central aromatic ring. Nearly all resulting multi-layer *3D* chiral products in this work displayed strong fluorescence activity of different colors and aggregation-induced emission (AIE) properties under UV irradiation. The conversions of cyanide functional group on multi-layer *3D* chiral products into many other groups and interdisciplinary collaboration on this project among chemistry, pharmaceutical and material sciences is now possible.

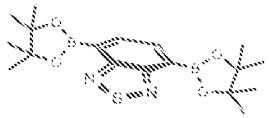
[0079] Unless otherwise stated, all reactions were magnetically stirred and conducted in oven-dried glassware in anhydrous solvents under Ar. Solvents and liquid reagents, as well as solutions of solid or liquid reagents were added via syringes, stainless steel or polyethylene cannulas through rubber septa or through a weak Ar counter-flow. Cooling baths were prepared in Dewar vessels, filled with ice/water (0°C) or dry ice/acetone (-78°C). Heated oil baths were used for reactions requiring elevated temperatures. Solvents were removed under reduced pressure at 40-65°C using a rotavapor. All given yields are isolated yields of chromatographically and NMR spectroscopically materials.

[0080] All commercially available chemicals were used as received without further purification. Solvents as follows: EtOH, toluene, hexane, EA, ether, DCM, dioxane, acetone, TEA, DMF, water were used without further purification. THF and DCM are delivered from an Innovation Technology solvent system.

[0081] The ^{1}H and ^{13}C NMR spectra were recorded in $CDCl_3$ or DMSO-d_6 on 400 MHz and 500 MHz instruments with TMS as internal standard. For referencing of the ^{1}H NMR spectra, the residual solvent signal ($\delta = 7.26$ for $CDCl_3$ and $\delta = 2.50$ for DMSO-d_6) were used. In the case of the ^{13}C NMR spectra, the signal of solvents ($\delta = 7.16$ for $CDCl_3$ and $\delta = 39.52$ for DMSO-d_6) were used. Chemical shifts(δ) were reported in ppm with respect to TMS. Data are represented as follows: chemical shift, multiplicity (s = singlet, d = doublet, t = triplet, m = multiplet), coupling constant (*J*, Hz), and integration. HRMS analyses were carried out using a TOF-MS instrument with an ESI source. Optical rotations were measured with a Rudolph Research Analytical APIV/2W Polarimeter at the indicated temperature with a sodium lamp. Measurements were performed in a 2 ml with concentrations (g/ (100 ml)) reported in the corresponding solvent. X-Ray crystallographic analysis was performed with a SMART CCD and a P4 diffractometer. X-ray data were collected on a Rigaku XtaLAB Synergy-*i* Kappa diffractometer equipped with a PhotonJet-*i* X-ray source operated at 50 W (50kV, 1 mA) to generate Cu Kα radiation ($\lambda = 1.54178$ Å) and a HyPix-6000HE HPC detector.

[0082] Synthetic Procedures and data

[0083] 2 and 3 were synthesized from 4,7-Dibromo-2,1,3-benzothiadiazole following the reported procedure [1] with very minor modification.



[0084] 4,7-bis(4,4,5,5-tetramethyl-1,3,2-dioxaborolan-2-yl)benzo[*c*][1,2,5]thiadiazole (2): yellow solid, 82% yield. ^{1}H NMR (400 MHz, CHLOROFORM-D) δ 8.10 (d, *J* = 8.8 Hz, 2H), 1.46 – 1.38 (m, 24H). MS(ESI): m/z, 389.2 $[M+H]^+$.



[0085] benzo[*c*][1,2,5]thiadiazole-4,7-diyldiboronic acid (3): yellow solid, 95% yield. ^{1}H NMR (400 MHz, DMSO-D6) δ 8.51 – 8.22 (m, 4H), 7.96 (s, 2H). MS(ESI): m/z, 225.0 $[M+H]^+$.

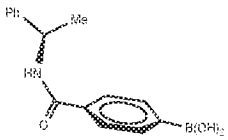
[0086] Data for 4



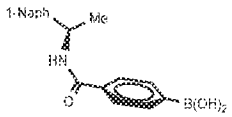
[0087] 4,7-bis(8-bromonaphthalen-1-yl)benzo[*c*][1,2,5]thiadiazole (4): green yellow solid, 55% yield. ^{1}H NMR (400 MHz, CHLOROFORM-D) δ 8.04 – 7.99 (m, 2H), 7.96 (dd, *J* = 8.2, 1.0 Hz, 2H), 7.79 – 7.57 (m, 8H), 7.34 (dd, *J* = 15.2, 7.3 Hz, 2H); ^{13}C NMR (101 MHz, CHLOROFORM-D) δ 155.55, 155.48, 136.58, 136.22, 136.17, 135.95, 135.82, 135.52, 133.83, 133.75, 132.02, 131.84, 130.58, 130.39, 130.37, 130.31, 129.42, 129.37, 129.18, 128.85, 126.51, 126.45, 125.71, 125.70, 120.64, 119.93. HRMS (ESI- TOF) *m/z* $[C_{26}H_{14}Br_2N_2S+H]^+$ calcd for 545.9395, found 545.9383.

[0088] General Procedure for 6a-6f

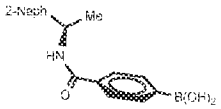
[0089] 4-Carboxybenzeneboronic acid (0.16 g, 1.0 mmol) was introduced into a round bottom flask followed by PyBOP (1.04 g, 2.0 mmol) and 5 ml DMF. The mixture was stirred for 5 min and chiral amine (2.0 mmol) was added. After 14 hours, the reaction mixture was diluted with EA (40 ml) and the organic layer was washed with water (3× 20 ml). The solvent was evaporated under reduced pressure and the residue was purified by flash chromatography on silica gel (hexane/EA, 10/1 to 4/1) to afford pure product. Or using acid-base purification by adjusting pH of the crude product to afford pure product as white solid.



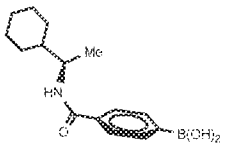
[0090] (*R*)-(4-((1-phenylethyl)carbamoyl)phenyl)boronic acid (6a): $[\alpha]_D^{25}$ = -28.0 (*c* = 1.1, MeOH); white solid, 67% yield. ^{1}H NMR (400 MHz, DMSO-D6) δ 8.75 (d, *J* = 5.7 Hz, 1H), 8.15 (d, *J* = 3.2 Hz, 2H), 7.92 – 7.67 (m, 4H), 7.41 – 7.12 (m, 5H), 5.19 – 5.01 (m, 1H), 1.43 (dd, *J* = 6.9, 2.9 Hz, 3H).



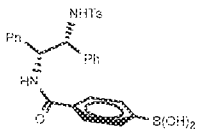
[0091] (*R*)-(4-((1-(naphthalen-1-yl)ethyl)carbamoyl)phenyl)boronic acid (6b): $[\alpha]_D^{25}$ = -108.8 (*c* = 1.0, MeOH); white solid, 75%. ^{1}H NMR (400 MHz, DMSO-D6) δ 8.95 (d, *J* = 7.9 Hz, 1H), 8.17 (d, *J* = 8.3 Hz, 1H), 7.95 (d, *J* = 8.4 Hz, 1H), 7.92 – 7.88 (m, 1H), 7.83 (s, 4H), 7.78 (d, *J* = 8.2 Hz, 1H), 7.69 (dt, *J* = 8.4, 0.9 Hz, 1H), 7.60 (d, *J* = 6.8 Hz, 1H), 7.55 – 7.33 (m, 4H), 5.93 (p, *J* = 7.0 Hz, 1H), 1.58 (d, *J* = 6.9 Hz, 3H); ^{13}C NMR (101 MHz, DMSO-D6) δ = 166.11, 140.97, 136.23, 134.43, 133.89, 130.95, 129.19, 127.75, 126.85, 126.71, 126.10, 126.03, 123.67, 123.11, 45.22, 22.02. HRMS (ESI- TOF) *m/z* $[C_{19}H_{18}BNO_3 + H]^+$ calcd for 320.1458, found 320.1448.



[0092] (*R*)-(4-((1-(naphthalen-2-yl)ethyl)carbamoyl)phenyl)boronic acid (6c): $[\alpha]_D^{25}$ = +42.9 (*c* = 0.7, MeOH); white solid, 79%. ^{1}H NMR (400 MHz, DMSO-D6) δ 8.93 (t, *J* = 12.1 Hz, 1H), 8.21 (s, 2H), 7.95 – 7.73 (m, 8H), 7.63 – 7.50 (m, 1H), 7.49 – 7.33 (m, 2H), 5.32 (p, *J* = 7.0 Hz, 1H), 1.54 (d, *J* = 7.0 Hz, 3H); ^{13}C NMR (101 MHz, DMSO-D6) δ = 166.13, 142.80, 136.16, 134.30, 133.23, 132.42, 128.27, 128.03, 127.82, 126.70, 126.48, 125.96, 125.41, 124.49, 49.00, 22.45. HRMS (ESI- TOF) *m/z* $[C_{19}H_{18}BNO_3 + H]^+$ calcd for 320.1458, found 320.1467.

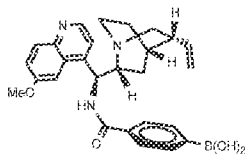


[0093] (*R*)-(4-((1-cyclohexylethyl)carbamoyl)phenyl)boronic acid (6d): $[\alpha]_D^{25}$ = -22.6 (*c* = 0.8, MeOH); white solid, 83%. ^{1}H NMR (400 MHz, DMSO-D6) δ 8.15 (s, 2H), 8.07 (d, *J* = 8.7 Hz, 1H), 7.82 – 7.76 (m, 2H), 7.74 (d, *J* = 8.2 Hz, 2H), 3.86 – 3.71 (m, 1H), 1.74 – 1.60 (m, 4H), 1.56 (d, *J* = 9.3 Hz, 1H), 1.36 (ddd, *J* = 11.1, 9.6, 5.9 Hz, 1H), 1.17 – 1.02 (m, 6H), 0.89 (td, *J* = 11.9, 3.2 Hz, 2H); ^{13}C NMR (101 MHz, DMSO-D6) δ = 166.21, 136.77, 134.34, 126.66, 49.71, 42.91, 29.82, 29.51, 26.55, 26.28, 18.22.



[0094] (4-(((1*R*,2*R*)-2-((4-methylphenyl)sulfonamido)-1,2-diphenylethyl)carbamoyl)phenyl)boronic acid (6e): $[\alpha]_D^{25}$ = +55.5 (*c* = 0.8, MeOH); white solid, 67%. ^{1}H NMR (400 MHz, DMSO-D6) δ 8.74 (d, *J* = 9.1 Hz, 1H), 8.54 (d, *J* = 9.4 Hz, 1H), 8.25 – 8.18 (m, 1H), 7.87 – 7.80 (m, 1H), 7.76 – 7.69 (m, 1H), 7.25 (d, *J* = 8.0 Hz, 1H), 7.20 – 7.04 (m, 7H), 6.94 (dt, *J* = 13.4, 7.7 Hz, 4H), 6.84 – 6.82 (m, 2H), 6.76 (d, *J* = 6.3 Hz, 1H), 5.48 – 4.78 (m, 1H), 4.63 – 4.42 (m, 1H), 2.19 – 2.13 (m, 4H), 1.71 – 1.62 (m, 2H); ^{13}C NMR (101 MHz, DMSO-D6) δ = 166.55, 142.64, 142.15, 140.64, 139.85, 139.06, 138.85, 138.51, 138.22, 136.06, 134.64,

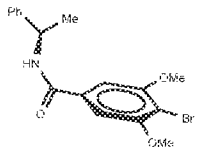
134.43, 129.39, 129.30, 128.35, 128.19, 128.10, 127.87, 127.69, 126.89, 126.71, 126.56, 126.49, 46.39, 46.35, 26.48, 26.40, 21.33. HRMS (ESI- TOF) *m/z* $[C_{28}H_{27}BN_2O_5S + H]^+$ calcd for 515.1812, found 515.1846.



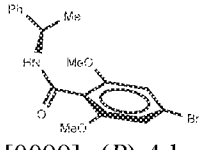
[0095] (4-(((1*S*)-(6-methoxyquinolin-4-yl)((2*R*,4*S*,5*R*)-5-vinylquinuclidin-2-yl)methyl)carbamoyl)phenyl)boronic acid (6f): $[\alpha]_D^{25}$ = -23.5 (*c* = 1.1, MeOH); pale orange solid, 47%. ^{1}H NMR (400 MHz, DMSO-D6) δ 9.07 (s, 1H), 8.75 (d, *J* = 4.5 Hz, 1H), 8.23 (s, 1H), 7.99 – 7.53 (m, 8H), 7.48 – 7.28 (m, 1H), 6.14 – 5.93 (m, 1H), 5.17 (dd, *J* = 22.7, 13.8 Hz, 1H), 4.34 (s, 1H), 3.88 (s, 3H), 3.63 – 3.08 (m, 6H), 2.69 (d, *J* = 15.8 Hz, 1H), 2.01 – 1.78 (m, 2H), 1.13 (d, *J* = 6.3 Hz, 1H); ^{13}C NMR (101 MHz, DMSO-D6) δ 168.05, 167.12, 158.21, 148.08, 144.69, 139.30, 135.05, 134.65, 134.33, 132.50, 131.92, 128.64, 127.25, 122.17, 120.79, 119.55, 117.11, 103.17, 59.13, 56.18, 53.92, 48.80, 42.10, 37.05, 26.68, 24.99, 24.01. HRMS (ESI- TOF) *m/z* $[C_{27}H_{30}BN_3O_4 + H]^+$ calcd for 472.2407, found 472.2405.

[0096] General procedure for 8a-8c

[0097] Different substituted benzoic acid (2 mmol) was introduced into a round bottom flask followed by PyBOP (4 mmol) and 50 ml DMF. The reaction mixture was stirred for 5 min and (*R*)-(+)-1-Phenylethylamine (4 mmol) was added. After 48 hours, the reaction mixture was diluted with EA (40 ml) and the organic layer was washed with water (3× 20 ml). The solvent was evaporated under reduced pressure and the residue was purified by flash chromatography (hexane/EA, 10/1 to 4/1) to afford pure product.

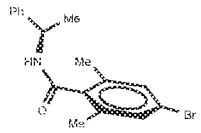


[0098] (*R*)-4-bromo-3,5-dimethoxy-*N*-(1-phenylethyl)benzamide (8a): $[\alpha]_D^{25}$ = -24.2 (*c* = 0.6, CH_2Cl_2); white solid, 80% yield. ^{1}H NMR (400 MHz, CHLOROFORM-D) δ 7.42 – 7.33 (m, 4H), 7.31 – 7.25 (m, 1H), 7.15 (d, *J* = 11.0 Hz, 2H), 6.94 (s, 2H), 6.43 (d, *J* = 7.6 Hz, 1H), 5.31 (p, *J* = 7.0 Hz, 1H), 3.90 (d, *J* = 7.8 Hz, 6H), 1.62 (d, *J* = 6.9 Hz, 3H); ^{13}C NMR (101 MHz, CHLOROFORM-D) δ 166.18, 157.20, 142.95, 135.03, 128.88, 127.67, 126.41, 104.77, 103.32, 56.75, 49.58, 21.66. HRMS (ESI- TOF) *m/z* $[C_{17}H_{18}BrNO_3 + H]^+$ calcd for 364.0548, found 364.0548.



[0099] (*R*)-4-bromo-2,6-dimethoxy-*N*-(1-phenylethyl)benzamide (8b): $[\alpha]_D^{25}$ = -25.2 (*c* = 0.7, CH_2Cl_2); white solid, 53% yield. ^{1}H NMR (400 MHz, CHLOROFORM-D) δ 7.40 – 7.22 (m, 5H), 6.91 (s, 2H), 6.53 (d, *J* = 7.2 Hz, 1H), 5.28 (p, *J* = 7.1 Hz, 1H), 3.86 (s, 6H), 1.59 (t, *J* = 7.4 Hz, 3H); ^{13}C NMR (101 MHz,

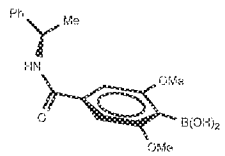
CHLOROFORM-D) δ 166.19, 157.19, 142.97, 135.02, 128.87, 127.66, 126.41, 104.75, 103.32, 56.73, 49.58, 21.66. HRMS (ESI- TOF) *m/z* $[C_{17}H_{18}BrNO_3+H]^+$ calcd for 364.0548, found 364.0555.



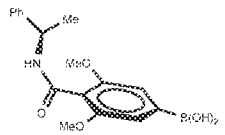
[0100] (*R*)-4-bromo-2,6-dimethyl-*N*-(1-phenylethyl)benzamide (8c): $[\alpha]_D^{25}$ = +3.0 (*c* = 1.1, CH_2Cl_2); white solid, 42% yield. ^{1}H NMR (400 MHz, CHLOROFORM-D) δ 7.33 – 7.20 (m, 5H), 7.05 (s, 2H), 6.60 (d, *J* = 8.3 Hz, 1H), 5.22 (dq, *J* = 14.0, 7.0 Hz, 1H), 2.09 (d, *J* = 6.1 Hz, 6H), 1.50 (d, *J* = 7.0 Hz, 3H); ^{13}C NMR (101 MHz, CHLOROFORM-D) δ 168.46, 143.14, 136.48, 136.31, 130.11, 128.64, 127.41, 126.46, 122.20, 48.78, 21.48, 18.82. HRMS (ESI- TOF) *m/z* $[C_{17}H_{18}BrNO+H]^+$ calcd for 332.065, found 332.066.

[0101] General procedure for 9a-9c

[0102] To a dried and argon-flushed round bottom flask with a stir bar, dissolved bromide substrate (8a-8c) (10 mmol) into anhydrous THF and stirred for 5 min at -78°C. Transferred 1.6 M *n*-butyllithium (25 mmol) solution dropwise with syringe, stirred at -78°C for 0.5 h. Then $B(OMe)_3$ (40 mmol) was added dropwise at -78°C; reaction mixture was warmed up to r.t. and stirred for 8 h. Added 1 M HCl (10 mmol) and stirred the reaction for 6 h. Monitored by TLC analysis and exacted with EA, dried for column directly (Hexane/EA = 5/1 to 1/1).

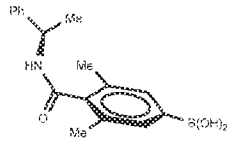


[0103] (*R*)-(2,6-dimethoxy-4-((1-phenylethyl)carbamoyl)phenyl)boronic acid (9a): $[\alpha]_D^{25}$ = -15.0 (*c* = 0.2, MeOH); white solid, 45% yield. ^{1}H NMR (400 MHz, CHLOROFORM-D) δ 7.42 – 7.33 (m, 4H), 7.31 – 7.25 (m, 1H), 7.15 (d, *J* = 11.0 Hz, 2H), 6.94 (s, 2H), 6.43 (d, *J* = 7.6 Hz, 1H), 5.31 (p, *J* = 7.0 Hz, 1H), 3.90 (d, *J* = 7.8 Hz, 6H), 1.62 (d, *J* = 6.9 Hz, 3H); ^{13}C NMR (101 MHz, CHLOROFORM-D) δ 166.02, 165.53, 165.52, 142.81, 139.29, 128.94, 128.93, 128.92, 127.75, 126.44, 126.43, 126.42, 103.06, 56.45, 56.44, 56.43, 56.42, 56.41, 49.62, 26.66, 21.62, 14.00. HRMS (ESI- TOF) *m/z* $[C_{17}H_{20}BNO_5+H]^+$ calcd for 330.1513, found 330.1523.



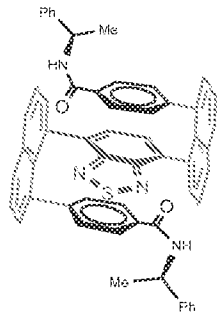
[0104] (*R*)-(3,5-dimethoxy-4-((1-phenylethyl)carbamoyl)phenyl)boronic acid (9b): $[\alpha]_D^{25}$ = -23.8 (*c* = 0.2, MeOH); white solid, 25% yield. ^{1}H NMR (400 MHz, CHLOROFORM-D) δ 7.45 – 7.28 (m, 5H), 7.27 – 7.23 (m, 2H), 6.91 (s, 1H), 6.64 (s, 1H), 6.02 (dd, *J* = 16.8, 8.2 Hz, 1H), 5.39 – 5.29 (m, 1H), 3.82 – 3.72 (m, 6H),

1.58 – 1.54 (m, 3H); ^{13}C NMR (101 MHz, DMSO-D6) δ 165.86, 161.93, 145.43, 136.58, 128.79, 127.12, 126.56, 103.25, 55.93, 48.89, 27.00, 25.61, 22.74, 14.45. HRMS (ESI- TOF) *m/z* [$C_{17}H_{20}BNO_5$+ H] $^+$ calcd for 330.1513, found 330.1516.

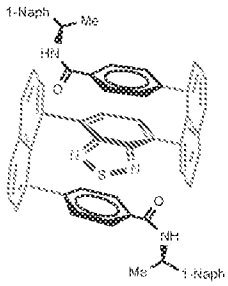


[0105] (*R*)-(3,5-dimethyl-4-((1-phenylethyl)carbamoyl)phenyl)boronic acid (9c): $[\alpha]_D^{25}$ = +24.6 (*c* = 1.0, MeOH); white solid, 21% yield. ^{1}H NMR (400 MHz, DMSO-D6) δ 8.62 (d, *J* = 7.4 Hz, 1H), 8.21 (s, 1H), 7.55 – 7.05 (m, 8H), 5.21 – 4.92 (m, 1H), 2.34 – 2.11 (m, 6H), 1.39 (dd, *J* = 21.5, 7.4 Hz, 3H); ^{13}C NMR (101 MHz, DMSO-D6) δ 166.34, 145.63, 138.98, 134.03, 128.72, 127.02, 126.54, 125.05, 48.78, 22.85, 22.43. HRMS (ESI- TOF) *m/z* [$C_{17}H_{20}BNO_3$+ H] $^+$ calcd for 298.1614, found 298.1624.

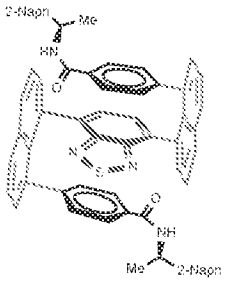
[0106] Data for 10a-10f



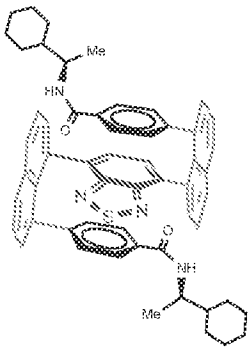
[0107] 4,4'-(benzo[*c*][1,2,5]thiadiazole-4,7-diylbis(naphthalene-8,1-diyl))bis(*N*-((*R*)-1-phenylethyl)benzamide) (10a): green yellow solid, 48% yield. ^{1}H NMR (400 MHz, CHLOROFORM-D) δ 7.95 (dddd, *J* = 32.8, 16.6, 8.2, 1.3 Hz, 4H), 7.60 (dt, *J* = 15.0, 7.5 Hz, 1H), 7.54 – 7.46 (m, 2H), 7.43 – 7.31 (m, 4H), 7.27 (dt, *J* = 3.8, 1.4 Hz, 2H), 7.24 – 7.08 (m, 12H), 7.01 (s, 1H), 6.88 (ddd, *J* = 23.6, 8.0, 1.7 Hz, 2H), 6.58 (ddd, *J* = 23.9, 8.0, 1.9 Hz, 2H), 6.44 (ddd, *J* = 8.1, 6.4, 1.8 Hz, 2H), 5.84 – 5.64 (m, 2H), 5.14 (dp, *J* = 32.6, 7.0 Hz, 2H), 1.48 (d, *J* = 6.9 Hz, 2H), 1.27 (d, *J* = 6.9 Hz, 4H); ^{13}C NMR (101 MHz, CHLOROFORM-D) δ 165.77, 165.46, 153.26, 153.24, 145.65, 145.16, 143.25, 142.65, 138.94, 135.84, 135.36, 134.87, 134.84, 134.82, 134.79, 131.35, 131.12, 130.79, 130.65, 130.29, 130.20, 130.18, 129.97, 129.80, 129.69, 129.66, 129.61, 129.39, 129.12, 128.61, 128.58, 127.22, 127.14, 126.78, 126.27, 126.13, 126.04, 125.63, 125.57, 125.32, 125.25, 125.07, 124.93, 122.82, 122.20, 49.17, 48.91, 21.73, 21.45. HRMS (ESI- TOF) *m/z* [$C_{56}H_{42}N_4O_2S$+ K] $^+$ calcd for 857.2816, found 875.2776.



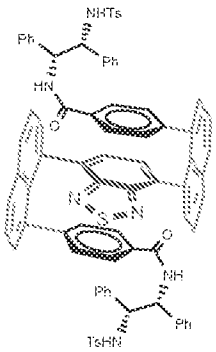
[0108] 4,4'-(benzo[*c*][1,2,5]thiadiazole-4,7-diylbis(naphthalene-8,1-diyl))bis(*N*-((*R*)-1-(naphthalen-1-yl)ethyl)benzamide) (10b): yellow solid, 16%. ^{1}H NMR (400 MHz, CHLOROFORM-D) δ 8.07 – 7.93 (m, 5H), 7.92 – 7.86 (m, 1H), 7.85 – 7.64 (m, 6H), 7.53 – 7.40 (m, 6H), 7.39 – 7.27 (m, 9H), 7.12 (d, *J* = 2.5 Hz, 2H), 7.11 – 6.82 (m, 4H), 6.66 – 6.36 (m, 4H), 6.01 – 5.72 (m, 4H), 1.65 (d, *J* = 5.7 Hz, 2H), 1.49 (d, *J* = 6.7 Hz, 4H); ^{13}C NMR (101 MHz, CHLOROFORM-D) δ = 165.78, 153.39, 145.38, 139.09, 138.44, 135.94, 135.07, 134.99, 134.00, 131.42, 131.08, 130.84, 130.46, 130.28, 129.91, 129.83, 129.77, 129.27, 128.87, 128.35, 126.95, 126.80, 126.55, 125.95, 125.90, 125.87, 125.55, 125.34, 125.22, 123.42, 123.38, 122.68, 122.41, 45.45, 20.97. HRMS (ESI- TOF) *m/z* [$C_{64}H_{46}N_4O_2S$+ Na] $^{+}$ calcd for 959.3390, found 959.3390.



[0109] 4,4'-(benzo[*c*][1,2,5]thiadiazole-4,7-diylbis(naphthalene-8,1-diyl))bis(*N*-((*R*)-1-(naphthalen-2-yl)ethyl)benzamide) (10c): yellow solid, 37%.^{1}H NMR (400 MHz, CHLOROFORM-D) δ 7.94 (d, *J* = 8.1 Hz, 2H), 7.80 – 7.68 (m, 5H), 7.66 – 7.56 (m, 5H), 7.55 – 7.41 (m, 6H), 7.40 – 7.35 (m, 3H), 7.35 – 7.30 (m, 2H), 7.29 – 7.25 (m, 1H), 7.24 – 7.02 (m, 6H), 6.91 – 6.83 (m, 2H), 6.65 – 6.41 (m, 4H), 5.84 (dd, *J* = 55.2, 7.3 Hz, 2H), 5.35 (p, *J* = 6.6 Hz, 1H), 5.26 (p, *J* = 7.0 Hz, 1H), 1.44 (dd, *J* = 69.7, 13.2 Hz, 6H); ^{13}C NMR (101 MHz, CHLOROFORM-D) δ = 165.66, 153.13, 145.45, 145.06, 140.41, 139.80, 138.74, 135.64, 134.66, 134.56, 133.08, 132.46, 132.41, 131.20, 130.48, 130.11, 129.93, 129.91, 129.59, 129.50, 129.46, 128.96, 128.22, 127.80, 127.66, 127.33, 127.25, 126.75, 125.92, 125.86, 125.59, 125.43, 125.12, 124.89, 124.63, 124.40, 124.38, 124.29, 122.11, 49.10, 29.48, 21.48. HRMS (ESI- TOF) *m/z* [$C_{64}H_{46}N_4O_2S$+ H] $^{+}$ calcd for 936.3492, found 936.3477.

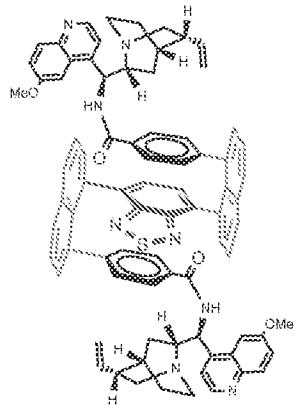


[0110] 4,4'-(benzo[*c*][1,2,5]thiadiazole-4,7-diylbis(naphthalene-8,1-diyl))bis(*N*-((*R*)-1-cyclohexylethyl)benzamide) (10d): yellow solid, 41%.^{1}H NMR (400 MHz, CHLOROFORM-D) δ 8.03 – 7.88 (m, 4H), 7.70 – 7.60 (m, 2H), 7.48 (t, *J* = 7.6 Hz, 2H), 7.39 – 7.27 (m, 4H), 7.14 (dt, *J* = 6.9, 4.9 Hz, 2H), 7.11 – 6.94 (m, 2H), 6.92 – 6.76 (m, 2H), 6.56 (ddd, *J* = 33.3, 8.0, 1.7 Hz, 2H), 6.46 – 6.38 (m, 2H), 5.49 (dd, *J* = 14.6, 6.8 Hz, 1H), 5.33 (d, *J* = 8.5 Hz, 1H), 3.94 – 3.80 (m, 2H), 1.59 (dd, *J* = 31.3, 21.6 Hz, 10H), 1.32 – 1.21 (m, 2H), 1.12 – 0.83 (m, 16H); ^{13}C NMR (101 MHz, CHLOROFORM-D) δ = 165.77, 153.24, 145.37, 144.98, 144.97, 138.97, 138.96, 135.75, 135.26, 134.88, 134.86, 131.80, 130.76, 130.60, 130.19, 129.66, 129.65, 129.51, 129.03, 127.35, 126.68, 125.67, 125.37, 125.02, 122.72, 121.93, 49.59, 43.00, 42.99, 29.05, 28.74, 26.30, 26.06, 26.04, 17.46. HRMS (ESI- TOF) *m/z* [$C_{56}H_{54}N_4O_2S$+ H] $^{+}$ calcd for 848.4118, found 848.4107.



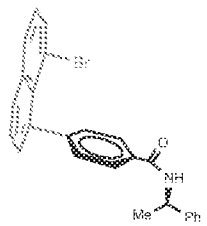
[0111] *N*-((1*R*,2*R*)-2-((4-methylphenyl)sulfonamido)-1,2-diphenylethyl)-4-(8-(7-(8-(4-(((1*R*,2*R*)-2-((4-methylphenyl)sulfonamido)-1,2-diphenylethyl)carbamoyl)phenyl)naphthalen-1-yl)benzo[*c*][1,2,5]thiadiazol-4-yl)naphthalen-1-yl)benzamide (10e): pale yellow solid, 31%.^{1}H NMR (400 MHz, CHLOROFORM-D) δ 7.97 – 7.74 (m, 4H), 7.43 (dd, *J* = 14.2, 7.2 Hz, 3H), 7.30 (t, *J* = 9.3 Hz, 5H), 7.12 (dd, *J* = 17.6, 6.8 Hz, 7H), 7.03 (d, *J* = 6.5 Hz, 4H), 6.95 (dd, *J* = 12.6, 6.8 Hz, 4H), 6.92 – 6.77 (m, 11H), 6.71 (t, *J* = 7.3 Hz, 3H), 6.61 (d, *J* = 7.9 Hz, 1H), 6.50 (d, *J* = 7.5 Hz, 1H), 6.34 (d, *J* = 7.9 Hz, 1H), 5.85 (t, *J* = 32.8 Hz, 2H), 5.16 (dd, *J* = 9.8, 6.7 Hz, 1H), 5.08 (dd, *J* = 13.6, 6.8 Hz, 1H), 4.49 (t, *J* = 9.2 Hz, 1H), 4.38 (t, *J* = 9.2 Hz, 1H), 2.21 (d, *J* = 10.6 Hz, 6H), 1.58 (s, 6H); ^{13}C NMR (126 MHz, cdcl$_3$) δ = 167.24, 166.90, 153.21, 153.06, 146.05, 142.91, 142.84, 139.22, 139.08, 138.09, 137.58, 137.42, 137.20, 135.81, 135.41, 134.93, 134.77, 134.70, 130.76, 130.52, 130.42, 130.15, 129.93, 129.80, 129.63, 129.16, 128.47, 128.39, 128.16, 128.00, 127.58, 127.33,

126.79, 126.48, 126.14, 125.84, 125.48, 125.03, 122.91, 72.53, 70.49, 69.92, 66.73, 63.71, 63.09, 61.84, 59.05, 31.93, 29.71, 22.70, 21.38, 15.09, 14.14. HRMS (ESI- TOF) *m/z* $[C_{82}H_{64}N_6O_6S_3+ H]^+$ calcd for 1326.4200, found 1326.4237.



[0112] 4,4'-(benzo[*c*][1,2,5]thiadiazole-4,7-diylbis(naphthalene-8,1-diyl))bis(*N*-((1*S*)-(6-methoxyquinolin-4-yl)((2*R*,4*S*,5*R*)-5-vinylquinuclidin-2-yl)methyl)benzamide) (10f): green yellow solid, 20% yield. ^{1}H NMR (400 MHz, DMSO-D6) δ 8.72 – 8.65 (m, 2H), 8.30 (s, 2H), 8.09 – 7.68 (m, 9H), 7.60 (d, *J* = 4.6 Hz, 2H), 7.56 – 7.24 (m, 8H), 7.08 – 6.85 (m, 4H), 6.83 – 6.70 (m, 6H), 6.50 – 6.37 (m, 1H), 6.28 (dd, *J* = 8.0, 1.5 Hz, 2H), 6.15 (dd, *J* = 8.0, 1.6 Hz, 1H), 5.77 (dt, *J* = 17.3, 7.7 Hz, 3H), 5.02 – 4.82 (m, 5H), 3.94 (d, *J* = 21.6 Hz, 6H), 3.06 – 2.96 (m, 2H), 2.61 (t, *J* = 21.8 Hz, 3H), 2.36 – 2.22 (m, 2H), 2.21 – 2.09 (m, 2H), 1.57 – 1.15 (m, 11H); ^{13}C NMR (101 MHz, CHLOROFORM-D) δ 214.17, 170.49, 170.00, 169.40, 161.05, 160.84, 156.39, 156.30, 151.26, 150.94, 149.15, 148.63, 147.94, 144.08, 142.35, 142.03, 139.04, 138.37, 138.28, 137.95, 137.84, 137.69, 136.95, 135.11, 134.98, 134.93, 134.17, 133.98, 133.92, 133.47, 133.37, 133.06, 132.62, 132.39, 132.19, 131.72, 130.58, 130.45, 130.02, 128.97, 128.54, 128.33, 128.23, 128.09, 126.50, 126.16, 124.79, 124.38, 118.26, 118.01, 105.36, 105.04, 72.73, 59.20, 58.89, 58.87, 58.79, 56.98, 44.17, 43.76, 43.29, 42.54, 42.45, 35.14, 34.98, 32.92, 32.58, 32.47, 30.92, 30.48, 30.42, 29.00, 25.92, 17.36, 4.24. HRMS (ESI- TOF) *m/z* $[C_{80}H_{70}N_8O_4S+ H]^+$ calcd for 1240.5392, found 1240.5392.

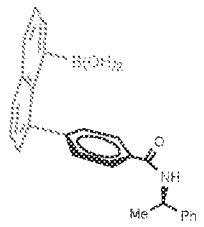
[0113] Data for 11



[0114] (*R*)-4-(8-bromonaphthalen-1-yl)-*N*-(1-phenylethyl)benzamide (11): white solid, 49% yield. ^{1}H NMR (400 MHz, CHLOROFORM-D) δ 7.89 (dt, *J* = 8.2, 1.5 Hz, 2H), 7.83 – 7.73 (m, 3H), 7.52 – 7.47 (m, 1H), 7.45 – 7.34 (m, 7H), 7.33 – 7.26 (m, 2H), 6.38 (d, *J* = 7.3 Hz, 1H), 5.38 (p, *J* = 7.0 Hz, 1H), 1.63 (t, *J* = 5.9 Hz, 3H); ^{13}C NMR (101 MHz, CHLOROFORM-D) δ 166.63, 146.50, 143.33, 139.38, 136.15, 133.92,

133.10, 131.23, 130.43, 130.41, 129.48, 129.43, 129.06, 128.86, 127.55, 126.46, 126.37, 126.26, 126.18, 125.40, 120.05, 49.38, 21.87. HRMS (ESI- TOF) *m/z* [$C_{25}H_{20}BrNO$+ H] $^+$ calcd for 430.0806, found 430.0825.

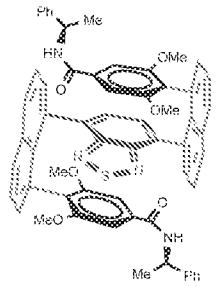
[0115] Synthesis for 12



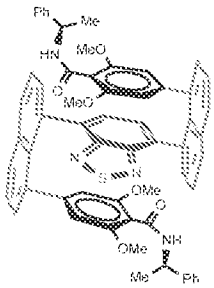
[0116] Synthesis of (*R*)-(8-(4-((1-phenylethyl)carbamoyl)phenyl)naphthalen-1-yl)boronic acid (12)

[0117] To a dried and argon-flushed round bottom flask with a stir bar, dissolved bromide substrate 11 (10 mmol) into anhydrous THF and stirred for 5 min at -78°C. Transferred 1.6 M *n*-butyllithium (25 mmol) solution dropwise with syringe, stir at -78°C for 0.5 h. $B(OMe)_3$ (40 mmol) was added dropwise at -78°C; reaction mixture was warmed up to r.t. and stirred for 8 h. Added 1 M HCl (10 mmol) and stirred the reaction for 6 h. Monitored by TLC analysis and exacted with EA. The organic phase was combined, dried with $MgSO_4$, and the solvent was evaporated under reduced pressure. The crude product was used without further purification.

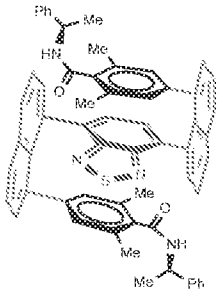
[0118] Data for 13a-13c



[0119] 4,4'-(benzo[*c*][1,2,5]thiadiazole-4,7-diylbis(naphthalene-8,1-diyl))bis(3,5-dimethoxy-*N*-((*R*)-1-phenylethyl)benzamide) (13a): bright yellow solid, 70% yield. ^{1}H NMR (400 MHz, CHLOROFORM-D) δ 8.01 – 7.87 (m, 4H), 7.57 – 7.47 (m, 3H), 7.43 – 7.36 (m, 1H), 7.31 – 7.19 (m, 12H), 7.07 (d, *J* = 7.0 Hz, 2H), 6.93 (d, *J* = 28.2 Hz, 2H), 6.56 (dd, *J* = 18.8, 0.8 Hz, 2H), 5.82 (dd, *J* = 54.8, 22.4 Hz, 4H), 5.17 (qd, *J* = 13.6, 6.8 Hz, 2H), 3.62 – 3.50 (m, 6H), 3.35 – 3.15 (m, 6H), 1.52 (t, *J* = 6.6 Hz, 2H), 1.37 (d, *J* = 6.9 Hz, 4H); ^{13}C NMR (101 MHz, DMSO-D6) δ 164.97, 164.89, 156.54, 156.44, 156.32, 156.31, 153.58, 153.57, 145.24, 135.89, 135.76, 134.86, 134.81, 134.03, 133.95, 133.47, 133.08, 131.91, 131.89, 131.39, 131.37, 131.10, 130.35, 130.24, 129.53, 128.96, 128.74, 127.10, 127.07, 126.69, 126.63, 125.65, 122.75, 122.48, 55.86, 55.61, 55.13, 54.94, 48.87, 48.81, 22.64, 22.60. HRMS (ESI- TOF) *m/z* [$C_{60}H_{50}N_4O_6S$+ H] $^+$ calcd for 956.3602, found 956.3585.



[0120] 4,4'-(benzo[*c*][1,2,5]thiadiazole-4,7-diylbis(naphthalene-8,1-diyl))bis(2,6-dimethoxy-*N*-((*R*)-1-phenylethyl)benzamide) (13b): bright yellow solid, 70% yield. ^{1}H NMR (400 MHz, CHLOROFORM-D) δ 8.02 – 7.88 (m, 3H), 7.83 (dt, *J* = 13.8, 6.9 Hz, 1H), 7.71 (dd, *J* = 7.0, 1.3 Hz, 1H), 7.61 – 7.53 (m, 2H), 7.53 – 7.44 (m, 2H), 7.32 – 7.24 (m, 5H), 7.23 – 7.13 (m, 8H), 7.04 (d, *J* = 14.4 Hz, 2H), 6.07 – 5.85 (m, 2H), 5.66 – 5.56 (m, 3H), 5.50 (d, *J* = 8.0 Hz, 1H), 5.24 – 5.07 (m, 2H), 3.67 – 3.53 (m, 6H), 3.37 – 3.23 (m, 6H), 1.34 (d, *J* = 6.9 Hz, 2H), 1.27 (d, *J* = 7.0 Hz, 4H); ^{13}C NMR (101 MHz, CHLOROFORM-D) δ 164.52, 164.39, 155.62, 155.40, 155.15, 154.82, 153.90, 153.65, 145.45, 144.91, 143.53, 143.36, 139.85, 139.77, 135.80, 135.31, 135.26, 134.96, 134.93, 134.87, 130.82, 130.78, 130.64, 130.43, 130.31, 129.87, 129.70, 129.58, 129.54, 129.01, 128.96, 128.45, 128.29, 126.97, 126.92, 126.43, 126.37, 126.01, 125.84, 125.12, 125.09, 113.16, 112.97, 106.60, 106.24, 105.73, 104.69, 55.85, 55.56, 55.43, 55.32, 49.09, 48.87, 29.79, 21.91, 14.22. HRMS (ESI- TOF) *m/z* $[C_{60}H_{50}N_4O_6S+H]^+$ calcd for 956.3602, found 956.3585.

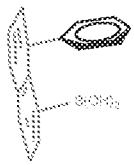


[0121] 4,4'-(benzo[*c*][1,2,5]thiadiazole-4,7-diylbis(naphthalene-8,1-diyl))bis(2,6-dimethyl-*N*-((*R*)-1-phenylethyl)benzamide) (13c): bright yellow solid, 23% yield. ^{1}H NMR (400 MHz, DMSO-D6) δ 8.20 (ddd, *J* = 31.9, 17.2, 10.9 Hz, 2H), 8.11 – 7.95 (m, 4H), 7.84 – 7.66 (m, 2H), 7.61 – 7.43 (m, 4H), 7.39 – 7.07 (m, 11H), 7.06 – 6.72 (m, 4H), 6.48 (ddd, *J* = 45.0, 29.6, 14.3 Hz, 2H), 6.02 – 5.68 (m, 1H), 5.10 (qd, *J* = 15.2, 8.0 Hz, 2H), 2.02 – 1.89 (m, 2H), 1.83 – 1.69 (m, 3H), 1.51 (d, *J* = 14.5 Hz, 1H), 1.40 – 1.04 (m, 12H); ^{13}C NMR (101 MHz, DMSO-D6) δ 168.79, 168.67, 168.43, 168.40, 154.03, 145.56, 145.50, 142.62, 142.55, 140.51, 140.44, 140.37, 140.35, 138.56, 138.28, 136.39, 136.33, 135.82, 135.36, 135.27, 135.20, 133.16, 132.69, 132.55, 132.35, 130.79, 130.25, 129.87, 129.64, 129.48, 129.41, 129.30, 129.17, 129.11, 129.06, 129.03, 127.60, 127.48, 127.18, 127.12, 127.05, 126.75, 126.27, 126.22, 125.79, 125.50, 48.90, 48.65, 42.22, 32.36, 32.02, 23.10, 22.82, 19.68, 19.57, 19.16, 19.01, 14.85. HRMS (ESI- TOF) *m/z* $[C_{60}H_{50}N_4O_2S+Na]^+$ calcd for 915.3714, found 915.3703.



[0122] Synthesis of 4,9-dibromonaphtho[2,3-*c*][1,2,5]thiadiazole (14)

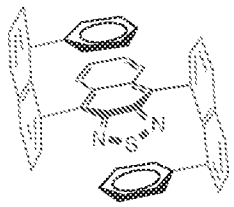
[0123] 14 was synthesized from 2,3-Diaminonaphthalene following the reported procedure [2] with very minor modification. ^{1}H NMR (400 MHz, CHLOROFORM-D) δ 8.45 – 8.38 (m, 2H), 7.63 – 7.56 (m, 2H).



[0124] Synthesis of (8-phenylnaphthalen-1-yl)boronic acid (15)

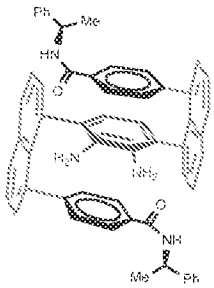
[0125] To a dried and argon-flushed round bottom flask with a stir bar, dissolved 1-bromo-8-phenylnaphthalene (10 mmol) into anhydrous THF and stirred for 5 min at -78°C. Transferred 1.6 M *n*-butyllithium (25 mmol) solution dropwise with syringe, stirred at -78°C for 0.5 h. $B(OMe)_3$ (40 mmol) was added dropwise at -78°C; reaction mixture was warmed up to r.t. and stirred for 8 h. Added 1 M HCl (10 mmol) and stirred the reaction for 6 h. Monitored by TLC analysis and exacted with EA. The organic phase was combined, dried with $MgSO_4$, and the solvent was evaporated under reduced pressure. The crude product was used without further purification.

[0126] Data for 16



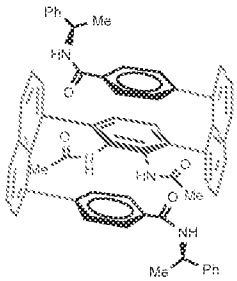
[0127] 4,9-bis(8-phenylnaphthalen-1-yl)naphtho[2,3-*c*][1,2,5]thiadiazole (16) : orange red solid, 70% yield. ^{1}H NMR (400 MHz, CHLOROFORM-D) δ 8.13 (dd, *J* = 8.3, 1.3 Hz, 2H), 8.02 (dd, *J* = 8.2, 1.3 Hz, 2H), 7.75 (dd, *J* = 8.2, 7.0 Hz, 2H), 7.54 – 7.46 (m, 2H), 7.38 (dd, *J* = 7.0, 1.4 Hz, 2H), 7.33 – 7.26 (m, 2H), 7.15 – 7.04 (m, 4H), 6.56 (tt, *J* = 7.4, 1.3 Hz, 2H), 6.38 – 6.30 (m, 2H), 6.25 – 6.13 (m, 4H), 6.09 (td, *J* = 7.4, 0.9 Hz, 2H); ^{13}C NMR (101 MHz, CHLOROFORM-D) δ 151.12, 141.96, 140.31, 135.05, 134.08, 132.47, 131.28, 130.61, 130.39, 130.02, 129.84, 128.96, 128.05, 127.12, 127.08, 125.67, 125.31, 125.27, 125.18, 124.41. HRMS (ESI- TOF) *m/z* $[C_{42}H_{26}N_2S+H]^+$ calcd for 591.1895, found 591.1932.

[0128] Data for 17

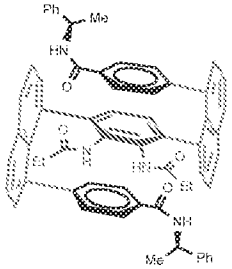


[0129] 4,4'-((2,3-diamino-1,4-phenylene)bis(naphthalene-8,1-diyl))bis(*N*-((*R*)-1-phenylethyl)benzamide) (17): green solid, 47% yield. ^{1}H NMR (400 MHz, CHLOROFORM-D) δ 7.87 (ddd, *J* = 30.8, 16.7, 10.6 Hz, 5H), 7.46 (dd, *J* = 14.1, 6.9 Hz, 4H), 7.41 – 7.29 (m, 6H), 7.28 – 7.16 (m, 7H), 7.15 – 7.04 (m, 9H), 7.02 (s, 1H), 6.90 – 6.79 (m, 2H), 6.50 – 6.27 (m, 2H), 6.17 – 5.95 (m, 2H), 5.27 – 5.04 (m, 2H), 1.53 (d, *J* = 6.8 Hz, 4H), 1.29 (d, *J* = 6.9 Hz, 2H); ^{13}C NMR (101 MHz, CHLOROFORM-D) δ 167.15, 166.94, 145.56, 145.45, 143.63, 139.63, 139.56, 135.20, 135.15, 132.13, 130.33, 128.85, 128.75, 128.59, 127.52, 127.39, 126.46, 126.26, 126.12, 125.04, 125.01, 124.25, 49.16, 21.96. HRMS (ESI- TOF) *m/z* [$C_{56}H_{46}N_4O_2$+ H] $^{+}$ calcd for 808.3772, found 808.3779.

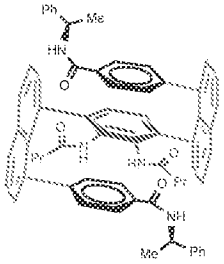
[0130] Data 18a-18f



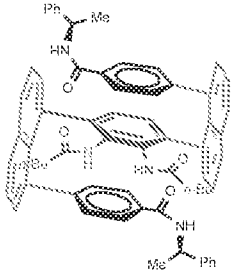
[0131] 4,4'-((2,3-diacetamido-1,4-phenylene)bis(naphthalene-8,1-diyl))bis(*N*-((*R*)-1-phenylethyl)benzamide) (18a): brown yellow solid, 56% yield. ^{1}H NMR (400 MHz, CHLOROFORM-D) δ 7.92 (d, *J* = 8.3 Hz, 4H), 7.65 (d, *J* = 7.5 Hz, 2H), 7.54 – 7.43 (m, 6H), 7.39 (dd, *J* = 10.3, 8.8 Hz, 6H), 7.28 (dd, *J* = 14.4, 6.6 Hz, 6H), 7.20 (t, *J* = 7.0 Hz, 2H), 7.12 – 6.97 (m, 4H), 6.85 (d, *J* = 7.8 Hz, 2H), 6.70 (s, 2H), 6.34 (s, 2H), 5.31 (p, *J* = 7.1 Hz, 2H), 1.80 (s, 6H), 1.56 (d, *J* = 7.0 Hz, 6H); ^{13}C NMR (101 MHz, CHLOROFORM-D) δ 169.44, 167.30, 145.67, 144.07, 139.44, 139.02, 135.48, 135.20, 132.69, 130.90, 130.62, 130.13, 130.11, 129.63, 129.43, 129.14, 129.00, 128.49, 128.48, 127.39, 127.33, 127.02, 126.84, 126.28, 125.38, 125.20, 100.00, 49.19, 29.72, 23.26, 22.35. HRMS (ESI- TOF) *m/z* [$C_{60}H_{50}N_4O_4$+ H] $^{+}$ calcd for 892.3983, found 892.3966.



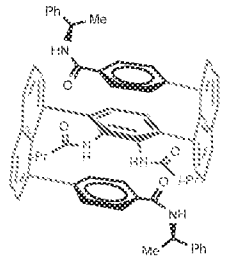
[0132] 4,4'-((2,3-dipropionamido-1,4-phenylene)bis(naphthalene-8,1-diyl))bis(*N*-((*R*)-1-phenylethyl)benzamide) (18b): gray yellow solid, 39% yield. ^{1}H NMR (400 MHz, CHLOROFORM-D) δ 7.95 – 7.71 (m, 4H), 7.58 – 7.27 (m, 17H), 7.24 – 7.16 (m, 4H), 7.11 – 7.04 (m, 2H), 7.00 – 6.86 (m, 5H), 6.79 (d, *J* = 19.6 Hz, 2H), 6.45 – 6.31 (m, 2H), 5.30 (dt, *J* = 13.6, 6.7 Hz, 2H), 2.00 – 1.78 (m, 4H), 1.49 (dd, *J* = 25.3, 18.6 Hz, 6H), 0.84 – 0.69 (m, 6H); ^{13}C NMR (101 MHz, CHLOROFORM-D) δ 172.55, 167.61, 167.26, 145.54, 145.43, 144.10, 143.76, 139.26, 139.17, 138.98, 135.46, 135.27, 135.09, 135.00, 132.78, 132.62, 131.63, 131.27, 131.06, 131.02, 130.66, 129.90, 129.86, 129.82, 129.76, 129.64, 129.45, 129.09, 129.03, 128.89, 128.81, 128.62, 128.43, 127.50, 127.11, 126.97, 126.95, 126.88, 126.64, 126.20, 125.62, 125.47, 125.12, 125.03, 49.47, 49.08, 29.77, 29.72, 22.51, 22.24, 9.77, 9.71. HRMS (ESI- TOF) *m/z* $[C_{62}H_{54}N_4O_4+H]^+$ calcd for 920.4296, found 920.4274.



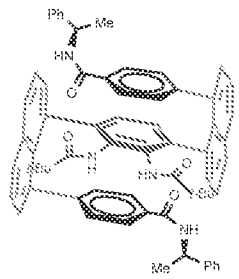
[0133] 4,4'-((2,3-dibutyramido-1,4-phenylene)bis(naphthalene-8,1-diyl))bis(*N*-((*R*)-1-phenylethyl)benzamide) (18c): light yellow solid, 42%. ^{1}H NMR (400 MHz, CHLOROFORM-D) δ 8.07 – 7.72 (m, 4H), 7.58 – 6.82 (m, 30H), 6.52 – 6.32 (m, 2H), 5.40 – 5.13 (m, 2H), 1.90 – 1.67 (m, 5H), 1.55 – 1.45 (m, 5H), 1.32 – 0.91 (m, 5H), 0.66 (dt, *J* = 10.3, 8.4 Hz, 5H); ^{13}C NMR (101 MHz, CHLOROFORM-D) δ = 171.43, 167.15, 145.22, 143.94, 139.07, 138.82, 135.36, 134.95, 132.44, 131.32, 130.59, 129.92, 129.73, 129.63, 129.21, 128.99, 128.94, 128.48, 128.29, 127.40, 126.88, 126.82, 126.58, 126.51, 126.08, 125.38, 124.94, 48.97, 38.46, 22.08, 18.75, 13.41. HRMS (ESI- TOF) *m/z* $[C_{64}H_{58}N_4O_4+H]^+$ calcd for 948.4609, found 948.4581.



[0134] 4,4'-((2,3-dipentanamido-1,4-phenylene)bis(naphthalene-8,1-diyl))bis(*N*-((*R*)-1-phenylethyl)benzamide) (18d): gray yellow solid, 47% yield. ^{1}H NMR (400 MHz, CHLOROFORM-D) δ 7.95 – 7.72 (m, 4H), 7.56 – 7.27 (m, 17H), 7.20 (ddd, *J* = 14.2, 7.8, 5.0 Hz, 5H), 7.09 – 6.80 (m, 8H), 6.42 (d, *J* = 23.1 Hz, 2H), 5.34 – 5.20 (m, 2H), 1.92 – 1.77 (m, 4H), 1.50 (t, *J* = 7.8 Hz, 6H), 1.18 – 0.95 (m, 8H), 0.78 – 0.68 (m, 6H); ^{13}C NMR (101 MHz, CHLOROFORM-D) δ 176.66, 171.73, 167.55, 167.19, 145.34, 145.27, 143.96, 143.65, 139.13, 138.99, 138.84, 135.39, 135.20, 134.96, 134.87, 132.58, 132.38, 131.30, 131.12, 130.60, 129.92, 129.79, 129.73, 129.68, 129.58, 129.27, 129.24, 128.97, 128.83, 128.71, 128.52, 128.50, 128.33, 128.31, 128.29, 127.55, 127.45, 126.99, 126.91, 126.84, 126.62, 126.53, 126.09, 125.54, 125.39, 124.97, 124.89, 49.39, 49.00, 36.35, 33.53, 29.61, 27.53, 27.46, 26.80, 22.35, 22.14, 22.03, 22.00, 21.97, 13.64, 13.63, 13.58. HRMS (ESI- TOF) *m/z* [$C_{66}H_{62}N_4O_4$+ H] $^+$ calcd for 976.4922, found 976.4926.



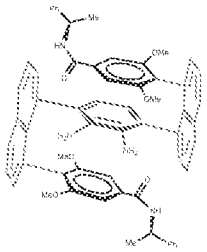
[0135] 4,4'-((2,3-diisobutyramido-1,4-phenylene)bis(naphthalene-8,1-diyl))bis(*N*-((*R*)-1-phenylethyl)benzamide) (18e): $[\alpha]_D^{25}$ = +92.0 (*c* = 1.0, CH_2Cl_2); pale brown solid, 38% yield. ^{1}H NMR (400 MHz, CHLOROFORM-D) δ 7.90 (dd, *J* = 14.2, 7.4 Hz, 3H), 7.79 – 7.73 (m, 1H), 7.55 – 7.26 (m, 18H), 7.19 (ddd, *J* = 10.6, 9.9, 4.9 Hz, 4H), 7.09 – 6.86 (m, 8H), 6.56 – 6.48 (m, 2H), 5.34 – 5.22 (m, 2H), 1.97 (ddt, *J* = 20.4, 13.8, 6.8 Hz, 2H), 1.49 (dd, J = 11.1, 6.9 Hz, 6H), 0.72 (dd, *J* = 9.3, 6.9 Hz, 6H), 0.66 – 0.58 (m, 6H); ^{13}C NMR (101 MHz, CHLOROFORM-D) δ 174.94, 174.79, 167.63, 167.30, 145.19, 145.14, 144.11, 143.76, 139.13, 138.95, 138.92, 138.89, 135.47, 135.28, 134.98, 134.88, 132.80, 132.61, 131.75, 131.62, 130.80, 130.78, 130.47, 130.38, 129.60, 129.55, 129.53, 129.36, 129.24, 129.17, 129.12, 129.08, 129.00, 128.84, 128.64, 128.43, 127.68, 127.54, 127.17, 127.08, 127.03, 126.94, 126.59, 126.35, 126.16, 125.77, 125.63, 125.07, 124.97, 49.46, 49.12, 35.73, 35.69, 30.31, 29.70, 22.47, 22.24, 19.39, 18.94. HRMS (ESI- TOF) *m/z* [$C_{64}H_{58}N_4O_4$+ H] $^+$ calcd for 948.4609, found 948.4583.



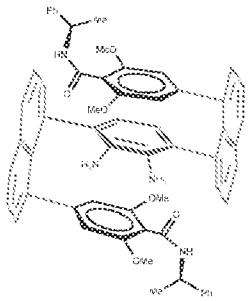
[0136] 4,4'-((2,3-dipivalamido-1,4-phenylene)bis(naphthalene-8,1-diyl))bis(*N*-((*R*)-1-phenylethyl)benzamide) (18f): $[\alpha]_D^{25}$ = +57.7 (*c* = 0.3, CH_2Cl_2); pale gray solid, 31% yield. ^{1}H NMR (400

MHz, CHLOROFORM-D) δ 7.89 (dd, *J* = 13.8, 7.3 Hz, 3H), 7.78 – 7.71 (m, 1H), 7.54 – 7.25 (m, 19H), 7.24 – 7.06 (m, 8H), 6.99 – 6.96 (m, 1H), 6.86 – 6.78 (m, 2H), 6.69 (d, *J* = 18.7 Hz, 2H), 5.35 – 5.25 (m, 2H), 1.51 (t, *J* = 6.4 Hz, 6H), 0.62 (d, *J* = 3.1 Hz, 18H); ^{13}C NMR (101 MHz, CHLOROFORM-D) δ 175.67, 175.55, 167.48, 144.66, 144.14, 143.76, 139.08, 138.93, 138.90, 134.81, 134.73, 132.03, 131.94, 131.15, 131.02, 130.78, 130.74, 129.42, 129.15, 129.03, 128.99, 128.94, 128.85, 128.64, 128.43, 127.60, 127.34, 127.06, 126.92, 126.51, 126.09, 125.87, 124.99, 124.89, 100.00, 49.37, 49.12, 38.74, 27.06, 22.36, 22.26. HRMS (ESI- TOF) *m/z* $[C_{66}H_{62}N_4O_4+H]^+$ calcd for 976.4922, found 976.4927.

[0137] Data for 19a-19c

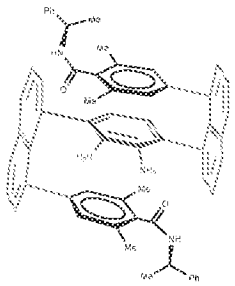


[0138] 4,4'-((2,3-diamino-1,4-phenylene)bis(naphthalene-8,1-diyl))bis(3,5-dimethoxy-*N*-((*R*)-1-phenylethyl)benzamide) (19a): light yellow solid, 84% yield. ^{1}H NMR (400 MHz, CHLOROFORM-D) δ 8.00 – 7.89 (m, 4H), 7.60 – 7.44 (m, 4H), 7.30 – 7.26 (m, 5H), 7.16 – 7.08 (m, 4H), 7.06 – 6.99 (m, 1H), 6.84 – 6.66 (m, 4H), 6.62 (d, *J* = 10.2 Hz, 2H), 6.50 (dd, *J* = 25.9, 9.3 Hz, 3H), 6.09 (dd, *J* = 19.5, 10.6 Hz, 2H), 5.25 – 4.79 (m, 2H), 3.56 – 3.40 (m, 12H), 1.57 (d, *J* = 6.7 Hz, 2H), 1.26 – 1.16 (m, 4H); ^{13}C NMR (101 MHz, CHLOROFORM-D) δ = 168.03, 157.01, 156.82, 143.58, 136.52, 135.52, 134.92, 131.41, 131.16, 130.78, 130.38, 130.27, 130.20, 129.35, 129.15, 129.01, 128.95, 128.56, 128.28, 127.14, 126.63, 126.17, 125.21, 125.11, 123.14, 120.66, 101.87, 101.81, 55.86, 54.97, 49.91, 49.17, 21.49. HRMS (ESI- TOF) *m/z* $[C_{60}H_{54}N_4O_6+H]^+$ calcd for 928.4194, found 928.4195.



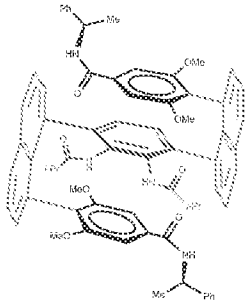
[0139] 4,4'-((2,3-diamino-1,4-phenylene)bis(naphthalene-8,1-diyl))bis(2,6-dimethoxy-*N*-((*R*)-1-phenylethyl)benzamide) (19b): pale solid, 72% yield. ^{1}H NMR (400 MHz, CHLOROFORM-D) δ 7.96 – 7.81 (m, 4H), 7.59 – 7.27 (m, 13H), 7.23 – 7.18 (m, 5H), 7.15 (dd, *J* = 7.0, 1.1 Hz, 1H), 7.08 – 7.02 (m, 2H), 6.00 (d, *J* = 9.7 Hz, 1H), 5.97 – 5.88 (m, 3H), 5.82 – 5.72 (m, 1H), 5.35 – 5.20 (m, 2H), 3.60 – 3.40 (m, 12H), 2.65 (s, 4H), 1.61 (d, *J* = 5.0 Hz, 2H), 1.48 (d, *J* = 6.9 Hz, 4H); ^{13}C NMR (101 MHz, CHLOROFORM-D) δ 165.25, 155.17, 154.87, 144.84, 143.39, 140.31, 136.25, 135.02, 131.96, 131.00, 130.10, 130.05, 129.95,

128.72, 128.64, 128.38, 128.26, 128.18, 128.16, 128.13, 127.07, 127.00, 126.90, 126.54, 125.35, 124.88, 122.91, 122.79, 114.32, 114.22, 106.28, 106.12, 104.70, 104.43, 100.00, 56.43, 54.95, 48.84, 29.67, 21.43, 14.11. HRMS (ESI- TOF) *m/z* $[C_{60}H_{54}N_4O_6+ H]^+$ calcd for 928.4194, found 928.4192.



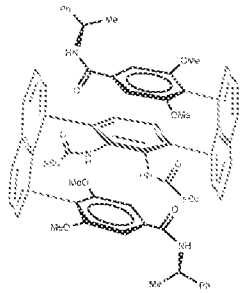
[0140] 4,4'-((2,3-diamino-1,4-phenylene)bis(naphthalene-8,1-diyl))bis(2,6-dimethyl-*N*-((*R*)-1-phenylethyl)benzamide) (19c): green yellow solid, 67% yield. ^{1}H NMR (400 MHz, CHLOROFORM-D) δ 7.98 – 7.81 (m, 4H), 7.70 – 7.28 (m, 9H), 7.21 – 6.90 (m, 9H), 6.67 – 5.82 (m, 8H), 5.31 – 5.07 (m, 2H), 2.75 – 2.40 (m, 4H), 2.39 – 1.86 (m, 12H), 1.66 – 1.45 (m, 6H); ^{13}C NMR (101 MHz, CHLOROFORM-D) δ = 169.46, 169.34, 169.31, 142.59, 142.48, 140.24, 140.12, 137.53, 137.08, 136.94, 136.84, 136.54, 135.66, 135.19, 135.15, 134.93, 134.74, 134.60, 131.77, 131.45, 130.79, 130.36, 130.17, 129.84, 129.35, 128.69, 128.51, 128.44, 128.38, 128.34, 128.22, 127.55, 127.31, 126.49, 126.44, 126.31, 126.23, 125.68, 125.57, 125.46, 125.01, 124.74, 122.27, 122.00, 121.93, 113.22, 49.10, 33.40, 31.99, 31.92, 30.23, 29.64, 22.44, 22.39, 20.74, 19.29, 19.17, 19.11, 13.98, 13.93. HRMS (ESI- TOF) *m/z* $[C_{60}H_{54}N_4O_2+ H]^+$ calcd for 864.4398, found 864.4378.

[0141] Data for 20a-20d

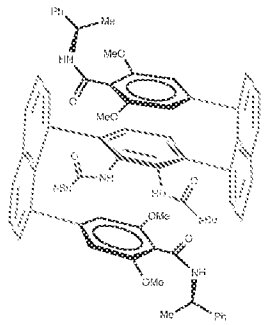


[0142] 4,4'-((2,3-diisobutyramido-1,4-phenylene)bis(naphthalene-8,1-diyl))bis(3,5-dimethoxy-*N*-((*R*)-1-phenylethyl)benzamide) (20a): $[\alpha]_D^{25}$ = +3.9 (*c* = 0.9, CH_2Cl_2); yellow solid, 97% yield. ^{1}H NMR (400 MHz, CHLOROFORM-D) δ 8.00 – 7.62 (m, 6H), 7.52 – 7.30 (m, 12H), 7.26 – 7.23 (m, 1H), 7.21 (d, *J* = 6.2 Hz, 1H), 7.12 (dd, *J* = 21.4, 6.3 Hz, 2H), 6.95 – 6.55 (m, 9H), 5.42 – 5.30 (m, 2H), 3.64 – 3.46 (m, 12H), 2.55 (hept, *J* = 7.0 Hz, 1H), 2.06 – 1.87 (m, 2H), 1.58 (dd, *J* = 23.5, 6.9 Hz, 6H), 0.80 – 0.55 (m, 12H); ^{13}C NMR (101 MHz, CHLOROFORM-D) δ = ^{13}C NMR (101 MHz, CHLOROFORM-D) δ = 175.39, 175.15, 168.25, 168.20, 156.74, 156.65, 156.01, 155.55, 144.54, 143.79, 140.56, 139.93, 136.36, 135.98, 135.23, 135.19, 134.52, 134.42, 132.17, 131.83, 131.25, 131.13, 130.97, 130.93, 130.90, 130.63, 130.19, 129.87, 129.08,

129.00, 128.82, 128.78, 128.60, 128.59, 128.56, 127.65, 127.45, 127.23, 126.99, 126.89, 126.24, 125.15, 124.96, 124.65, 124.20, 123.73, 106.93, 103.76, 103.72, 56.97, 56.65, 55.45, 55.44, 49.96, 49.48, 35.72, 35.61, 29.79, 22.86, 22.74, 19.62, 19.43, 18.99, 18.90, 18.83. HRMS (ESI- TOF) *m/z* $[C_{68}H_{66}N_4O_8+ H]^+$ calcd for 1068.5031, found 1068.5034.

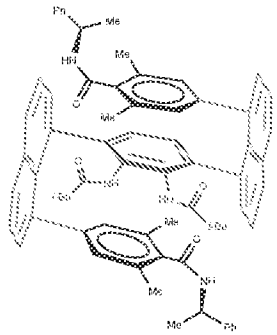


[0143] 4,4'-((2,3-dipivalamido-1,4-phenylene)bis(naphthalene-8,1-diyl))bis(3,5-dimethoxy-N-((R)-1-phenylethyl)benzamide) (20b): $[\alpha]_D^{25}$ = +46.4 (*c* = 1.1, CH_2Cl_2); grey white solid, 72% yield. ^{1}H NMR (400 MHz, CHLOROFORM-D) δ 8.10 (s, 1H), 7.96 – 7.80 (m, 4H), 7.68 (dd, *J* = 11.5, 4.1 Hz, 2H), 7.50 – 7.40 (m, 8H), 7.36 – 7.29 (m, 5H), 7.25 (d, *J* = 1.6 Hz, 1H), 7.15 (dd, *J* = 7.1, 1.3 Hz, 2H), 6.86 (dt, *J* = 3.1, 1.6 Hz, 3H), 6.75 – 6.72 (m, 3H), 5.46 – 5.18 (m, 2H), 3.56 (dd, *J* = 20.3, 8.9 Hz, 12H), 1.59 (d, *J* = 7.0 Hz, 6H), 0.73 – 0.63 (m, 18H); 13C NMR (101 MHz, CHLOROFORM-D) δ = 176.15, 168.10, 156.72, 156.40, 143.84, 139.81, 136.23, 134.95, 134.32, 132.35, 131.17, 130.90, 130.80, 130.27, 129.58, 128.85, 128.75, 128.49, 127.25, 127.14, 126.83, 124.95, 124.84, 124.21, 107.24, 103.28, 57.18, 55.43, 49.80, 38.46, 29.80, 27.25, 22.50. HRMS (ESI- TOF) m/z [C70H70N4O8+ Na] + calcd for 1118.5169, found 1118.5176. HRMS (ESI- TOF) *m/z* $[C_{70}H_{70}N_4O_8+ Na]^+$ calcd for 1118.5169, found 1118.5176.



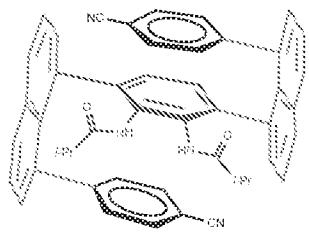
[0144] 4,4'-((2,3-dipivalamido-1,4-phenylene)bis(naphthalene-8,1-diyl))bis(2,6-dimethoxy-*N*-((*R*)-1-phenylethyl)benzamide) (20c): $[\alpha]_D^{25}$ = +109.2 (*c* = 0.8, CH_2Cl_2); pale solid, 68% yield. ^{1}H NMR (400 MHz, CHLOROFORM-D) δ 8.64 (d, *J* = 8.8 Hz, 1H), 8.04 (s, 1H), 7.99 – 7.93 (m, 2H), 7.87 – 7.79 (m, 2H), 7.69 (dd, *J* = 7.0, 5.7 Hz, 2H), 7.63 – 7.56 (m, 1H), 7.45 (tdd, *J* = 21.0, 10.2, 4.8 Hz, 6H), 7.33 – 7.25 (m, 6H), 7.19 (t, *J* = 7.5 Hz, 3H), 7.15 – 7.07 (m, 3H), 6.84 (s, 1H), 6.74 (s, 1H), 6.20 (d, *J* = 1.0 Hz, 1H), 6.09 (s, 1H), 5.88 (d, *J* = 0.9 Hz, 1H), 5.45 – 5.36 (m, 1H), 4.60 (q, *J* = 6.7 Hz, 1H), 3.81 (d, *J* = 1.0 Hz, 6H), 3.62 (d, *J* = 6.3 Hz, 3H), 3.39 – 3.34 (m, 3H), 1.56 (d, *J* = 3.3 Hz, 6H), 0.62 (d, *J* = 8.3 Hz, 9H), 0.35 (s, 9H); ^{13}C NMR (101 MHz, CHLOROFORM-D) δ 190.94, 176.40, 173.63, 168.93, 165.15, 156.06, 155.92, 155.73, 154.82,

145.45, 144.89, 142.77, 141.64, 140.34, 139.90, 138.96, 137.76, 137.15, 134.71, 134.68, 134.42, 133.57, 132.42, 131.45, 130.26, 129.68, 129.53, 129.47, 129.33, 129.10, 128.80, 128.56, 128.53, 128.15, 127.89, 127.77, 127.65, 127.22, 126.72, 126.67, 126.47, 126.08, 125.02, 124.57, 115.06, 111.40, 108.38, 107.80, 104.58, 103.63, 58.24, 55.50, 55.30, 54.86, 48.42, 44.10, 38.91, 38.17, 31.90, 29.67, 27.77, 26.92, 26.87, 22.90, 22.67, 19.41, 14.10. HRMS (ESI- TOF) *m/z* $[C_{70}H_{70}N_4O_8+ K]^+$ calcd for 1135.4982, found 1135.4937.



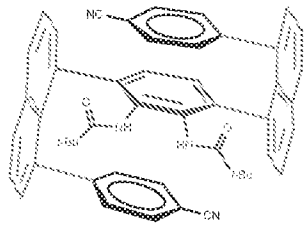
[0145] 4,4'-((2,3-dipivalamido-1,4-phenylene)bis(naphthalene-8,1-diyl))bis(2,6-dimethyl-*N*-((*R*)-1-phenylethyl)benzamide) (20d): $[\alpha]_D^{25}$ = +64.8 (*c* = 0.9, CH_2Cl_2); pale green solid, 58% yield. ^{1}H NMR (400 MHz, CHLOROFORM-D) δ 7.92 – 7.82 (m, 4H), 7.66 – 7.54 (m, 3H), 7.48 – 7.36 (m, 8H), 7.35 – 7.25 (m, 6H), 7.24 – 7.16 (m, 4H), 7.14 – 6.82 (m, 5H), 6.47 – 6.38 (m, 2H), 5.42 (dd, *J* = 14.5, 7.8 Hz, 2H), 2.17 – 2.10 (m, 4H), 1.97 – 1.89 (m, 5H), 1.60 (dd, *J* = 13.8, 6.8 Hz, 9H), 0.57 – 0.36 (m, 18H); ^{13}C NMR (101 MHz, CHLOROFORM-D) δ 175.47, 169.61, 169.43, 143.55, 140.27, 140.16, 139.77, 139.57, 139.49, 139.28, 138.69, 137.30, 136.39, 135.83, 135.29, 134.89, 134.82, 133.84, 133.74, 132.28, 132.21, 132.13, 131.83, 131.43, 131.35, 131.25, 131.20, 130.98, 129.71, 129.42, 129.20, 129.13, 128.92, 128.86, 128.67, 128.53, 128.46, 128.37, 127.19, 127.05, 126.89, 126.81, 126.30, 126.23, 126.11, 125.50, 125.10, 125.02, 48.67, 48.60, 38.69, 38.59, 33.37, 32.27, 31.36, 29.78, 27.01, 27.00, 22.78, 21.88, 19.19, 14.14. HRMS (ESI-TOF) *m/z* $[C_{70}H_{70}N_4O_4+ K]^+$ calcd for 1071.5185, found 1071.5209.

[0146] Data for 21a-21f

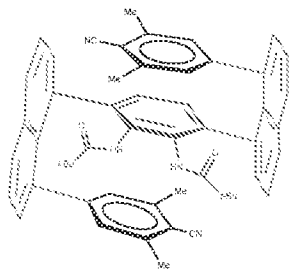


[0147] *N,N'*-(3,6-bis(8-(4-cyanophenyl)naphthalen-1-yl)-1,2-phenylene)bis(2-methylpropanamide) (21a): $[\alpha]_D^{25}$ = +40.8 (*c* = 0.8, CH_2Cl_2); pale green solid, 49% yield. ^{1}H NMR (400 MHz, CHLOROFORM-D) δ 8.04 – 7.92 (m, 5H), 7.83 (dd, *J* = 10.2, 4.9 Hz, 1H), 7.74 (d, *J* = 8.0 Hz, 1H), 7.56 – 7.30 (m, 9H), 7.12 (dd, *J* = 10.5, 7.5 Hz, 2H), 6.88 (d, *J* = 7.6 Hz, 1H), 6.83 – 6.72 (m, 2H), 6.64 (dd, *J* = 23.2, 7.9 Hz, 2H), 6.41 (d,

J = 8.0 Hz, 1H), 2.78 – 2.63 (m, 1H), 1.62 (dt, *J* = 12.5, 6.3 Hz, 1H), 1.42 (dd, *J* = 17.1, 6.8 Hz, 3H), 1.25 – 1.16 (m, 3H), 0.71 – 0.64 (m, 3H), -0.01 (t, *J* = 20.6 Hz, 3H); ^{13}C NMR (101 MHz, CHLOROFORM-D) δ 179.40, 158.76, 147.79, 144.62, 139.26, 137.46, 135.90, 135.15, 134.80, 134.57, 132.66, 131.76, 131.27, 130.44, 130.02, 129.94, 129.64, 129.54, 129.35, 129.26, 129.13, 129.08, 129.00, 128.58, 128.29, 127.84, 126.85, 126.31, 126.18, 125.96, 125.68, 125.47, 124.42, 124.21, 118.51, 118.26, 108.35, 107.71, 39.01, 29.15, 26.96, 22.87, 21.19, 19.68. HRMS (ESI- TOF) *m/z* [$C_{48}H_{38}N_4O_2$+ K] $^+$ calcd for 743.2783, found 743.2204.

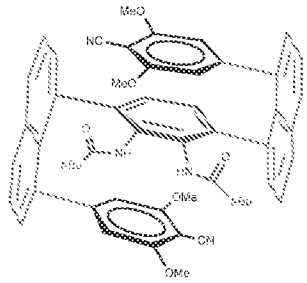


[0148] *N*,*N*'-(3,6-bis(8-(4-cyanophenyl)naphthalen-1-yl)-1,2-phenylene)bis(2,2-dimethylpropanamide) (21b): $[\alpha]_D^{25}$ = 133.8 (*c* = 1.2, CH_2Cl_2); pale yellow solid, 61% yield. ^{1}H NMR (400 MHz, CHLOROFORM-D) δ 7.97 (dd, *J* = 8.1, 3.0 Hz, 4H), 7.73 (t, *J* = 7.6 Hz, 2H), 7.49 (t, *J* = 7.6 Hz, 2H), 7.42 (dd, *J* = 7.7, 1.3 Hz, 2H), 7.32 (dd, *J* = 7.0, 0.9 Hz, 2H), 7.23 (tdd, *J* = 4.9, 3.2, 1.6 Hz, 6H), 6.97 (s, 2H), 6.88 (dd, *J* = 7.9, 1.1 Hz, 2H), 6.45 (s, 2H), 0.59 (s, 18H); ^{13}C NMR (101 MHz, CHLOROFORM-D) δ 176.11, 146.95, 138.65, 138.09, 135.40, 134.79, 132.61, 131.33, 131.05, 130.67, 130.30, 130.04, 129.75, 129.56, 129.11, 129.10, 128.30, 126.22, 124.93, 119.27, 109.39, 38.71, 29.68, 26.99. HRMS (ESI- TOF) *m/z* [$C_{50}H_{42}N_4O_2$+ H] $^+$ calcd for 732.3459, found 732.3459.

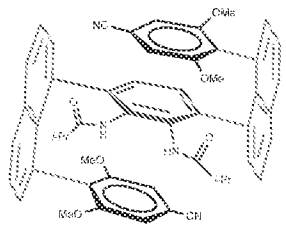


[0149] *N*,*N*'-(3,6-bis(8-(4-cyano-3,5-dimethylphenyl)naphthalen-1-yl)-1,2-phenylene)bis(2,2-dimethylpropanamide) (21c): $[\alpha]_D^{25}$ = +68.7 (*c* = 0.7, CH_2Cl_2); yellow solid, 78% yield. ^{1}H NMR (400 MHz, CHLOROFORM-D) δ 7.95 (ddd, *J* = 19.7, 11.0, 6.5 Hz, 3H), 7.87 – 7.73 (m, 2H), 7.62 – 7.43 (m, 3H), 7.39 – 7.28 (m, 3H), 7.19 – 6.97 (m, 4H), 6.92 – 6.77 (m, 3H), 6.50 (ddd, *J* = 24.3, 16.6, 9.9 Hz, 2H), 2.50 – 2.09 (m, 12H), 0.84 (ddd, *J* = 12.1, 5.7, 3.3 Hz, 6H), 0.52 – 0.42 (m, 18H); ^{13}C NMR (126 MHz, cdcl3) δ 175.75, 174.84, 139.25, 139.19, 134.92, 132.27, 131.75, 131.57, 131.36, 131.27, 130.83, 130.73, 130.61, 130.30, 129.83, 129.78, 129.72, 129.67, 129.60, 129.51, 129.18, 128.88, 128.50, 128.07, 127.90, 127.72, 127.67, 127.48, 126.77, 126.41, 126.09, 125.79, 125.36, 125.18, 124.89, 124.78, 124.74, 31.93, 31.67, 30.44, 30.19,

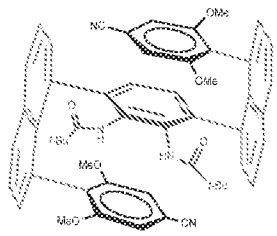
22.70, 22.42, 20.63, 20.54, 14.14, 13.96. HRMS (ESI- TOF) *m/z* $[C_{54}H_{50}N_4O_2+ Na]^+$ calcd for 811.3982, found 811.3972.



[0150] *N,N'*-(3,6-bis(8-(4-cyano-3,5-dimethoxyphenyl)naphthalen-1-yl)-1,2-phenylene)bis(2,2-dimethylpropanamide) (21d): $[\alpha]_D^{25}$ = +36.4 (*c* = 0.3, CH_2Cl_2); pale yellow solid, 80% yield. ^{1}H NMR (400 MHz, CHLOROFORM-D) δ 8.49 (dd, *J* = 36.4, 8.6 Hz, 1H), 8.12 – 7.91 (m, 3H), 7.82 – 7.47 (m, 5H), 7.35 – 7.25 (m, 4H), 7.23 – 7.06 (m, 4H), 6.99 – 6.83 (m, 3H), 4.22 – 4.18 (m, 3H), 4.13 – 4.06 (m, 2H), 3.93 – 3.90 (m, 1H), 3.75 (ddd, *J* = 8.2, 7.6, 0.7 Hz, 4H), 3.69 (dd, *J* = 6.4, 0.7 Hz, 1H), 3.62 (s, 1H), 0.94 – 0.86 (m, 18H); ^{13}C NMR (101 MHz, DMSO-D6) δ 176.15, 157.93, 157.74, 140.15, 136.54, 135.02, 133.22, 131.41, 131.01, 130.53, 130.07, 129.94, 127.45, 126.19, 125.72, 125.24, 120.49, 111.04, 110.80, 107.98, 56.99, 56.71, 38.82, 27.61. HRMS (ESI- TOF) *m/z* $[C_{54}H_{50}N_4O_6+ H]^+$ calcd for 875.3779, found 875.3708.



[0151] *N,N'*-(3,6-bis(8-(4-cyano-2,6-dimethoxyphenyl)naphthalen-1-yl)-1,2-phenylene)bis(2-methylpropanamide) (21e): $[\alpha]_D^{25}$ = +51.4 (*c* = 0.9, CH_2Cl_2); grey yellow solid, 43% yield. ^{1}H NMR (400 MHz, CHLOROFORM-D) δ 7.96 – 7.83 (m, 4H), 7.72 – 7.59 (m, 2H), 7.52 – 7.40 (m, 3H), 7.28 (dt, *J* = 8.2, 4.1 Hz, 1H), 7.18 – 7.12 (m, 1H), 7.05 – 6.95 (m, 1H), 6.67 (d, *J* = 1.2 Hz, 1H), 6.60 – 6.53 (m, 1H), 6.47 – 6.36 (m, 2H), 5.97 – 5.78 (m, 2H), 3.84 – 3.52 (m, 6H), 3.31 – 3.22 (m, 1H), 3.11 (t, *J* = 32.7 Hz, 6H), 1.90 (dq, *J* = 13.3, 6.6 Hz, 1H), 1.54 (t, *J* = 26.3 Hz, 2H), 1.39 (d, *J* = 6.8 Hz, 3H), 1.00 (d, *J* = 6.8 Hz, 3H), 0.65 (d, *J* = 7.2 Hz, 3H), 0.24 (d, *J* = 6.5 Hz, 3H); ^{13}C NMR (101 MHz, CHLOROFORM-D) δ = 179.06, 158.95, 157.19, 156.80, 156.66, 156.62, 139.23, 136.94, 135.21, 135.11, 134.87, 131.71, 131.49, 131.29, 131.27, 130.74, 130.47, 130.26, 129.82, 129.80, 129.51, 129.48, 129.21, 128.50, 127.02, 125.68, 125.44, 125.28, 125.12, 124.67, 124.63, 124.54, 124.36, 119.14, 119.04, 110.59, 110.42, 107.14, 106.52, 105.81, 105.64, 56.01, 55.95, 55.61, 54.81, 38.56, 29.66, 27.08, 22.36, 21.79, 19.90, 17.01. HRMS (ESI- TOF) *m/z* $[C_{52}H_{46}N_4O_6+ Na]^+$ calcd for 847.3466, found 847.3983.



[0152] *N,N'*-(3,6-bis(8-(4-cyano-2,6-dimethoxyphenyl)naphthalen-1-yl)-1,2-phenylene)bis(2,2-dimethylpropanamide) (21f): $[\alpha]_D^{25}$ = +210.0 (*c* = 1.1, CH_2Cl_2); grey white solid, 81% yield. ^{1}H NMR (400 MHz, CHLOROFORM-D) δ 7.91 (dd, *J* = 7.7, 3.1 Hz, 4H), 7.67 – 7.56 (m, 2H), 7.55 – 7.40 (m, 2H), 7.10 (dd, *J* = 8.9, 3.2 Hz, 4H), 6.93 (s, 4H), 6.51 (d, *J* = 50.1 Hz, 4H), 3.63 (d, *J* = 79.1 Hz, 12H), 0.62 (s, 18H); ^{13}C NMR (101 MHz, CHLORORM-D) δ = 175.86, 157.43, 157.07, 139.68, 135.41, 134.34, 132.73, 130.68, 130.34, 130.16, 129.87, 129.28, 129.03, 126.44, 125.61, 125.07, 124.82, 119.42, 110.76, 110.15, 106.43, 56.24, 55.50, 38.22, 26.99. HRMS (ESI- TOF) *m/z* $[C_{54}H_{50}N_4O_6+ Na]^+$ calcd for 875.3379, found 875.3707.



[0153] 1*H*,3*H*-naphtho[1,8-*cd*][1,2,6]oxadiborinine-1,3-diol: pale grey solid, 150mg, 76% yield. ^{1}H NMR (400 MHz, D_2O) δ 7.71 (dd, *J* = 16.8, 7.1 Hz, 4H), 7.36 (t, *J* = 7.4 Hz, 2H); ^{13}C NMR (101 MHz, DMSO-D6) δ = 135.21, 133.49, 131.94, 130.97, 129.28, 128.87, 126.67, 126.48, 123.70. HRMS (ESI- TOF) *m/z* $[C10H8B_2O_3+ H]^+$ calcd for 199.0738, found 199.0759.

[0154] It is contemplated that any embodiment discussed in this specification can be implemented with respect to any method, kit, reagent, or composition of the invention, and vice versa. Furthermore, compositions of the invention can be used to achieve methods of the invention.

[0155] It will be understood that particular embodiments described herein are shown by way of illustration and not as limitations of the invention. The principal features of this invention can be employed in various embodiments without departing from the scope of the invention. Those skilled in the art will recognize, or be able to ascertain using no more than routine experimentation, numerous equivalents to the specific procedures described herein. Such equivalents are considered to be within the scope of this invention and are covered by the claims.

[0156] All publications and patent applications mentioned in the specification are indicative of the level of skill of those skilled in the art to which this invention pertains. All publications and patent applications are herein incorporated by reference to the same extent as if each individual publication or patent application was specifically and individually indicated to be incorporated by reference.

[0157] The use of the word "a" or "an" when used in conjunction with the term "comprising" in the claims and/or the specification may mean "one," but it is also consistent with the meaning of "one or more," "at least one," and "one or more than one." The use of the term "or" in the claims is used to mean "and/or" unless explicitly indicated to refer to alternatives only or the alternatives are mutually exclusive, although the disclosure supports a definition that refers to only alternatives and "and/or." Throughout this application, the term "about" is used to indicate that a value includes the inherent variation of error for the device, the method being employed to determine the value, or the variation that exists among the study subjects.

[0158] As used in this specification and claim(s), the words "comprising" (and any form of comprising, such as "comprise" and "comprises"), "having" (and any form of having, such as "have" and "has"), "including" (and any form of including, such as "includes" and "include") or "containing" (and any form of containing, such as "contains" and "contain") are inclusive or open-ended and do not exclude additional, unrecited elements or method steps. In embodiments of any of the compositions and methods provided herein, "comprising" may be replaced with "consisting essentially of" or "consisting of". As used herein, the phrase "consisting essentially of" requires the specified integer(s) or steps as well as those that do not materially affect the character or function of the claimed invention. As used herein, the term "consisting" is used to indicate the presence of the recited integer (e.g., a feature, an element, a characteristic, a property, a method/process step or a limitation) or group of integers (e.g., feature(s), element(s), characteristic(s), property(ies), method/process steps or limitation(s)) only.

[0159] The term "or combinations thereof" as used herein refers to all permutations and combinations of the listed items preceding the term. For example, "A, B, C, or combinations thereof" is intended to include at least one of: A, B, C, AB, AC, BC, or ABC, and if order is important in a particular context, also BA, CA, CB, CBA, BCA, ACB, BAC, or CAB. Continuing with this example, expressly included are combinations that contain repeats of one or more item or term, such as BB, AAA, AB, BBC, AAABCCCC, CBBAAA, CABABB, and so forth. The skilled artisan will understand that typically there is no limit on the number of items or terms in any combination, unless otherwise apparent from the context.

[0160] As used herein, words of approximation such as, without limitation, "about", "substantial" or "substantially" refers to a condition that when so modified is understood to not necessarily be absolute or perfect but would be considered close enough to those of ordinary skill in the art to warrant designating the condition as being present. The extent to which the description may vary will depend on how great a change can be instituted and still have one of ordinary skill in the art recognize the modified feature as still having the required characteristics and capabilities of the unmodified feature. In general, but subject to the preceding discussion, a numerical value herein that is modified by a word of approximation such as "about" may vary from the stated value by at least ±1, 2, 3, 4, 5, 6, 7, 10, 12 or 15%.

[0161] All of the compositions and/or methods disclosed and claimed herein can be made and executed without undue experimentation in light of the present disclosure. While the compositions and methods of this invention have been described in terms of preferred embodiments, it will be apparent to those of skill in the art that variations may be applied to the compositions and/or methods and in the steps or in the sequence of steps of the method described herein without departing from the concept, spirit and scope of the invention. All such similar substitutes and modifications apparent to those skilled in the art are deemed to be within the spirit, scope and concept of the invention as defined by the appended claims.

[0162] To aid the Patent Office, and any readers of any patent issued on this application in interpreting the claims appended hereto, applicants wish to note that they do not intend any of the appended claims to invoke paragraph 6 of 35 U.S.C. § 112, U.S.C. § 112 paragraph (f), or equivalent, as it exists on the date of filing hereof unless the words "means for" or "step for" are explicitly used in the particular claim.

[0163] For each of the claims, each dependent claim can depend both from the independent claim and from each of the prior dependent claims for each and every claim so long as the prior claim provides a proper antecedent basis for a claim term or element.

REFERENCES

[0164] 1. Eliel EL and Wilen SH. Stereochemistry of Organic Compounds. New York: John Wiley & Sons, 1994; 1172-5.

[0165] 2. Wagner I and Musso, H. New naturally occurring amino acids. Angew Chem Int Ed 1983; 22: 816-28.

[0166] 3. William RM. Synthesis of Optically Active α-Amino Acids. Oxford: Pergamon Press 1990.

[0167] 4. Pace CN and Scholtz JM. A helix propensity scale based on experimental studies of peptides and proteins. Biophys J 1998; 75: 422-7.

[0168] 5. Dunitz, JD. Pauling's left-handed α-helix. Angew Chem Int Ed 2001; 40: 4167-73.

[0169] 6. Wang A-J, Fujii S and Van Boom J et al. Right-handed and left-handed double-helical DNA: structural studies. Cold Spring Harb Symp Quant Biol 1983; 47: 33-44.

[0170] 7. Corey EJ, Czakó B and Kürti L. Molecules and medicine. New Jersey: John Wiley & Sons, 2007.

[0171] 8. Ojima I. Catalytic Asymmetric Synthesis. New Jersey: John Wiley & Sons, 2010.

[0172] 9. Hikaru K, Takashi N and Kayo S et al. Isolation of Notaamid S and Enantiomeric 6-epi-Stephacidin A from the Fungus Aspergillus: Biogenetic Implication. Org Lett 2015; 17: 700-3.

[0173] 10. Nicolaou KC and Snyder SA. Classics in Total Synthesis II: More Target, Strategies, Methods. Weinheim: Wiley-VCH, 2003.

[0174] 11. Jacobsen EN, Pfaltz A and Yamamoto, H. Comprehensive asymmetric catalysis. New York: Springer, 2003.

[0175] 12. Carreira EM and Kvaerno, L. Classics in stereoselective synthesis. Weinheim: Wiley-VCH, 2009.

[0176] 13. Shi S-L, Wong ZL and Buchwald SL. Copper-catalysed enantioselective stereodivergent synthesis of amino alcohols. Nature 2016; 532: 353.

[0177] 14. MacMillan DW. The advent and development of organocatalysis. Nature 2008; 455: 304-8.

[0178] 15. Xie J-H and Zhou Q-L. Chiral diphosphine and monodentate phosphorus ligands on a spiro scaffold for transition-metal-catalyzed asymmetric reactions. Acc Chem Res 2008; 41: 581-93.

[0179] 16. Ding K, Han Z and Wang Z. Spiro skeletons: A class of privileged structure for chiral ligand design. Chem Asian J 2009; 4: 32-41.

[0180] 17. Liu X, Zheng H and Xia Y et al. Asymmetric Cycloaddition and Cyclization Reactions Catalyzed by Chiral N, N′-Dioxide–Metal Complexes. Acc Chem Res 2017; 50: 2621-31.

[0181] 18. Ye L-W, Zhou J and Tang, Y. Phosphine-triggered synthesis of functionalized cyclic compounds. Chem Soc Rev 2008; 37: 1140-52.

[0182] 19. Cai Z-J, Liu C-X and Wang, Q et al. Thioketone-directed rhodium (I) catalyzed enantioselective CH bond arylation of ferrocenes. Nat Commun 2019; 10(1): 1-8.

[0183] 20. List, B. Asymmetric aminocatalysis. Synlett 2001; 11: 1675-86.

[0184] 21. Kolb HC, VanNieuwenhze MS and Sharpless, KB. Catalytic asymmetric dihydroxylation. Chem Rev 1994; 94: 2483-547.

[0185] 22. Wei Y and Shi M. Recent advances in organocatalytic asymmetric morita–baylis–hillman/aza-morita–baylis–hillman reactions. Chem Rev 2013; 113: 6659-90.

[0186] 23. Zbieg JR, Yamaguchi E and McInturff, EL et al. Enantioselective CH crotylation of primary alcohols via hydrohydroxyalkylation of butadiene. Science 2012; 336: 324-7.

[0187] 24. Cao Z-Y, Wang X and Tan, C et al. Highly stereoselective olefin cyclopropanation of diazooxindoles catalyzed by a C 2-symmetric spiroketal bisphosphine/Au (I) complex. J Am Chem Soc 2013; 135: 8197-200.

[0188] 25. Phipps RJ, Hamilton GL and Toste, FD. The progression of chiral anions from concepts to applications in asymmetric catalysis. Nat Chem 2012; 4: 603.

[0189] 26. Gustafson JL, Lim D and Miller SJ. Dynamic kinetic resolution of biaryl atropisomers via peptide-catalyzed asymmetric bromination. Science 2010; 328: 1251-5.

[0190] 27. Cui X, Xu X and Lu, H et al. Enantioselective cyclopropenation of alkynes with acceptor/acceptor-substituted diazo reagents via Co (II)-based metalloradical catalysis. J Am Chem Soc 2011; 133: 3304-7.

[0191] 28. Chen J and Huang Y. Asymmetric catalysis with N-heterocyclic carbenes as non-covalent chiral templates. Nat Chem 2014; 5: 3437.

[0192] 29. Liu H, Dagousset G and Masson G et al. Chiral Brønsted acid-catalyzed enantioselective three-component Povarov reaction. J Am Chem Soc 2009; 131: 4598-9.

[0193] 30. Huang XL, He L and Shao PL et al. [4+ 2] Cycloaddition of Ketenes with N-Benzoyldiazenes Catalyzed by N-Heterocyclic Carbenes. Angew Chem Int Ed 2009; 48: 192-5.

[0194] 31. Guo J, Wang H and Xing, S et al. Cobalt-Catalyzed Asymmetric Synthesis of gem-Bis (silyl) alkanes by Double Hydrosilylation of Aliphatic Terminal Alkynes. Chem 2019; 5: 881-95.

[0195] 32. Guo W, Wu B and Zhou X et al. Formal Asymmetric Catalytic Thiolation with a Bifunctional Catalyst at a Water–Oil Interface: Synthesis of Benzyl Thiols. Angew Chem Int Ed 2015; 54: 4522-6.

[0196] 33. Luo J, Zhang T and Wang L et al. Enantioselective Synthesis of Biaryl Atropisomers by Pd-Catalyzed C− H Olefination using Chiral Spiro Phosphoric Acid Ligands. Angew Chem Int Ed 2019; 131: 6780-4.

[0197] 34. Fu Z, Xu J and Zhu T et al. β-Carbon activation of saturated carboxylic esters through N-heterocyclic carbene organocatalysis. Nat Chem 2013; 5: 835.

[0198] 35. Li G and Sharpless KB. Short Taxol Side-chain Synthesis. Acta Chem Scand 1996; 50: 649-51.

[0199] 36. Shen Y and Chen C-F. Helicenes: synthesis and applications. Chem Rev 2011; 112: 1463-535.

[0200] 37. Huang G, Wen R and Wang Z et al. Novel chiral aggregation induced emission molecules: self-assembly, circularly polarized luminescence and copper (ii) ion detection. Mater Chem Front 2018; 2: 1884-92.

[0201] 38. Tang H, Gu Z and Ding H et al. Nanoscale Crystalline Sheets and Vesicles Assembled from Nonplanar Cyclic π-Conjugated Molecules. Research 2019; 2019: 1953926.

[0202] 39. Wang X, Lou X-Y and Jin X-Y et al. A Binary Supramolecular Assembly with Intense Fluorescence Emission, High pH Stability, and Cation Selectivity: Supramolecular Assembly-Induced Emission Materials. Research 2019; 2019: 1454562.

[0203] 40. Dai L-X, Tu T and You S-L et al. Asymmetric catalysis with chiral ferrocene ligands. Acc Chem Res 2003; 36: 659-67.

[0204] 41. Alberico D, Scott ME and Lautens M. Aryl− aryl bond formation by transition-metal-catalyzed direct arylation. Chem Rev 2007; 107: 174-238.

[0205] 42. Fu GC. Enantioselective nucleophilic catalysis with "planar-chiral" heterocycles. Acc Chem Res 2000; 33: 412-20.

[0206] 43. Schwamb CB, Fitzpatrick KP and Brueckner AC et al. Enantioselective Synthesis of α-Amidoboronates Catalyzed by Planar-Chiral NHC-Cu (I) Complexes. J Am Chem Soc 2018; 140(34) 10644-8.

[0207] 44. Schwartz LA, Holmes M and Brito GA et al. Cyclometalated Iridium–PhanePhos Complexes Are Active Catalysts in Enantioselective Allene–Fluoral Reductive Coupling and Related Alcohol-Mediated Carbonyl Additions That Form Acyclic Quaternary Carbon Stereocenters. J Am Chem Soc 2019; 141: 2087-96.

[0208] 45. Mishra S, Liu J and Aponick A. Enantioselective Alkyne Conjugate Addition Enabled by Readily Tuned Atropisomeric P, N-Ligands. J Am Chem Soc 2017; 139: 3352-5.

[0209] 46. Zhang P-C, Wang Y and Zhang Z-M et al. Gold (I)/Xiang-Phos-Catalyzed Asymmetric Intramolecular Cyclopropanation of Indenes and Trisubstituted Alkenes. Org Lett 2018; 20: 7049-52.

[0210] 47. Han J, Zhou W and Zhang P-C et al. Design and Synthesis of WJ-Phos, and Application in Cu-Catalyzed Enantioselective Boroacylation of 1, 1-Disubstituted Allenes. ACS Catal 2019; 9: 6890-5.

[0211] 48. 48 Sandoval CA, Ohkuma T and Muñiz K et al. Mechanism of asymmetric hydrogenation of ketones catalyzed by BINAP/1, 2-diamine− ruthenium (II) complexes. J Am Chem Soc 2003; 125: 13490-503.

[0212] 49. Trost BM. Designing a receptor for molecular recognition in a catalytic synthetic reaction: allylic alkylation. Acc Chem Res 1996; 29: 355-64.

[0213] 50. Evans DA, Woerpel KA and Hinman MM et al. Bis (oxazolines) as chiral ligands in metal-catalyzed asymmetric reactions. Catalytic, asymmetric cyclopropanation of olefins. J. Am. Chem Soc 1991; 113: 726-8.

[0214] 51. Denmark SE, Stavenger RA and Wong K-T et al. Chiral phosphoramide-catalyzed aldol additions of ketone enolates. Preparative aspects. J Am Chem Soc 1999; 121: 4982-91.

[0215] 52. Akiyama T. Stronger brønsted acids. Chem Rev 2007; 107: 5744-58.

[0216] 53. Tang W and Zhang X. New chiral phosphorus ligands for enantioselective hydrogenation. Chem Rev 2003; 103: 3029-70.

[0217] 54. Xu G, Senanayake CH and Tang W. P-Chiral Phosphorus Ligands Based on a 2, 3-Dihydrobenzo [d][1, 3] oxaphosphole Motif for Asymmetric Catalysis. Acc Chem Res 2019; 52: 1101-12.

[0218] 55. Handa S, Andersson MP and Gallou F et al. HandaPhos: a general ligand enabling sustainable ppm levels of palladium-catalyzed cross-couplings in water at room temperature. Angew Chem Int Ed 2016; 55: 4914-8.

[0219] 56. Zhang Z, Butt NA and Zhang W. Asymmetric hydrogenation of nonaromatic cyclic substrates. Chem Rev 2016; 116: 14769-827.

[0220] 57. Pu L. 1, 1 '-Binaphthyl dimers, oligomers, and polymers: molecular recognition, asymmetric catalysis, and new materials. Chem Rev 1998; 98: 2405-94.

[0221] 58. Chen D-F, Han Z-Y and Zhou X-L et al. Asymmetric organocatalysis combined with metal catalysis: concept, proof of concept, and beyond. Acc Chem Res 2014; 47: 2365-77.

[0222] 59. Cai Y, Liu X and Zhou P et al. Asymmetric Catalytic Halofunctionalization of α, β-Unsaturated Carbonyl Compounds. J Org Chem 2018; 84: 1-13.

[0223] 60. Yu J, Shi F and Gong L-Z. Brønsted-acid-catalyzed asymmetric multicomponent reactions for the facile synthesis of highly enantioenriched structurally diverse nitrogenous heterocycles. Acc Chem Res 2011; 44: 1156-71.

[0224] 61. Lorion MM, Maindan K and Kapdi AR et al. Heteromultimetallic catalysis for sustainable organic syntheses. Chem Soc Rev 2017; 46: 7399-420.

[0225] 62. Chen Y, Yekta S and Yudin AK. Modified BINOL ligands in asymmetric catalysis. Chem Rev 2003; 103: 3155-212.

[0226] 63. Zhang J, Yu P and Li SY et al. Asymmetric phosphoric acid-catalyzed four-component Ugi reaction. Science 2018; 361: 1087-96.

[0227] 64. Lin JS, Li TT and Jiao GY et al. Chiral Brønsted Acid Catalyzed Dynamic Kinetic Asymmetric Hydroamination of Racemic Allenes and Asymmetric Hydroamination of Dienes. Angew. Chem Int Ed 2019; 58: 7092-6.

[0228] 65. Yoon H, Marchese AD and Lautens M. Carboiodination Catalyzed by Nickel. J Am Chem Soc 2018; 140: 10950-4.

[0229] 66. Liu Y and Zhang W. Iridium-Catalyzed Asymmetric Hydrogenation of α-Alkylidene Succinimides. Angew Chem Int Ed 2013; 52: 2203-6.

[0230] 67. Ye C-X, Melcamu YY and Li H-H et al. Dual catalysis for enantioselective convergent synthesis of enantiopure vicinal amino alcohols. Nat Commun 2018; 9: 410.

[0231] 68. Yang G, Guo D and Meng D et al. NHC-catalyzed atropoenantioselective synthesis of axially chiral biaryl amino alcohols via a cooperative strategy. Nat Commun 2019; 10: 3062.

[0232] 69. Zhao C, Guo D, Munkerup K, et al, nantioselective [3+3] atroposelective annulation catalyzed by N-heterocyclic carbenes, Nature Comm, 2018; 9, 611. DOI: 10.1038/s41467-018-02952-3.

[0233] 70. Zhu Y, Zhang L and Luo S. Asymmetric α-photoalkylation of β-ketocarbonyls by primary amine catalysis: facile access to acyclic all-carbon quaternary stereocenters. J Am Chem Soc 2014; 136: 14642-5.

[0234] 71. Zhang HH, Wang CS and Li C et al. Design and Enantioselective Construction of Axially Chiral Naphthyl-Indole Skeletons. Angew Chem Int Ed 2017; 56: 116-21.

[0235] 72. Shen D, Chen Q and Yan P et al. Enantioselective dearomatization of naphthol derivatives with allylic alcohols by cooperative iridium and Brønsted acid catalysis. Angew Chem Int Ed 2017; 56: 3242-6.

[0236] 73. Li G, Liang T and Wojtas L et al. An asymmetric Diels-Alder reaction catalyzed by chiral phosphate magnesium complex: highly enantioselective synthesis of chiral spirooxindoles. Angew. Chem Int Ed 2013; 125: 4726-30.

[0237] 74. Wu G, Liu Y and Yang Z et al. Multilayer 3D Chirality and Its Synthetic Assembly. Research 2019; 2019: 6717104.

[0238] 75. An G, Seifert C and Li, G. N-Phosphonyl/phosphinyl imines and group-assisted purification (GAP) chemistry/technology. Org Biomol Chem 2015; 13: 1600-17.

[0239] 76. Xie J-b, Luo J and Winn TR et al. Group-assisted purification (GAP) chemistry for the synthesis of Velcade via asymmetric borylation of N-phosphinylimines. Beilstein J Org Chem 2014; 10: 746-51.

[0240] 77. Kaur P, Wever W and Pindi S et al. The GAP chemistry for chiral N-phosphonyl imine-based Strecker reaction. Green Chem 2011; 13: 1288-92.

[0241] 78. Seifert CW, Paniagua A and White GA et al. GAP Peptide Synthesis through the Design of a GAP Protecting Group: An Fmoc/tBu Synthesis of Thymopentin Free from Polymers, Chromatography and Recrystallization. Eur J Org Chem 2016; 2016: 1714-9.

[0242] 79. Kaur P, Pindi S and Wever W et al. Asymmetric catalytic N-phosphonyl imine chemistry: The use of primary free amino acids and Et2AlCN for asymmetric catalytic Strecker reaction. J Org Chem 2010; 75: 5144-50.

[0243] 80. Seifert C. New Synthetic Methodology for Chiral Amines and Peptides via GAP Technology. Ph. D. Thesis. Texas Tech University Department of Chemistry and Biochemistry 2017.

[0244] 81. Corey E and Cheng X-M. The Logic of Chemical Synthesis. Chichester: John Wiley & Sons, 1989.

[0245] 82. Noland WE, Narina VS and Britton D. Synthesis and crystallography of 8-halonaphthalene-1-carbonitriles and naphthalene-1, 8-dicarbonitrile. J Chem Res 2011; 35: 694-7.

[0246] 83. Guram AS and Buchwald SL. Palladium-catalyzed aromatic aminations with in situ generated aminostannanes. J Am Chem Soc 1994; 116: 7901-2.

[0247] 84. Anil S and Stephen LB. Palladium-Catalyzed Aromatic Aminations with in situ Generated Aminostannanes. J Am Chem Soc 1994; 116: 7902-41.

[0248] 85. Bhunia S, Pawar GG and Kumar, SV et al. Selected Copper-Based Reactions for C− N, C− O, C− S, and C− C Bond Formation. Angew Chem Int Ed 2017; 56: 16136-79.

[0249] 86. Miyaura N and Suzuki A. Palladium-catalyzed cross-coupling reactions of organoboron compounds. Chem Rev 1995; 95: 2457-83.

[0250] 87. Ding X, Chen L and Honsho Y et al. An n-channel two-dimensional covalent organic framework. J Am Chem Soc 2011; 133: 14510-3.

[0251] 88. Kotha S, Lahiri K and DHURKE K. Recent applications of the Suzuki–Miyaura cross-coupling reaction in organic synthesis. Tetrahedron 2002; 58: 9633-95

[0252] 89. Mothana S, Grassot JM and Hall, DG. Multistep Phase-Switch Synthesis by Using Liquid–Liquid Partitioning of Boronic Acids: Productive Tags with an Expanded Repertoire of Compatible Reactions. Angew Chem Int Ed 2010; 49: 2883-7.

[0253] 90. Zhu K, Baggi G and Loeb SJ. Ring-through-ring molecular shuttling in a saturated [3] rotaxane. Nat Chem 2018; 10: 625.

[0254] 91. Alder RW, Hyland NP and Jeffery JC et al. Poly (1, 1-bis (dialkylamino) propan-1, 3-diyl) s; conformationally-controlled oligomers bearing electroactive groups. Org Biomol Chem 2009; 7: 2704-15.

[0255] 92. Gampe DM, Schramm S and Ziemann S et al. From Highly Fluorescent Donors to Strongly Absorbing Acceptors: The Tunable Properties of Fluorubines. J Org Chem 2017; 82: 6153-62.

[0256] 93. Zhou Y, Kijima T and Izumi T. The synthesis and application of 2-acetyl-6-(1-naphthyl)-pyridine oxime as a new ligand for palladium precatalyst in Suzuki coupling reaction. J Heterocycl Chem 2009; 46: 116-8.

[0257] 94. Geng H and Huang P-Q. Versatile and chemoselective transformation of aliphatic and aromatic secondary amides to nitriles. Tetrahedron 2015; 71: 3795-801.

[0258] 95. Metallinos C, Nerdinger, S and Snieckus V. N-cumyl benzamide, sulfonamide, and aryl O-carbamate directed metalation groups. Mild hydrolytic lability for facile manipulation of directed ortho metalation derived aromatics. Org Lett 1999; 1: 1183-6.

[0259] 96. Hu X, Zhao X and He B et al. A Simple Approach to Bioconjugation at Diverse Level: Metal Free Clcik Reaction of Activated Alkynes with Native Groups of Biotargets without Prefunctionalization. Research 2018; 2018: 3152870,1-12.

[0260] 97. Mei J, Leung NL and Kwok, RT et al. Aggregation-induced emission: together we shine, united we soar! Chem Rev 2015; 115: 11718-940.

[0261] 98. Li Y, Li C and Jiang T et al. Aptamer-Anchored Rubrene-Loaded Organic Nanoprobes for Cancer Cell Targeting and Imaging. CCS Chemistry 2019; 1: 251-60.

[0262] 99. Liu Q, Bi C and Li J et al. Generating Giant Membrane Vesicles from Live Cells with Preserved Cellular Properties. Research 2019; 2019: 6523970.

What is claimed is:

1. A multi-layer 3D material comprising: a first, a second, and a third layer, wherein each of the layers are arranged in a nearly parallel fashion with chirality along a center plane.

2. The material of claim 1, wherein each of the first, second, and third layers are parallel.

3. The material of claim 1, wherein the multi-layer 3D material has a right-hand chirality, a left-hand chirality, or both a left- and a right-handed chirality.

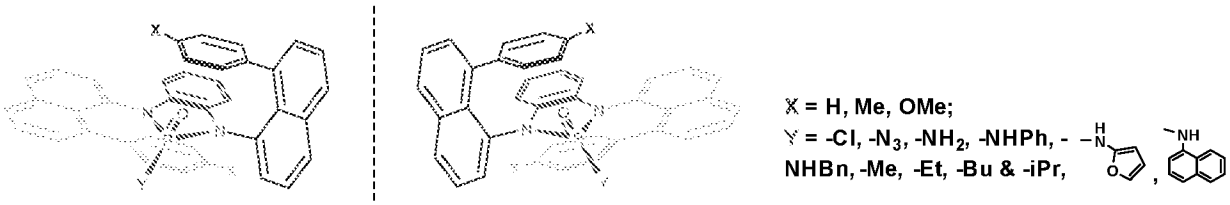
4. The material of claim 1, wherein each of the first, second, and third layers are at least one of: *anti, syn,* or both *anti* and *syn* isomers.

5. The material of claim 1, wherein each of the first, second, and third layers are *N,N*-phosphornyl amides.

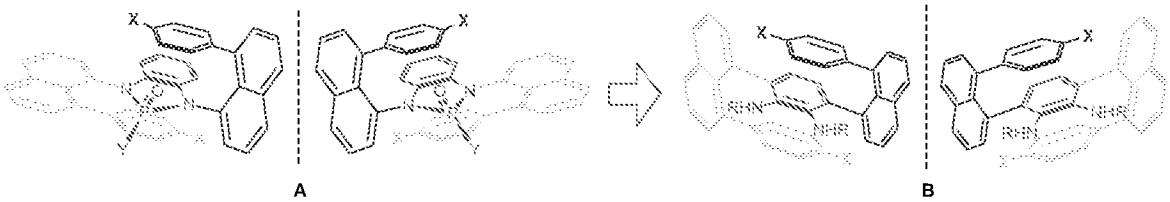
6. The material of claim 1, wherein each of the first, second, and third layers comprise chiral or achiral *N*-phosphonyl- or *N*-phosphinyl groups.

7. The material of claim 1, wherein each of the first, second, and third layers comprise a Multi-Layer Organic Framework (M-LOF) of single organic molecules with pseudo C_2-chiral characteristics.

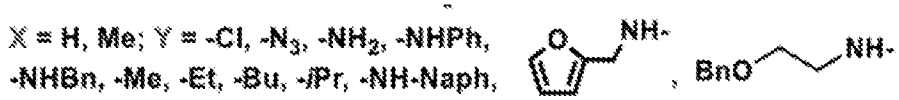
8. The material of claim 1, wherein each of the first, second, and third layers comprises:



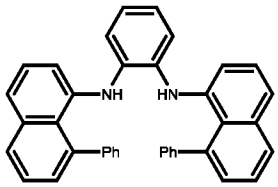
9. The material of claim 1, wherein each of the first, second, and third layers comprises:



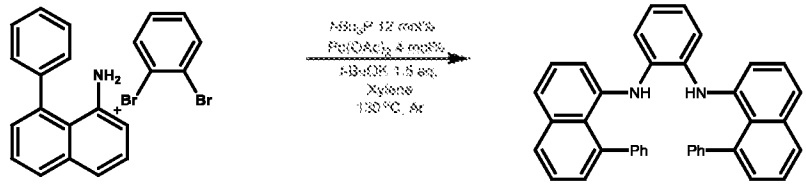
Wherein



10. The material of claim 1, wherein one or more of the first, second, or third layers are made by:

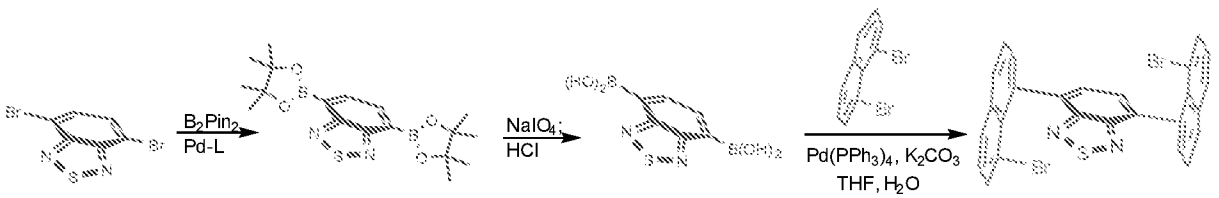


is produced by the following:



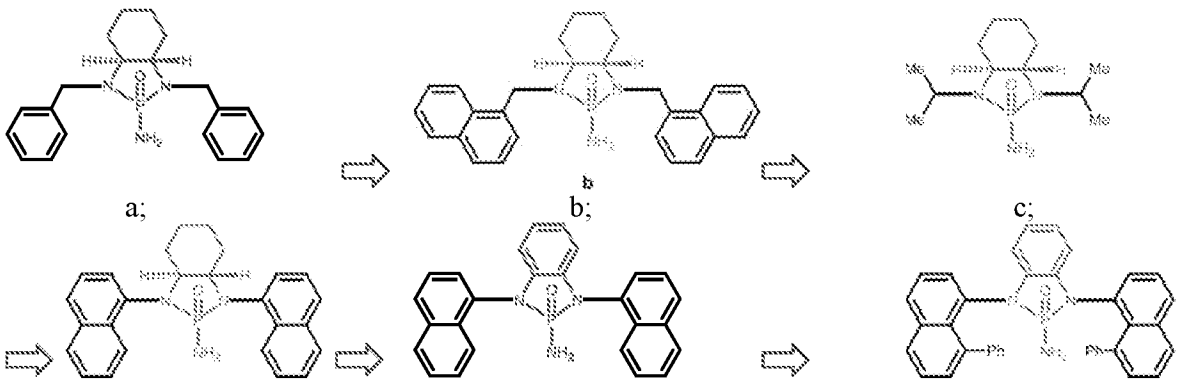
.

11. The material of claim 1, wherein one or more of the first, second, or third layers are made by:

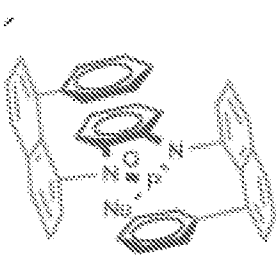
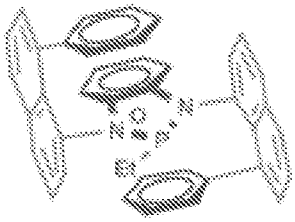
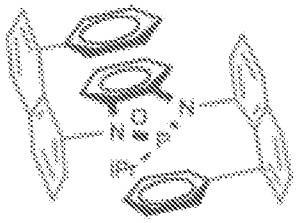


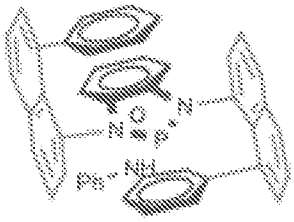
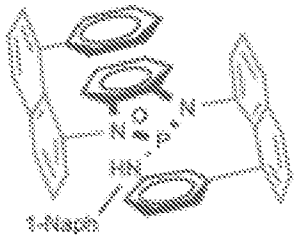
.

12. The material of claim 1, wherein monomeric precursors of the multi-layer 3D material is selected from at least one of:



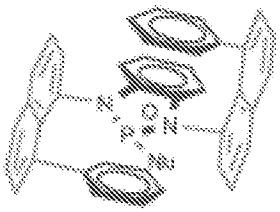
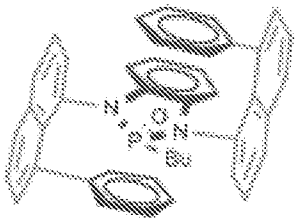
13. The material of claim 1, wherein the multi-layer 3D material is selected from at least one of:

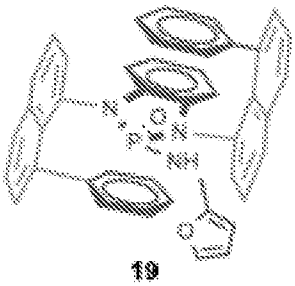

; 
20 ; 
21 ;


22 ; 
23 ; 
24 ; or


25 .

14. The material of claim 1, wherein the multi-layer 3D material is selected from at least one of:


; 
17 ; 
18 ; or

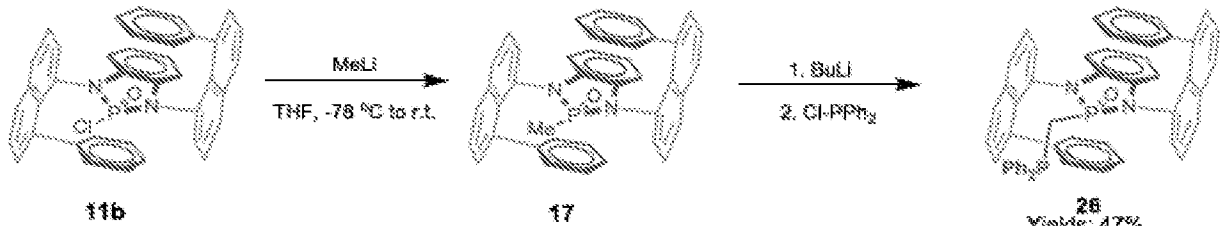

19 .

15. The material of claim 1, wherein the product of formula:



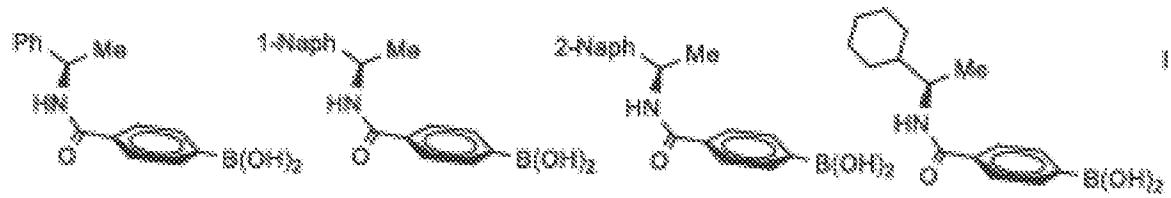
26

is made by a method comprising:

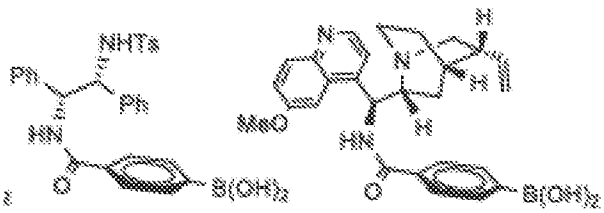


11b 17 28

16. The material of claim 1, wherein the product of at least one compound of formula 2a to 2f:

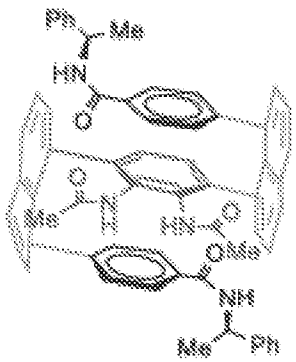


2a 2b 2c 2d



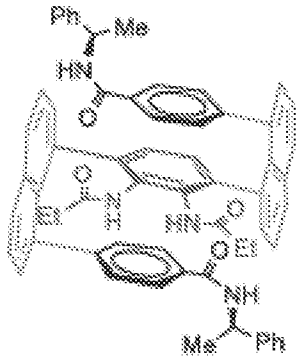
2e 2f

17. The material of claim 1, wherein the product of at least one compound of formula



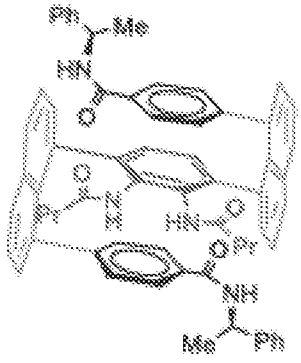
yield 56%

8a



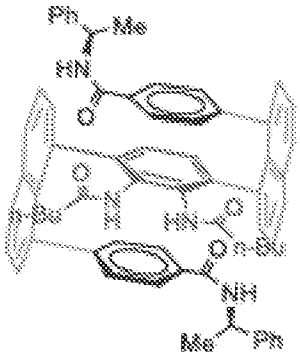
yield 39%

8b



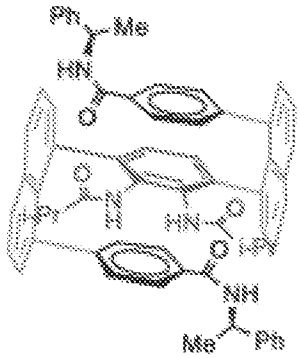
yield 42%

8c



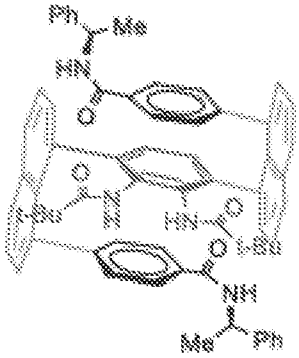
yield 47%

8d



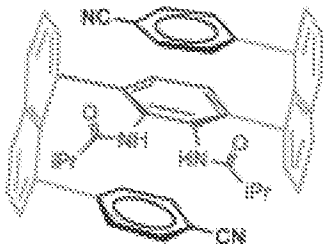
yield 38%, $[\alpha]_D^{25}$ = 92°

8e

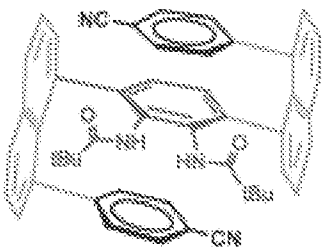


yield 31%, $[\alpha]_D^{25}$ = 58°

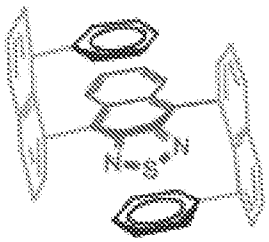
8f



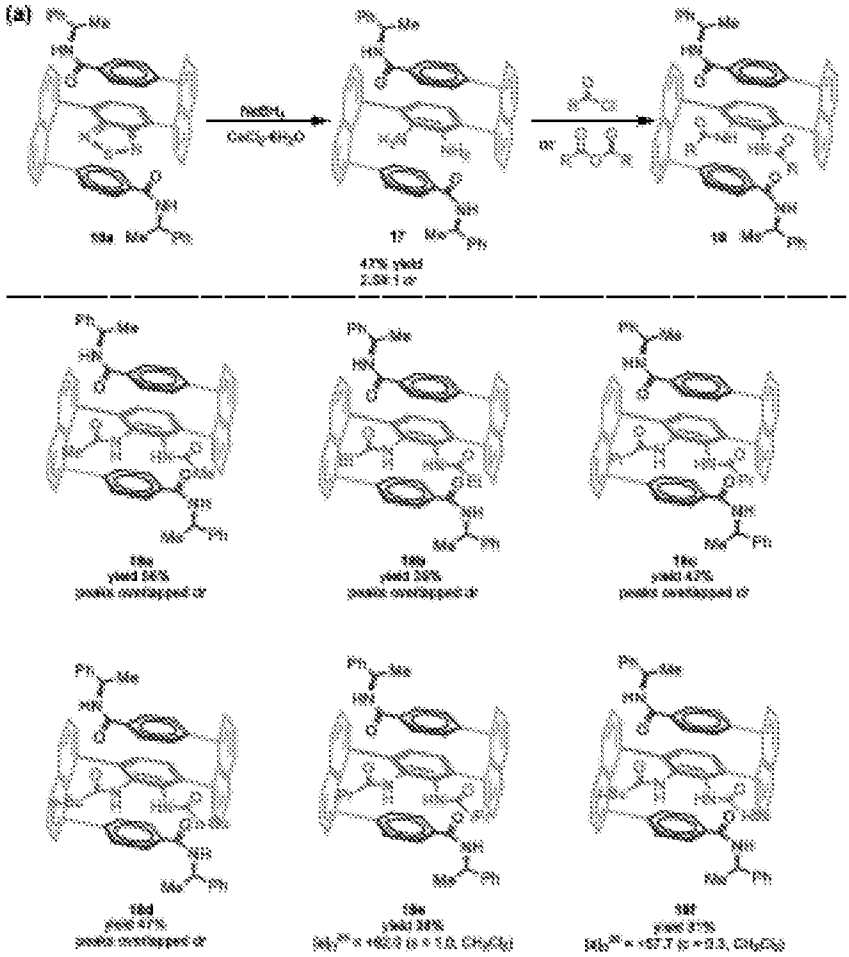
14a

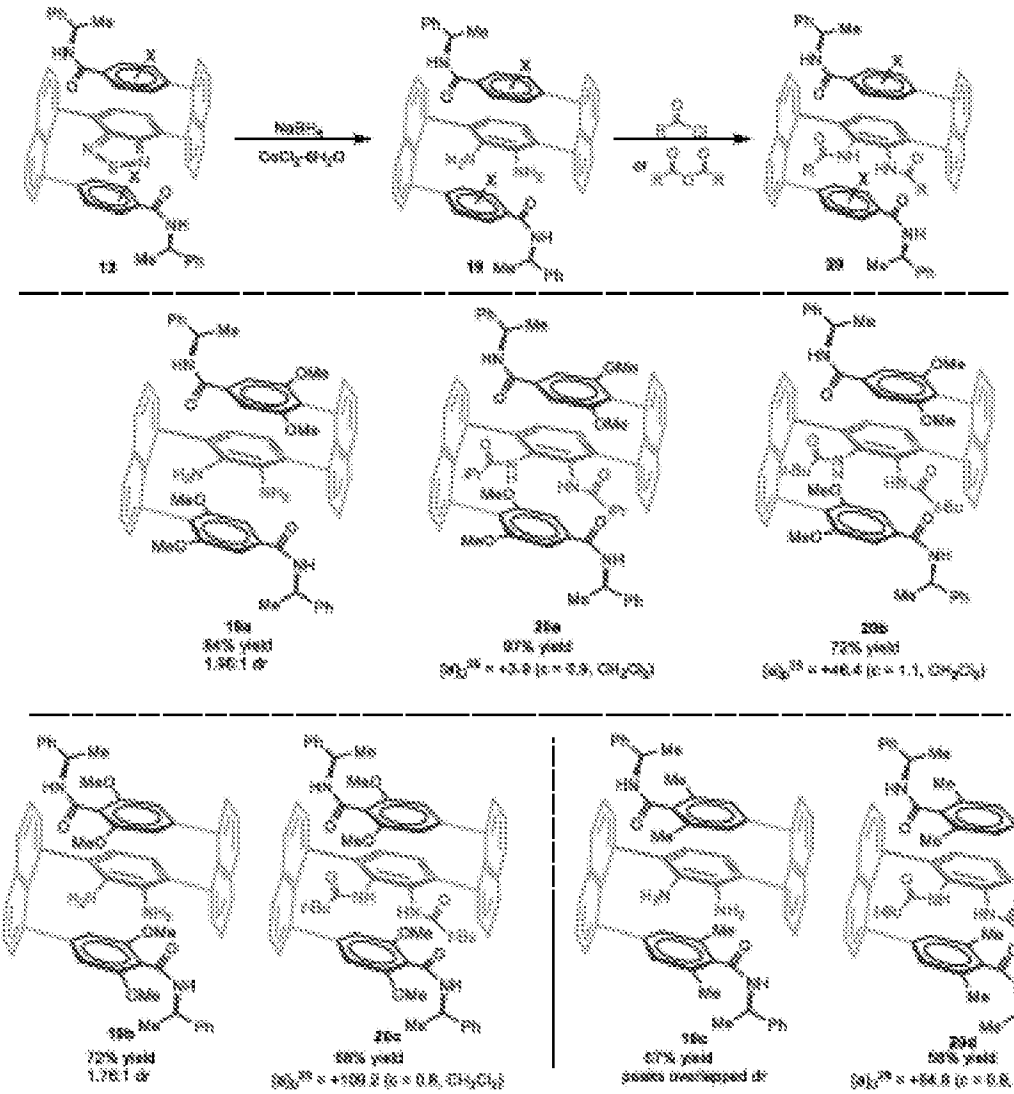


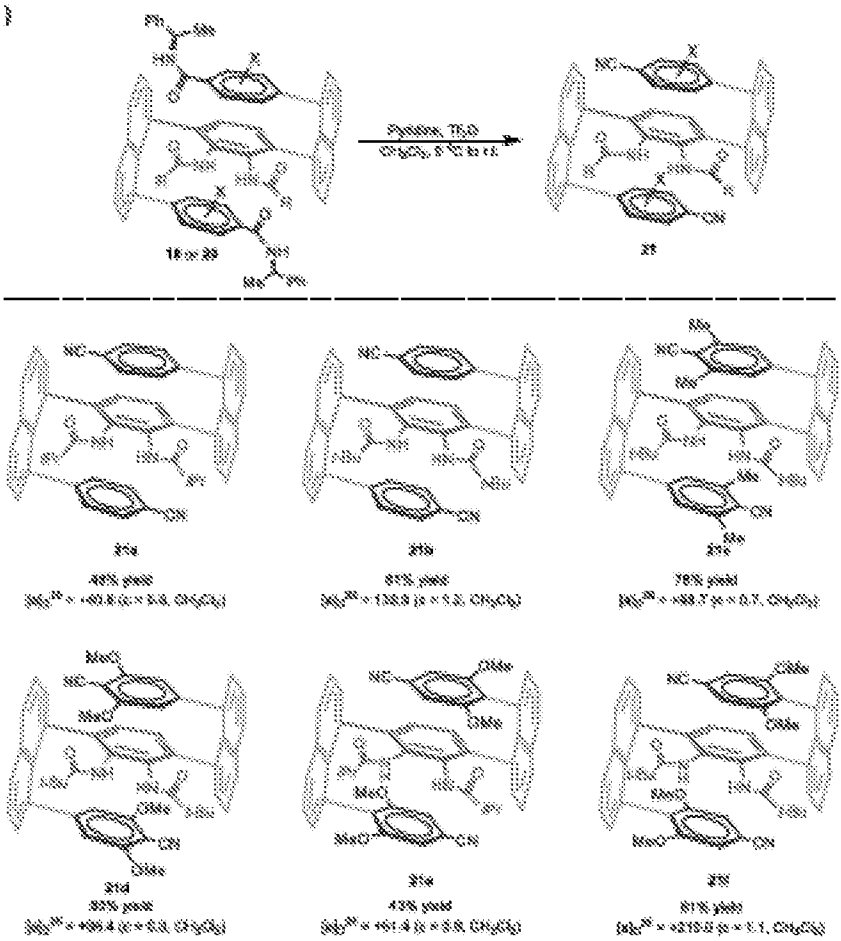
14b

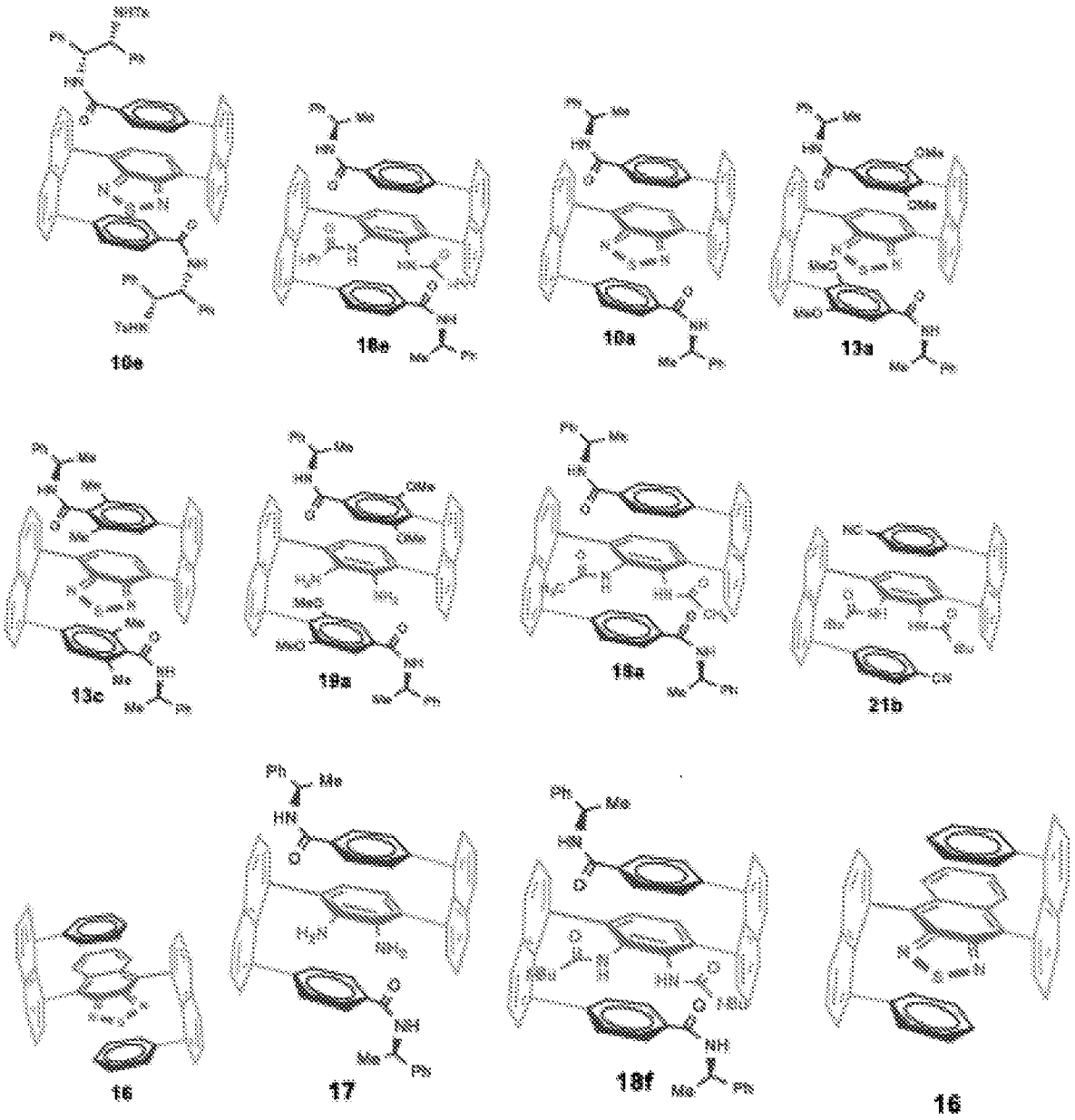


15

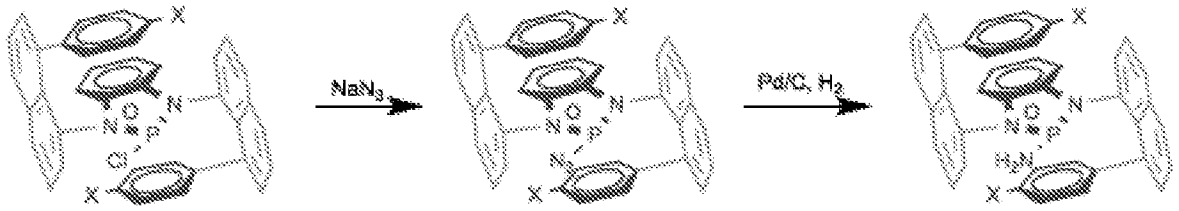








18. A method of making a multi-layer 3D material comprising: a first, a second, and a third layer, wherein each of the layers are arranged in a nearly parallel fashion with chirality along a center plane comprising:

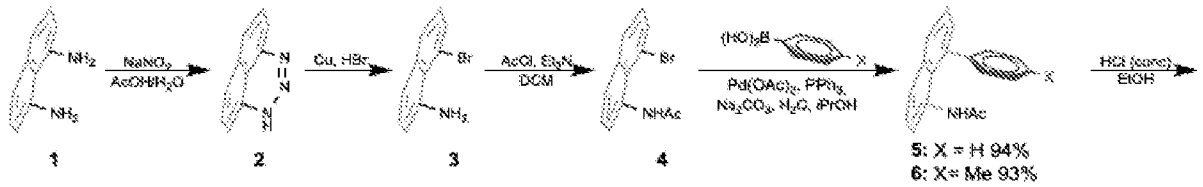


11a: X = H
12a: X= Me

13a: X = H
14a: X= Me

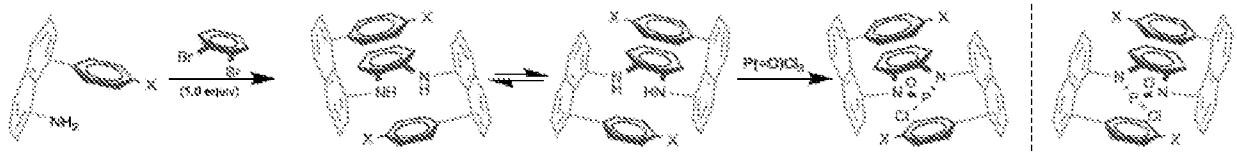
15a: X = H 81%
16a: X= Me 78%

; or



1 **2** **3** **4**

5: X = H 94%
6: X= Me 93%

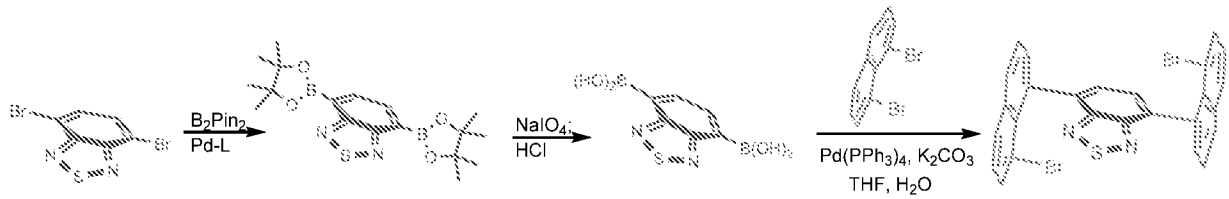


7: X = H 98%
8: X= Me 96%

9: X = H 27%
10: X= Me 24%

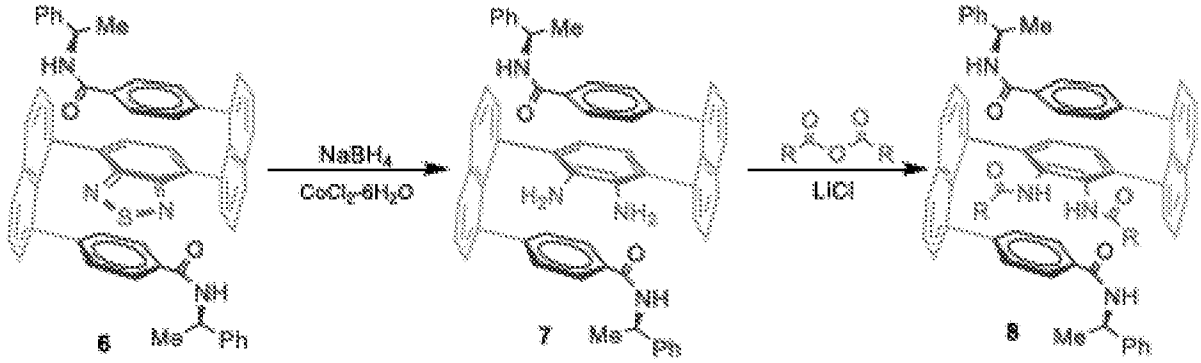
a **11: X = H 39%** **b**
12: X= Me 45%

;



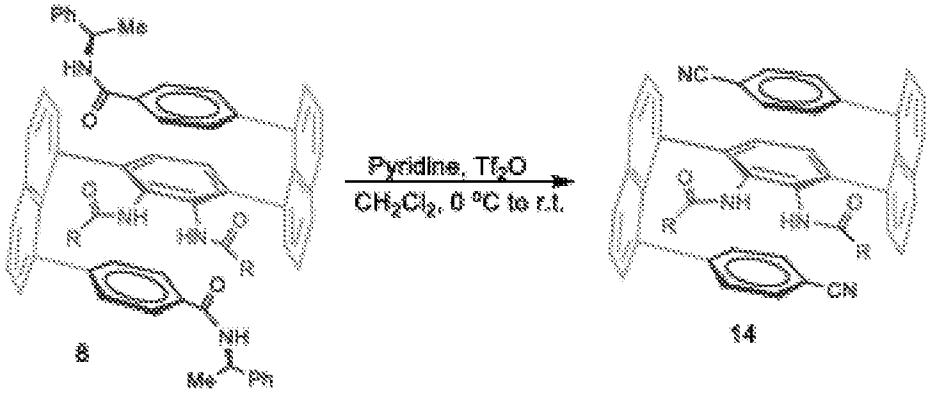
82% 95% 55%

;



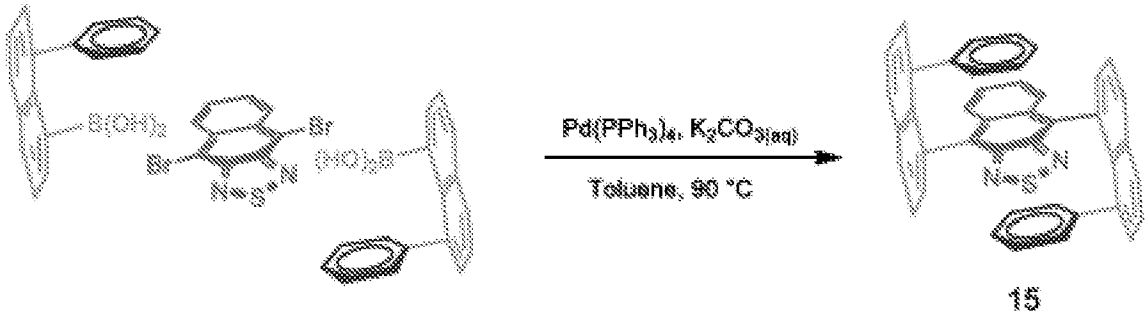
6 **7** **8**

;



8 14

; or

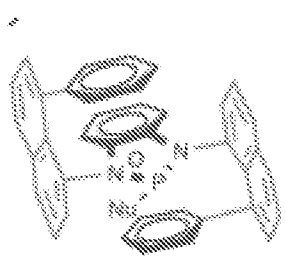


15

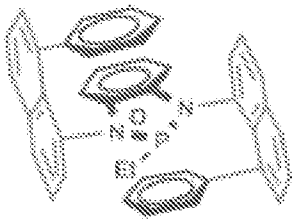
.

19. The method of claim 18, wherein the multi-layer 3D material is a 2-amino-1,3-bis(8-phenylnaphthalen-1-yl)-1,3-dihydrobenzo[d][1,3,2]diazaphosphole 2-oxide (**15a**).

20. The method of claim 18, wherein the multi-layer 3D material is selected from at least one of:



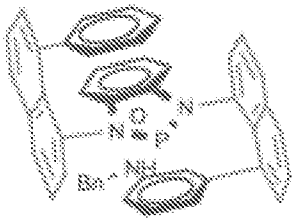
;



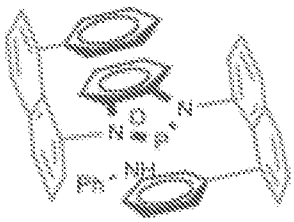
20 ;



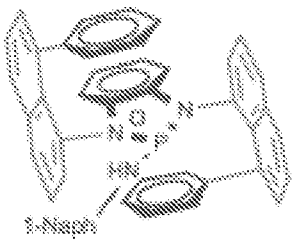
21 ;



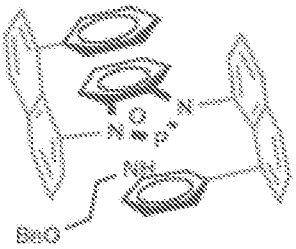
22 ;



23 ;

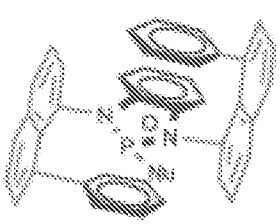


24 ; or



25 .

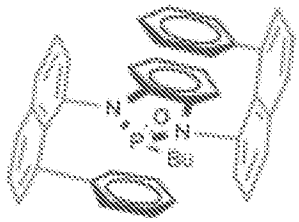
21. The method of claim 18, wherein the multi-layer 3D material is selected from at least one of:



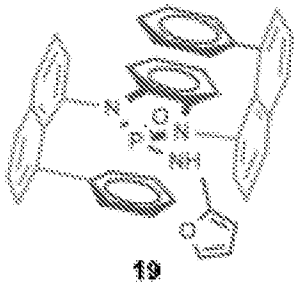
;



17 ;



18 ; or



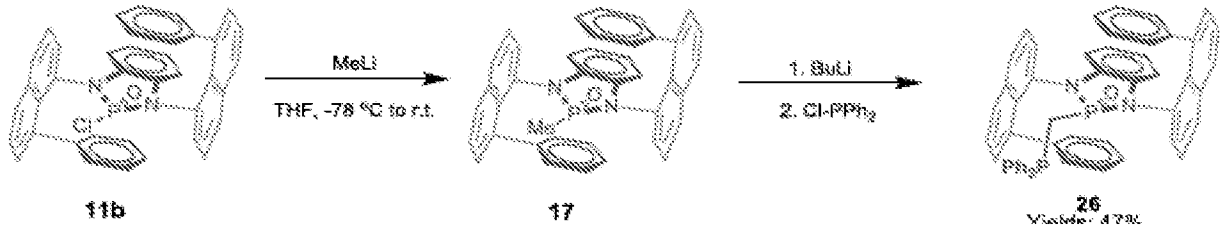
19 .

5 22. The method of claim 18, wherein the product of formula comprises:



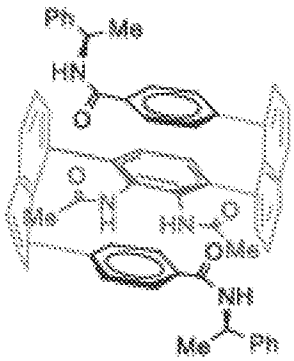
26

is made by a method comprising:



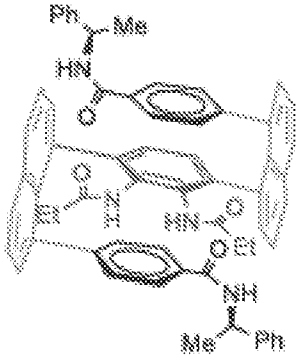
11b 17 26 .

23. The method of claim 18, wherein the product of formula comprises:



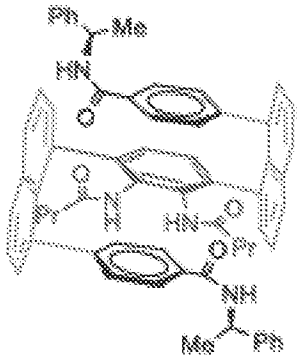
yield 56%

8a



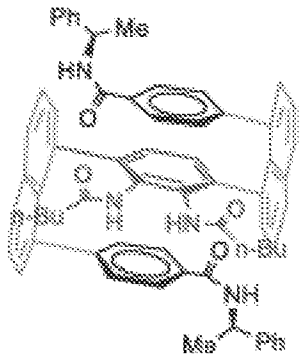
yield 39%

8b



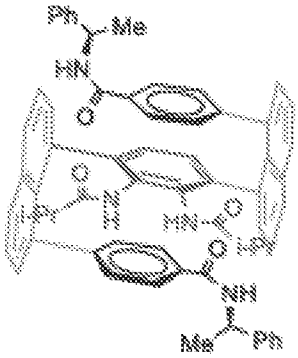
yield 42%

8c



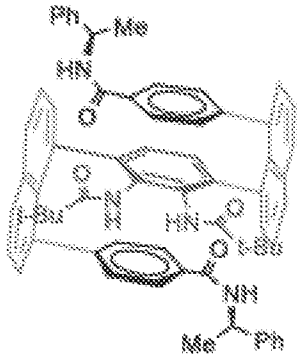
yield 47%

8d



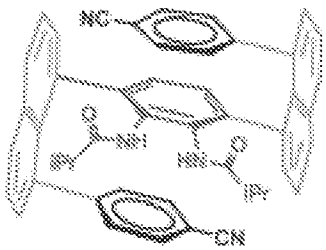
yield 38%, $[\alpha]_D^{25}$ = 92°

8e

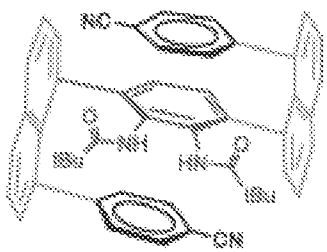


yield 31%, $[\alpha]_D^{25}$ = 58°

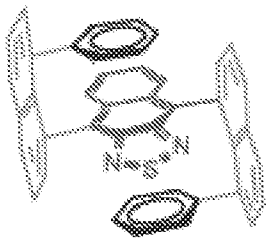
8f



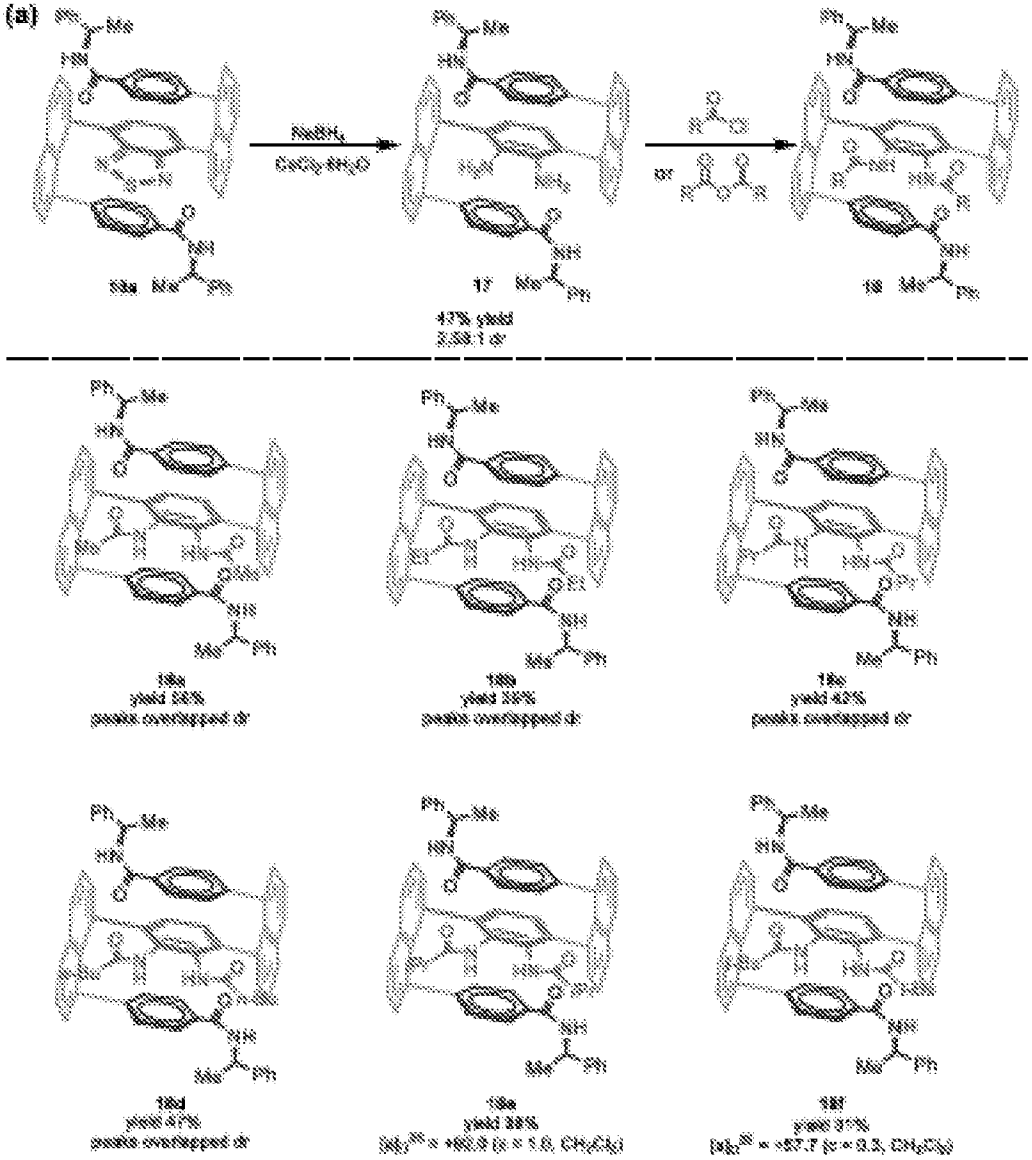
14a

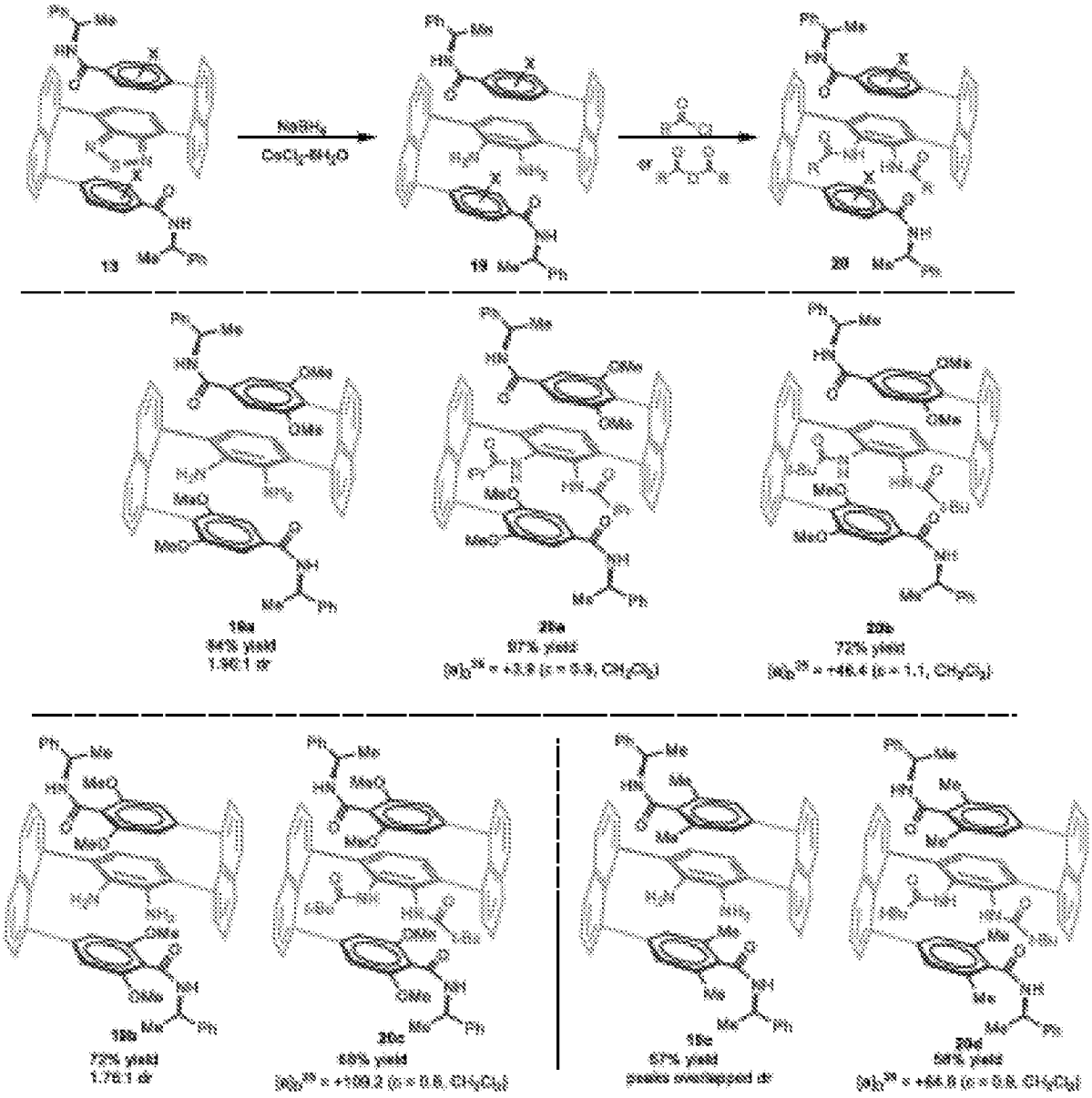


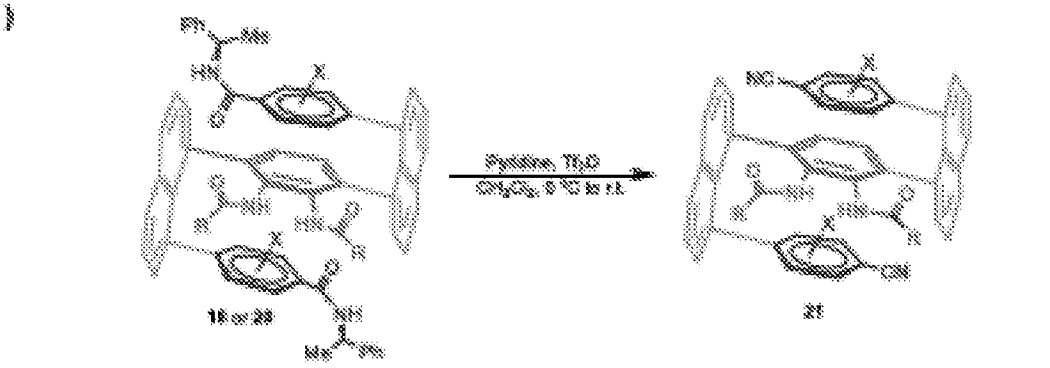
14b

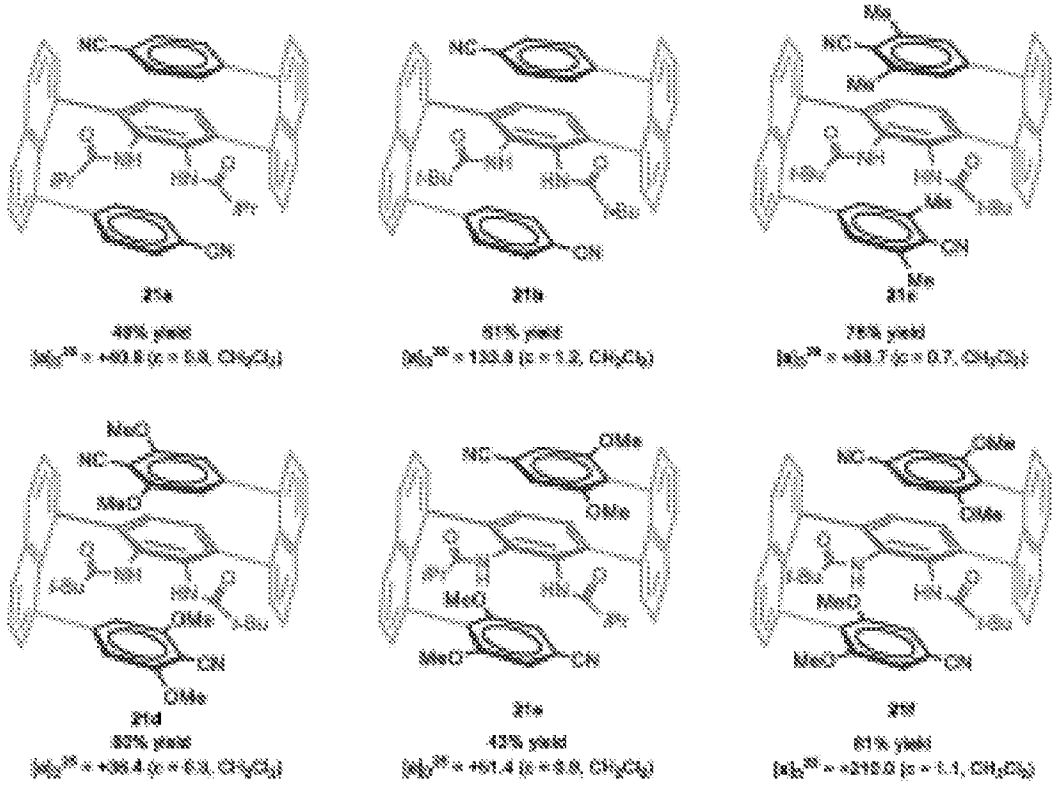


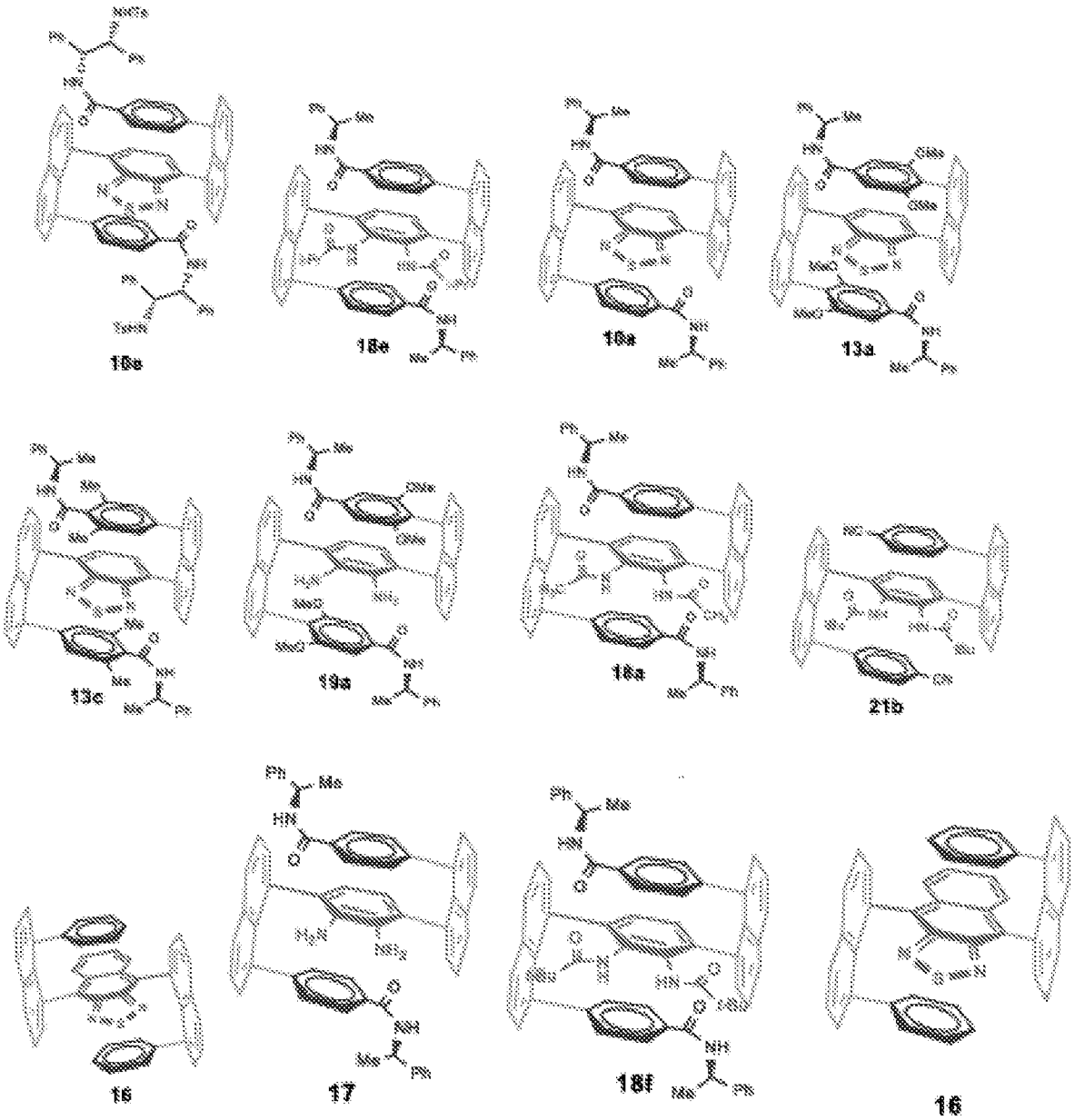
15







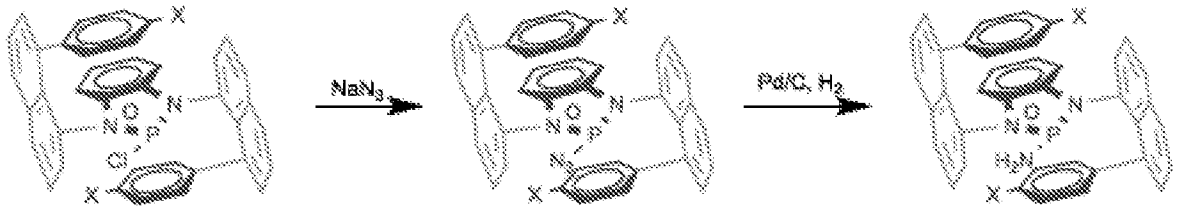




24. A Group-Assisted Purification (GAP) catalyst comprising:

a multi-layer 3D material comprising: a first, a second, and a third layer, wherein each of the layers are arranged in a nearly parallel fashion with chirality along a center plane comprising the GAP-catalyst anchored by *N,N*-phosphonyl groups.

25. The catalyst of claim 24, the multi-layer 3D material comprises a first, a second, and a third layer, wherein each of the layers are arranged in a nearly parallel fashion with chirality along a center plane comprising:

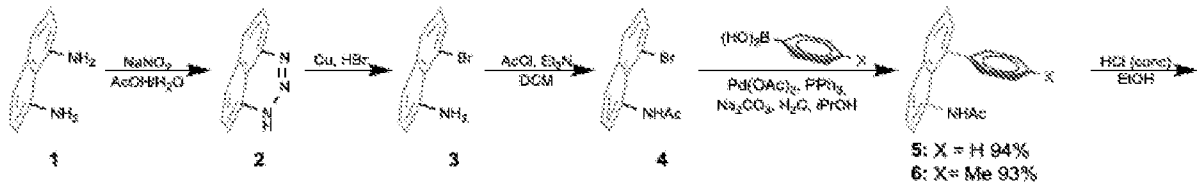


11a: X = H
12a: X= Me

13a: X = H
14a: X= Me

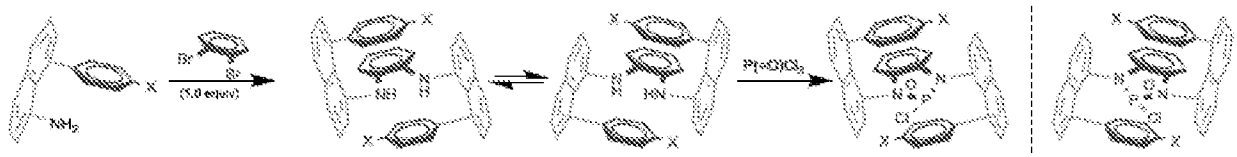
15a: X = H 81%
16a: X= Me 78%

; or



1 2 3 4

5: X = H 94%
6: X= Me 93%



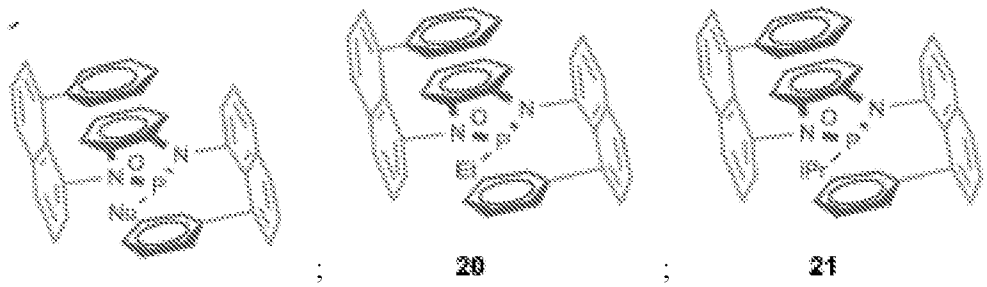
7: X = H 98%
8: X= Me 96%

9: X = H 27%
10: X= Me 24%

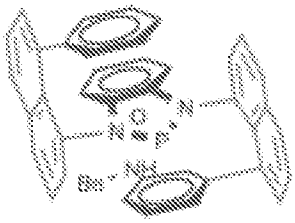
a **11: X = H 39%**
12: X= Me 45% b

26. The catalyst of claim 24, wherein the multi-layer 3D material is a 2-amino-1,3-bis(8-phenylnaphthalen-1-yl)-1,3-dihydrobenzo[d][1,3,2]diazaphosphole 2-oxide (**15a**).

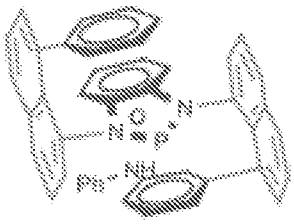
27. The catalyst of claim 24, wherein the multi-layer 3D material is selected from at least one of:



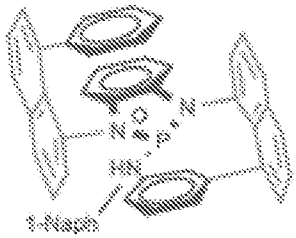
; **20** ; **21** ;



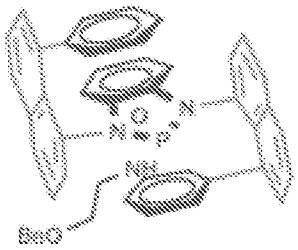
22 ;



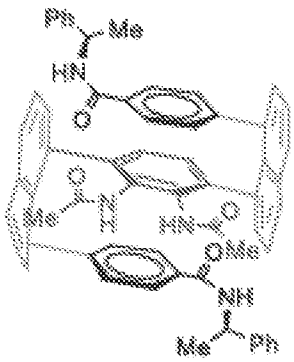
23 ;



24 ; or

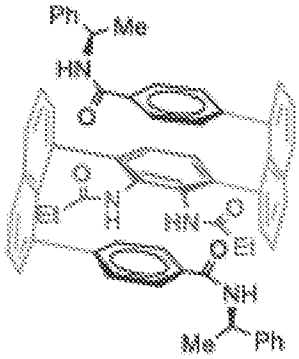


25



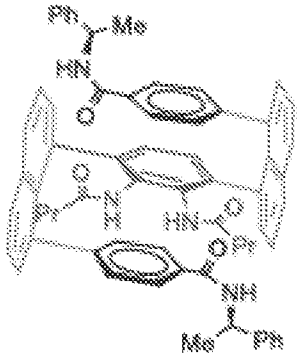
yield 56%

8a



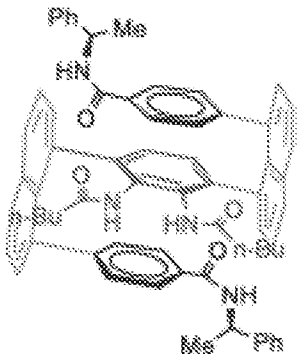
yield 39%

8b



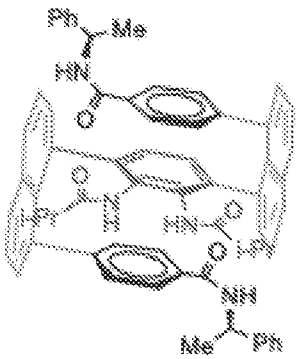
yield 42%

8c



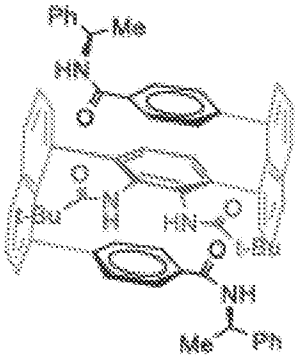
yield 47%

8d



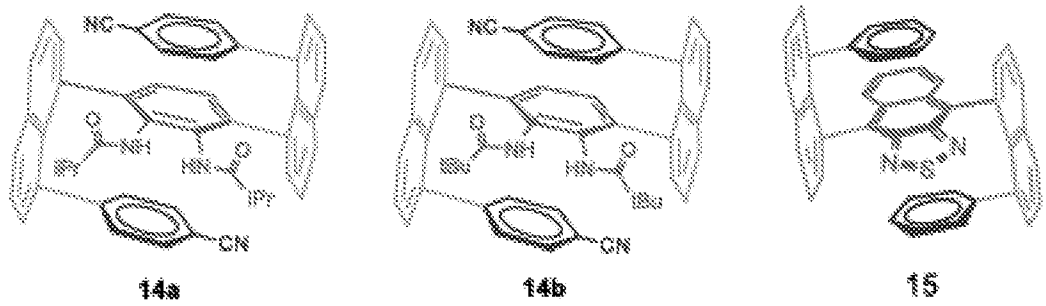
yield 38%, $[\alpha]_D^{25}$ = 82°

8e

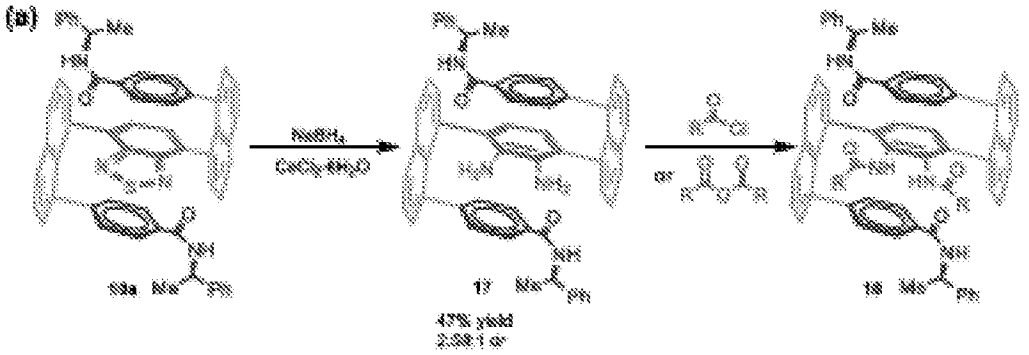


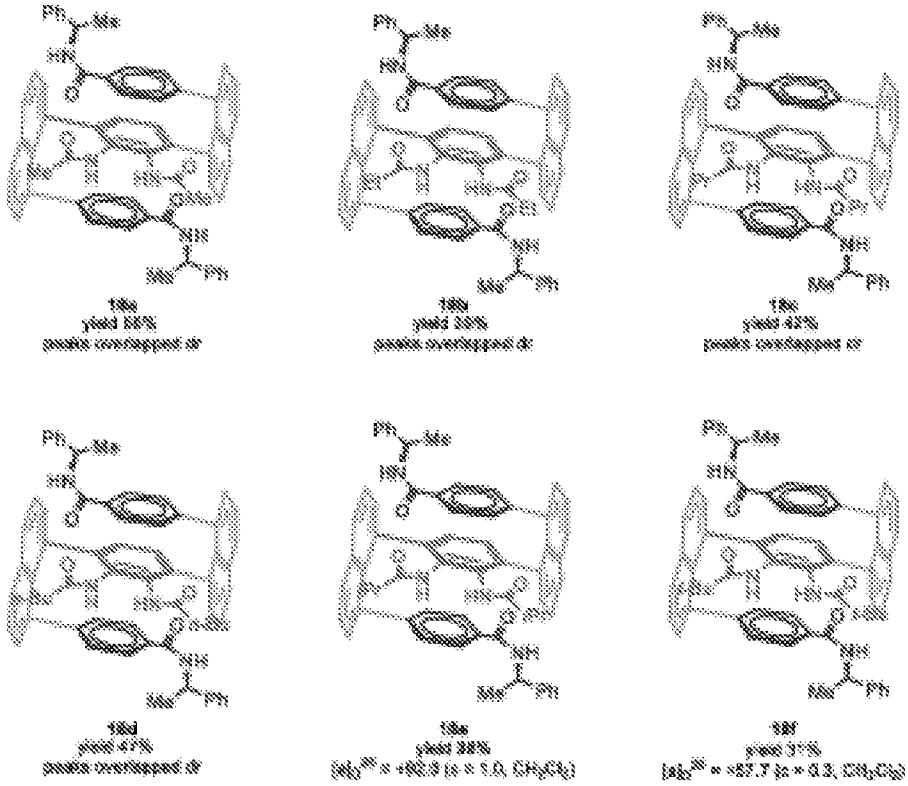
yield 31%, $[\alpha]_D^{25}$ = 58°

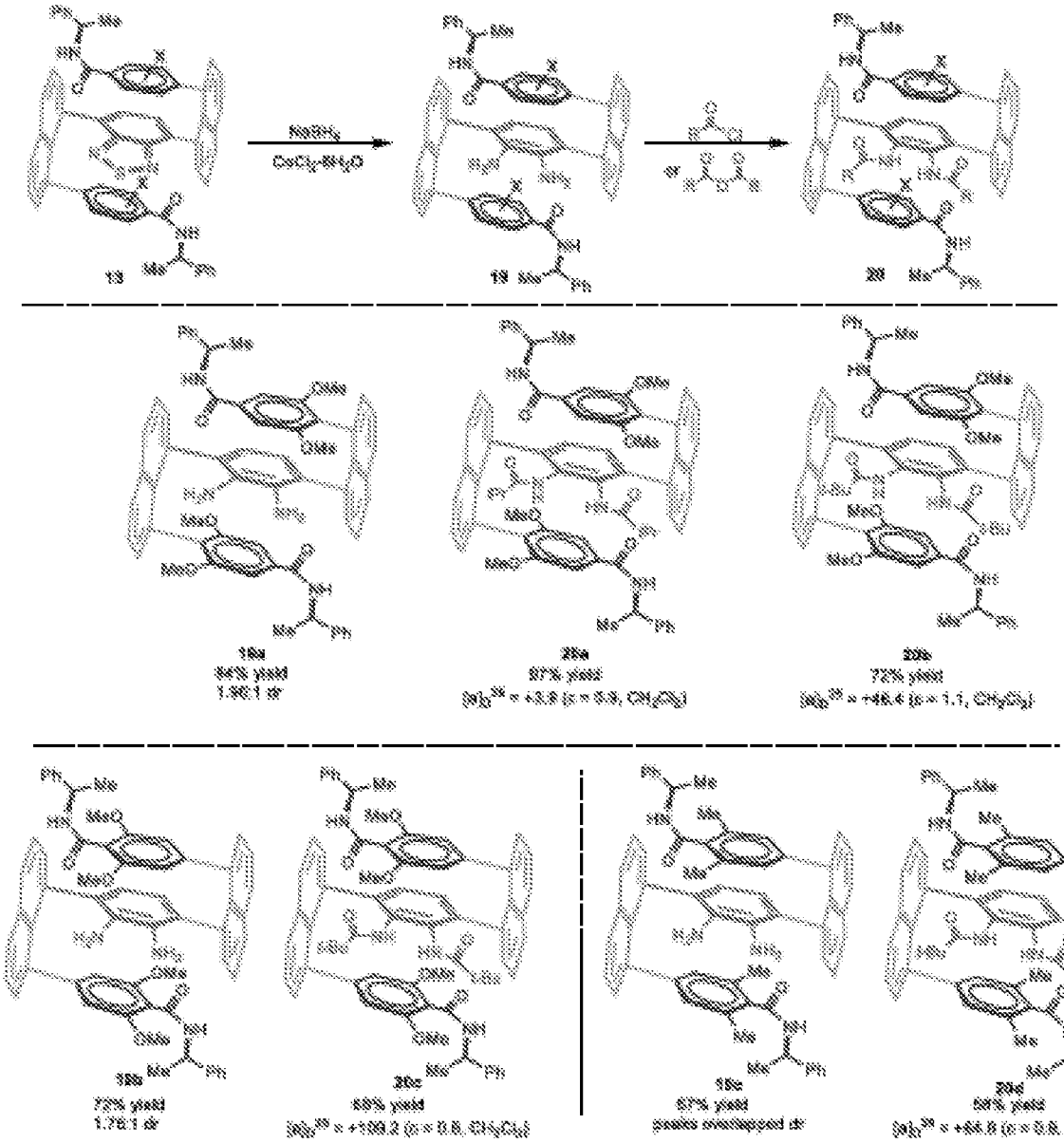
8f

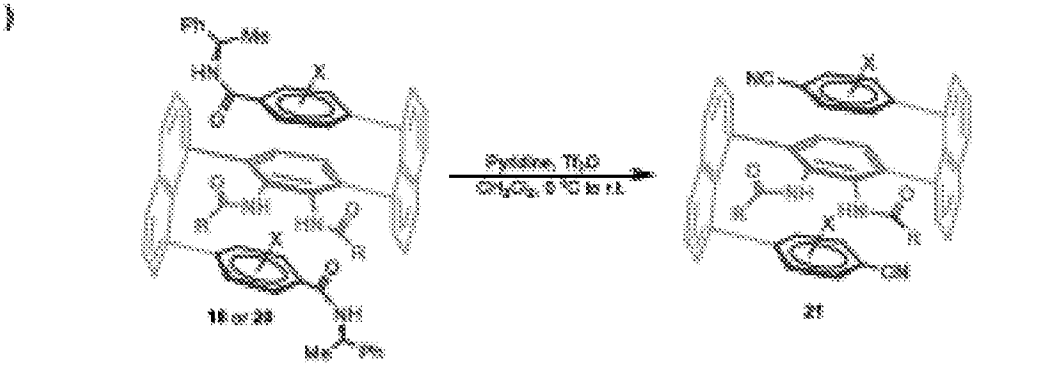


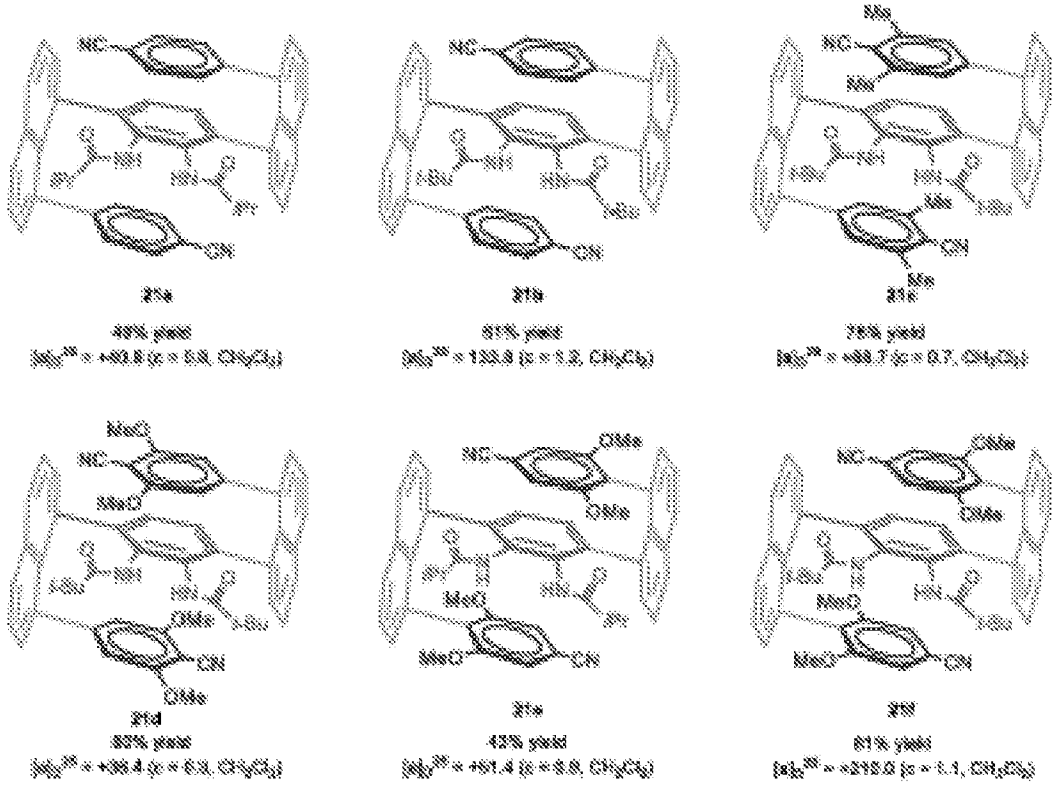
14a 14b 15

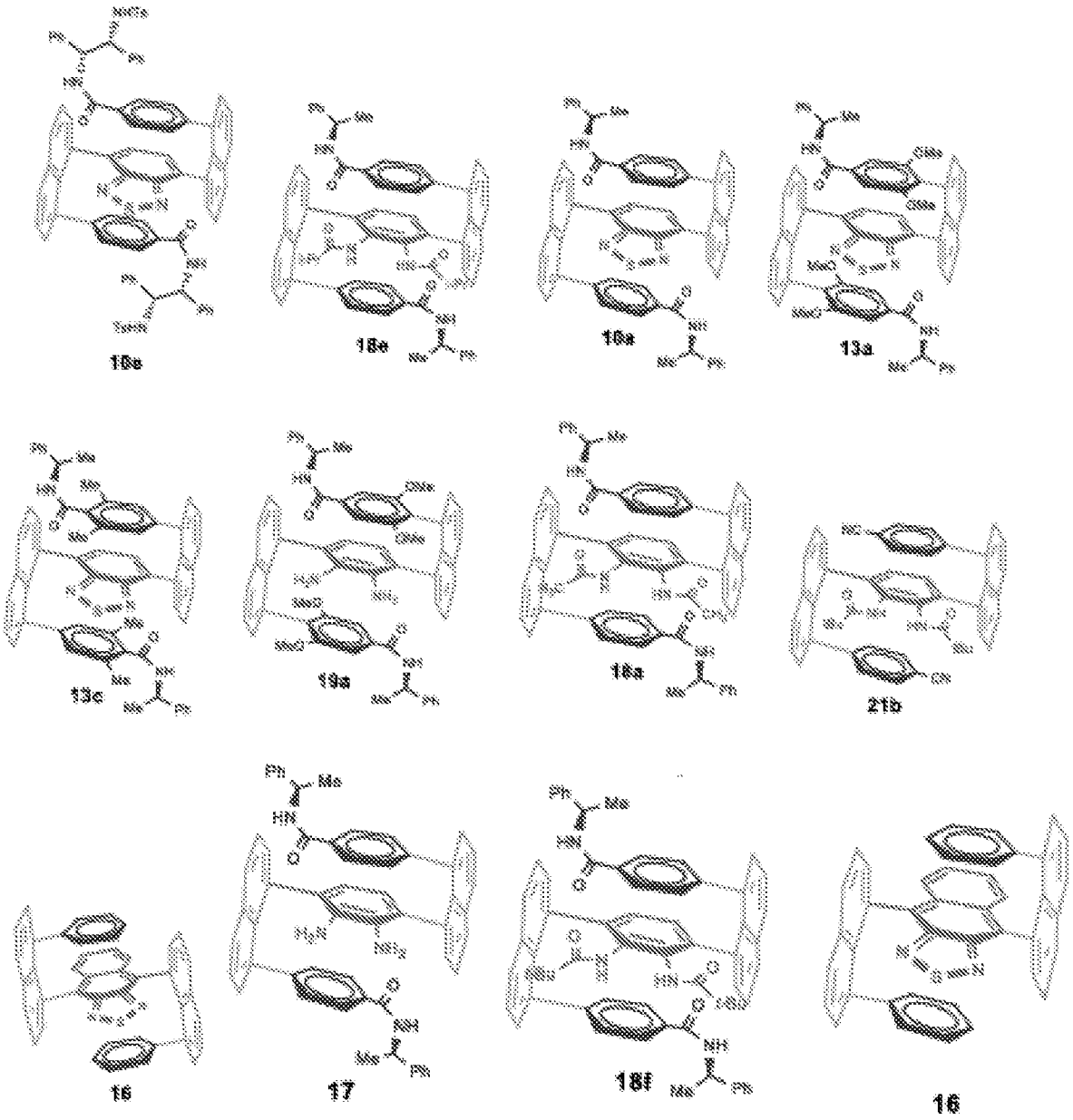




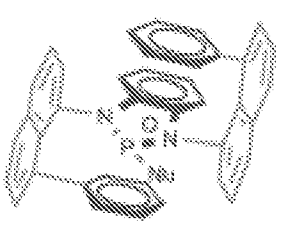




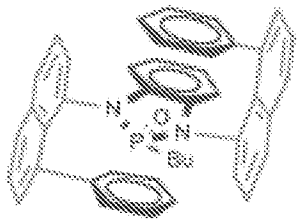




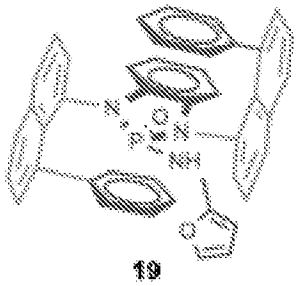
28. The catalyst of claim 24, wherein the multi-layer 3D material is selected from at least one of:



; 

17 ; 

18 ; or



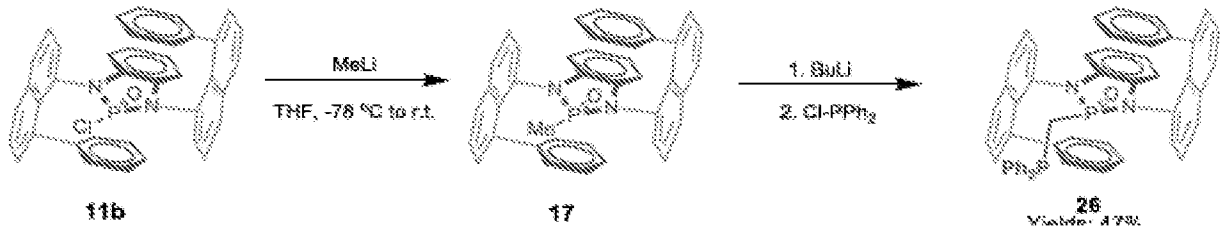
19 .

29. The catalyst of claim 24, wherein the product of formula:



26

is made by a method comprising:



11b 17 26 .

30. A method of conducting a synthetic reaction comprising:

providing a Group-Assisted Purification (GAP) catalyst comprising a multi-layer 3D material comprising: a first, a second, and a third layer, wherein each of the layers are arranged in a nearly parallel fashion with chirality along a center plane comprising the GAP-catalyst anchored by *N,N*-phosphonyl groups; and

catalyzing a reaction in the presence of the GAP-catalyst.

31. The method of claim 30, wherein the multi-layer 3D material has a right-hand chirality, a left-hand chirality, or both a left- and a right-handed chirality.

32. The method of claim 30, wherein each of the first, second, and third layers are at least one of: *anti, syn,* or both *anti* and *syn* isomers.

33. The method of claim 30, wherein each of the first, second, and third layers are *N,N*-phosphornyl amides.

34. The method of claim 30, wherein each of the first, second, and third layers comprise chiral or achiral *N*-phosphonyl- or *N*-phosphinyl groups.

35. The method of claim 30, wherein each of the first, second, and third layers comprise a Multi-Layer Organic Framework (M-LOF) of single organic molecules with pseudo C_2-chiral characteristics.

36. The method of claim 30, wherein the first, the second, and the third layers have: a right-hand chirality, a left-hand chirality, or both the left- and the right-handed chirality.

37. The method of claim 30, wherein the first, the second, and the third layers each comprise a plane, and wherein: (a) one of the three planes is replaced by carbon-carbon triple bond (alkyne bridges and arms); (b) further comprising two additional layers having a right-hand chirality, a left-hand chirality, or both the left- and the right-handed chirality,

38. The method of claims 37, wherein the additional layers comprise at least one of: 4,4'-(2,7-dimethoxynaphthalene-1,8-diyl)bis(3-methoxybenzonitrile); N,N'-(1,8-bis(2-methoxyphenyl)naphthalene-2,7-diyl)bis(4-methylbenzenesulfonamide); 8,8"-dibromo-2,2",7,7"-tetramethoxy-1,1':8',1"-ternaphthalene; (1'R)-8,8"-dibromo-2',7'-dimethoxy-1,1':8',1"-ternaphthalene; wherein, Br can be H, aliphatics, aromatics; MeO can be NHAc, NHTs, NH-protection groups, aromatics, alkylyl, alkenyls; N-(1-((8-([1,1'-biphenyl]-4-yl)naphthalen-1-yl)ethynyl)naphthalen-2-yl)-4-methylbenzenesulfonamide (Ts can be Ac, Ns, Fmoc, t-Boc, CBZ, etc., para Ph can be a halo, alkyl, Aryl, CN, N3, or NHAc.

39. The method of claim 30, wherein the multi-layer 3D material is a polymer and the first, the second, and the third layers can have a right-hand chirality, a left-hand chirality, or both the left- and the right-handed chirality.

40. The method of claims 39, wherein monomers are formed into one or more additional layers that can be above, below, or both above and below the first, the second, and the third layers.

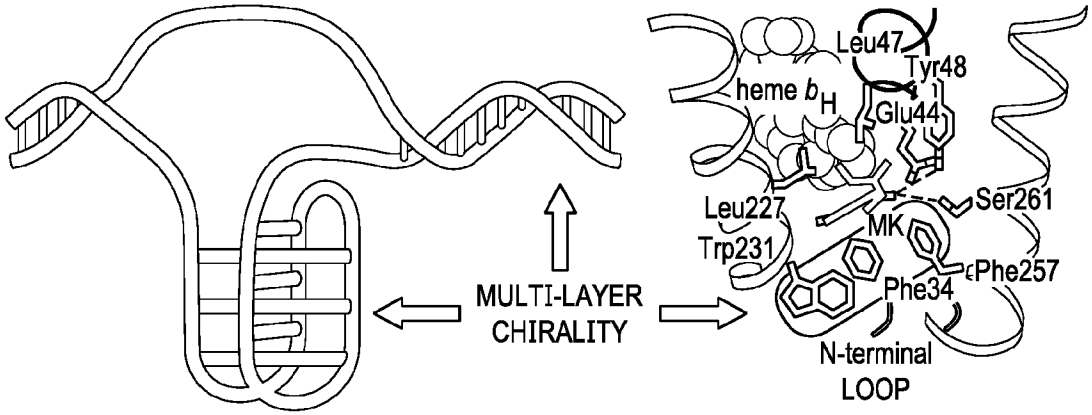


FIG. 1A
(PRIOR ART)

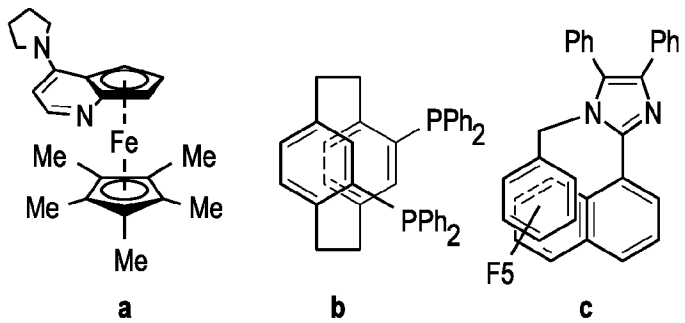
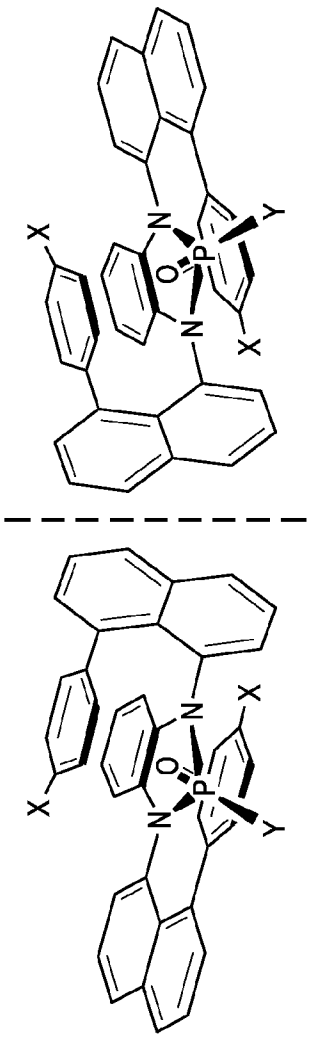


FIG. 1B
(PRIOR ART)



X = H, Me, OMe;
Y = -Cl, -N_3, -NH_2, -NHPh, -NHBn, -Me, -Et, -Bu AND -iPr,

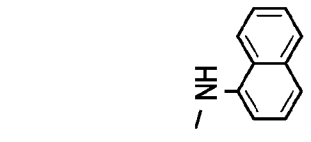


FIG. 1C

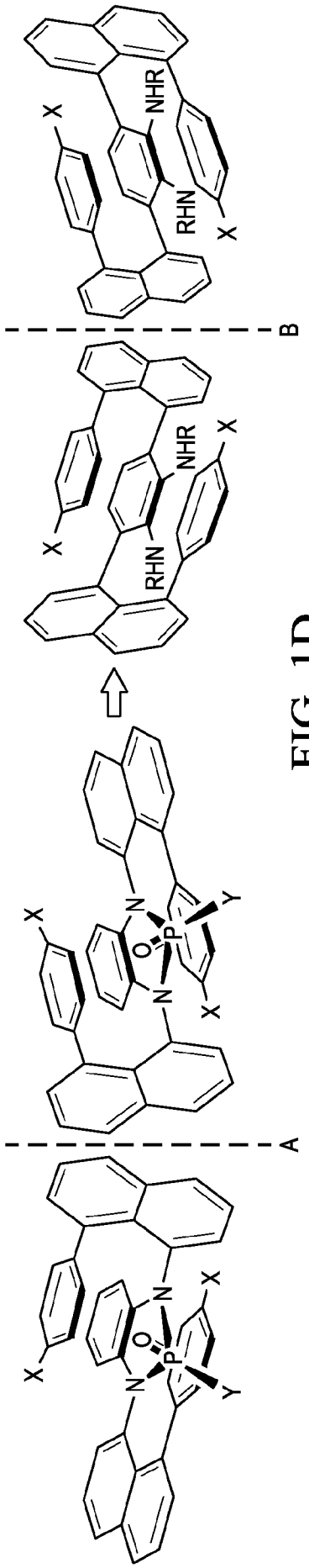


FIG. 1D

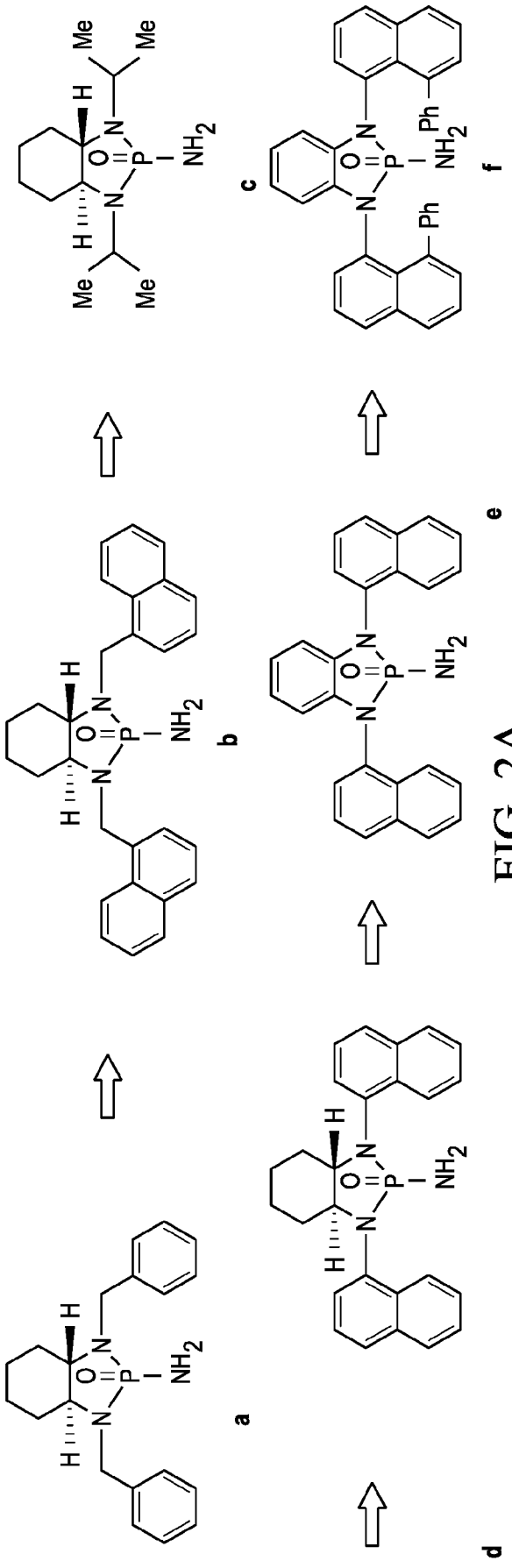


FIG. 2A

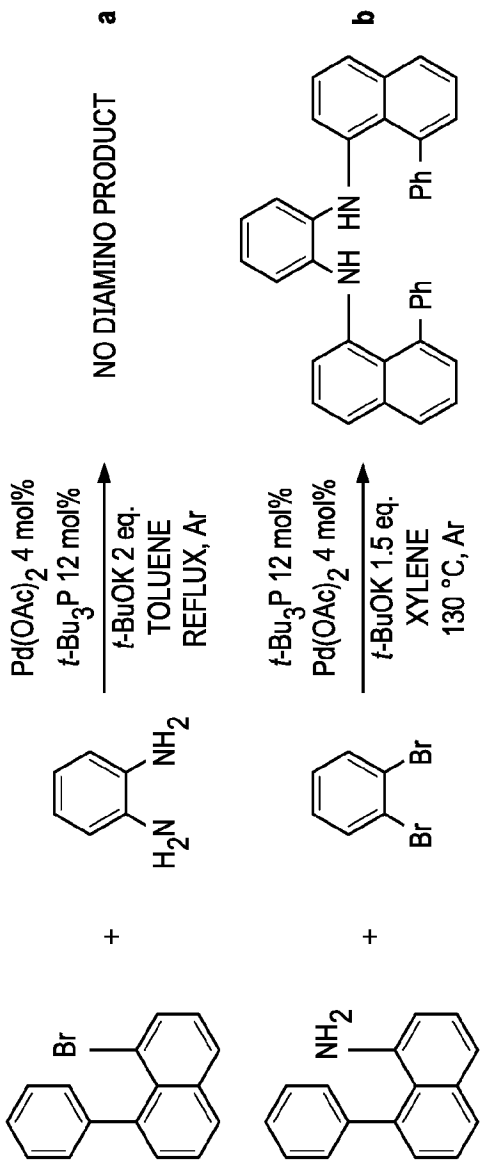

a
NO DIAMINO PRODUCT
Pd(OAc)2 4 mol%
t-Bu3P 12 mol%
t-BuOK 2 eq.
TOLUENE
REFLUX, Ar
NH2
H2N
Br
+
b
t-Bu3P 12 mol%
Pd(OAc)2 4 mol%
t-BuOK 1.5 eq.
XYLENE
130 °C, Ar
Br
Br
+
NH2
NH HN
Ph
Ph

FIG. 2B

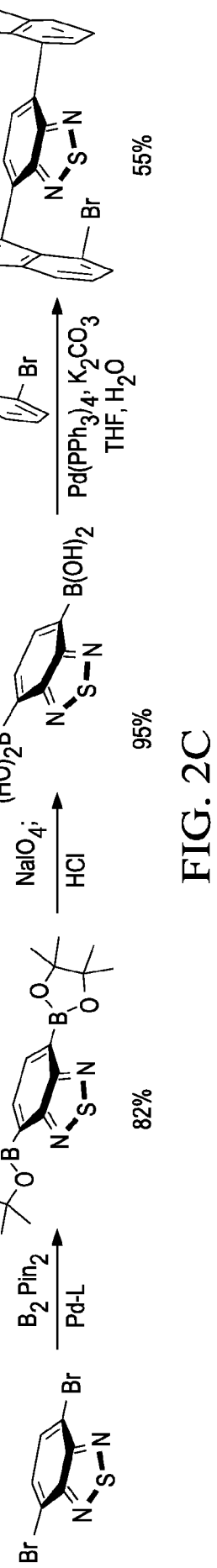

Br
Br
B2 Pin2
Pd-L
NaIO4;
HCl
(HO)2B
B(OH)2
Pd(PPh3)4, K2CO3
THF, H2O
82%
95%
55%

FIG. 2C

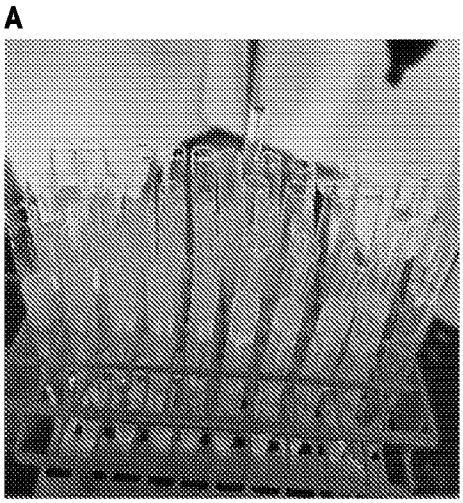


FIG. 3A

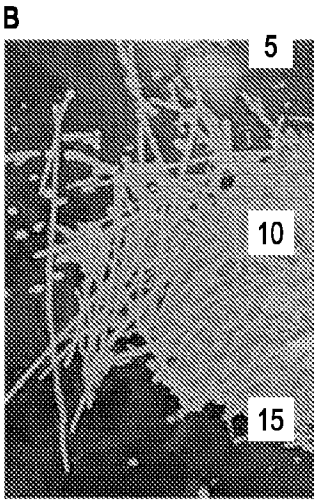


FIG. 3B

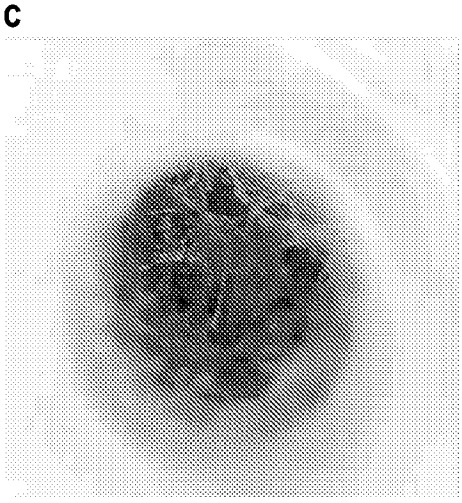


FIG. 3C

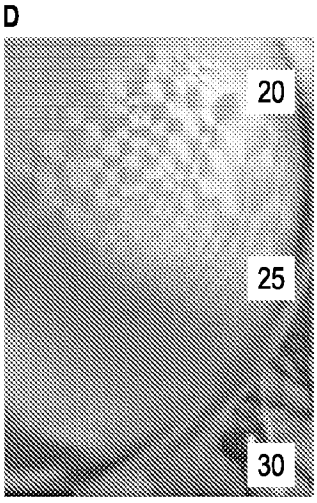


FIG. 3D

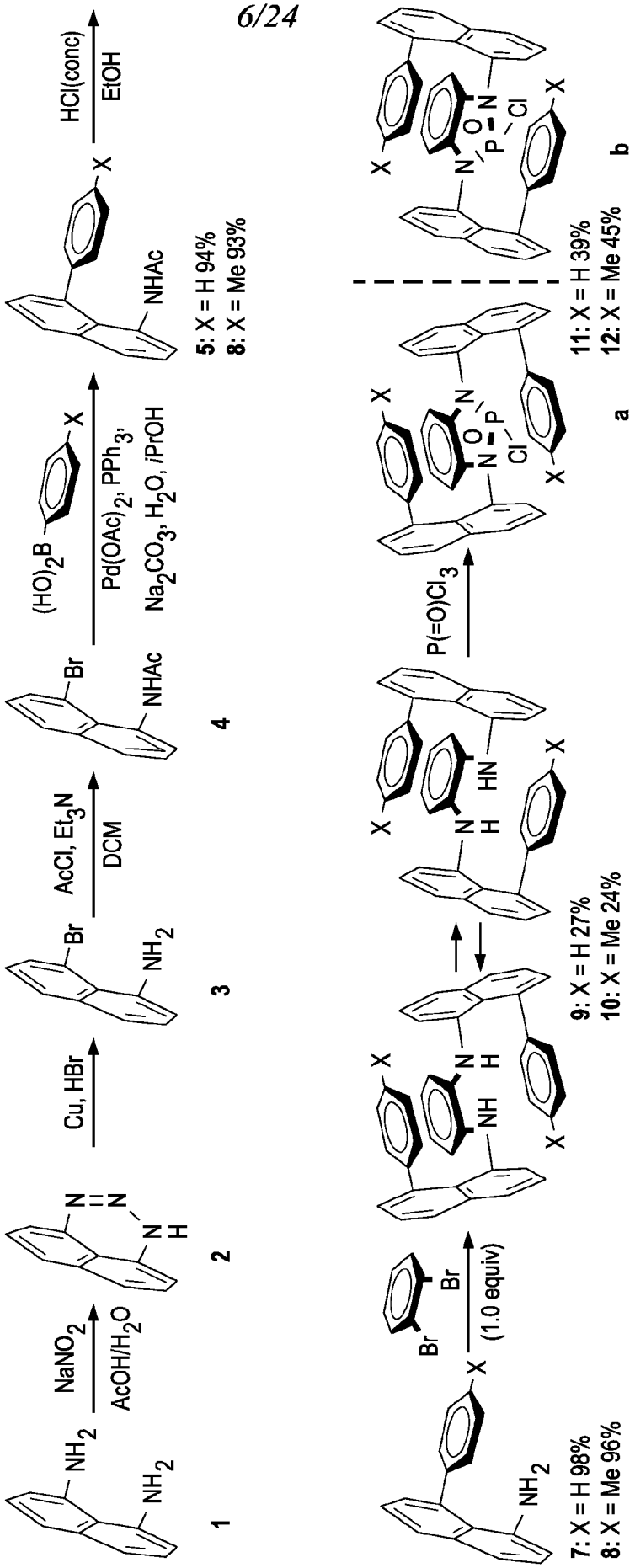

NaNO2
AcOH/H2O
Cu, HBr
AcCl, Et3N
DCM
(HO)2B
Pd(OAc)2, PPh3,
Na2CO3, H2O, iPrOH
HCl(conc)
EtOH
P(=O)Cl3
(1.0 equiv)
1
2
3
4
5: X = H 94%
8: X = Me 93%
7: X = H 98%
8: X = Me 96%
9: X = H 27%
10: X = Me 24%
11: X = H 39%
12: X = Me 45%
a
b

FIG. 4A

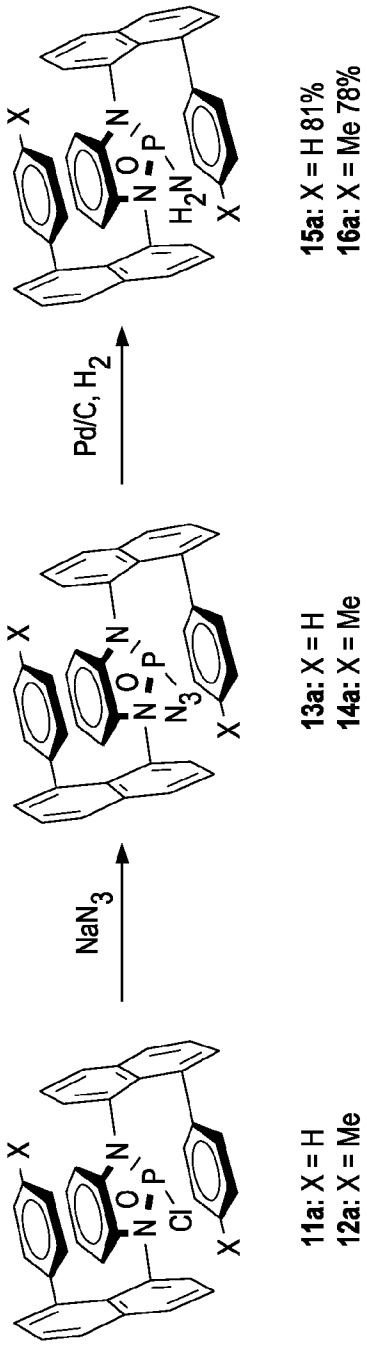


FIG. 4B

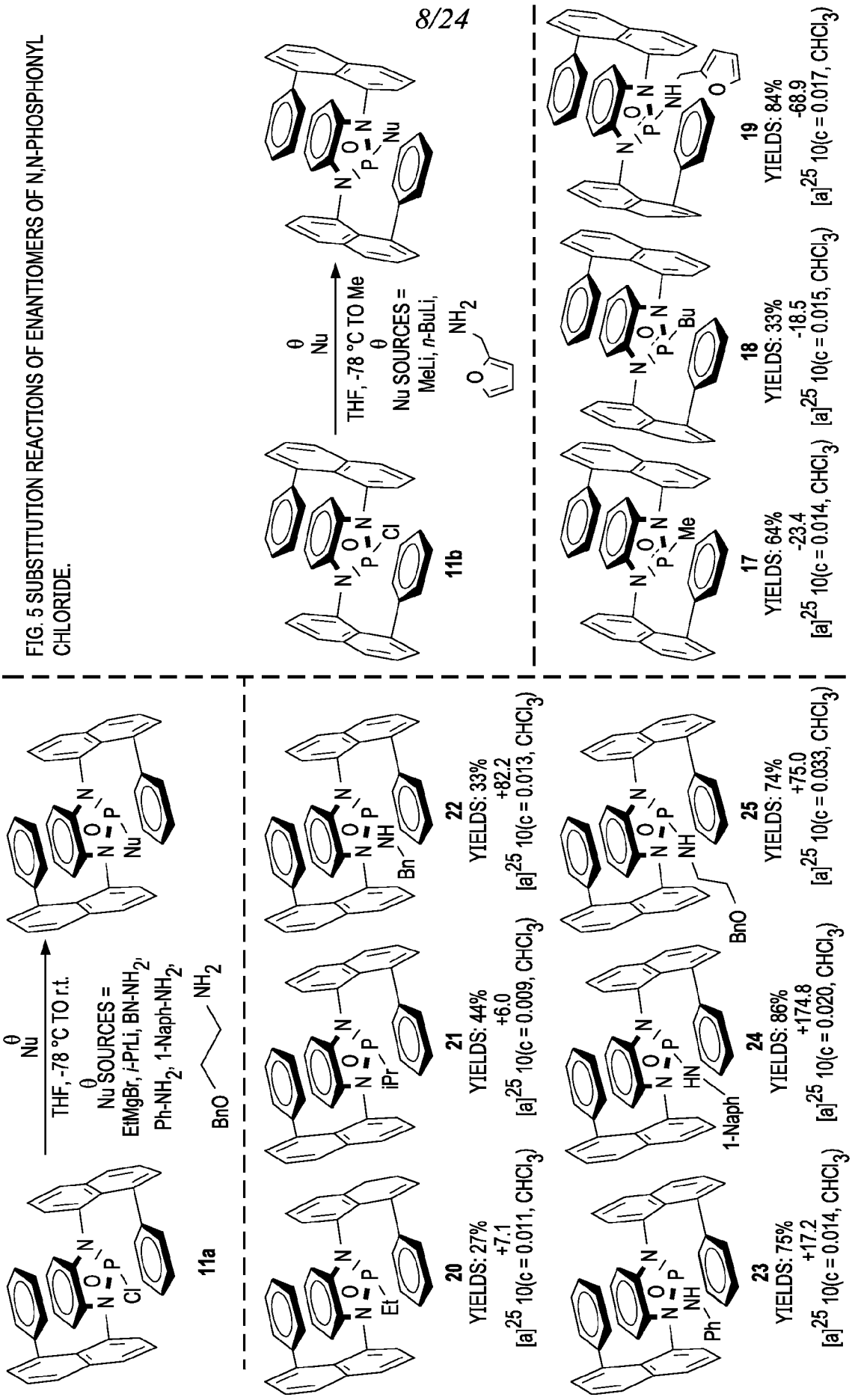

FIG. 5 SUBSTITUTION REACTIONS OF ENANTIOMERS OF N,N-PHOSPHONYL CHLORIDE.
θ Nu
THF, -78 °C TO r.t.
θ Nu SOURCES = EtMgBr, i-PrLi, BN-NH2, Ph-NH2, 1-Naph-NH2,
BnO NH2
11a
θ Nu
THF, -78 °C TO Me
θ Nu SOURCES = MeLi, n-BuLi,
NH2
O
11b
20 YIELDS: 27% +7.1 [a]25 10(c = 0.011, CHCl3)
21 YIELDS: 44% +6.0 [a]25 10(c = 0.009, CHCl3)
22 YIELDS: 33% +82.2 [a]25 10(c = 0.013, CHCl3)
23 YIELDS: 75% +17.2 [a]25 10(c = 0.014, CHCl3)
24 YIELDS: 86% +174.8 [a]25 10(c = 0.020, CHCl3)
25 YIELDS: 74% +75.0 [a]25 10(c = 0.033, CHCl3)
17 YIELDS: 64% -23.4 [a]25 10(c = 0.014, CHCl3)
18 YIELDS: 33% -18.5 [a]25 10(c = 0.015, CHCl3)
19 YIELDS: 84% -68.9 [a]25 10(c = 0.017, CHCl3)

FIG. 5

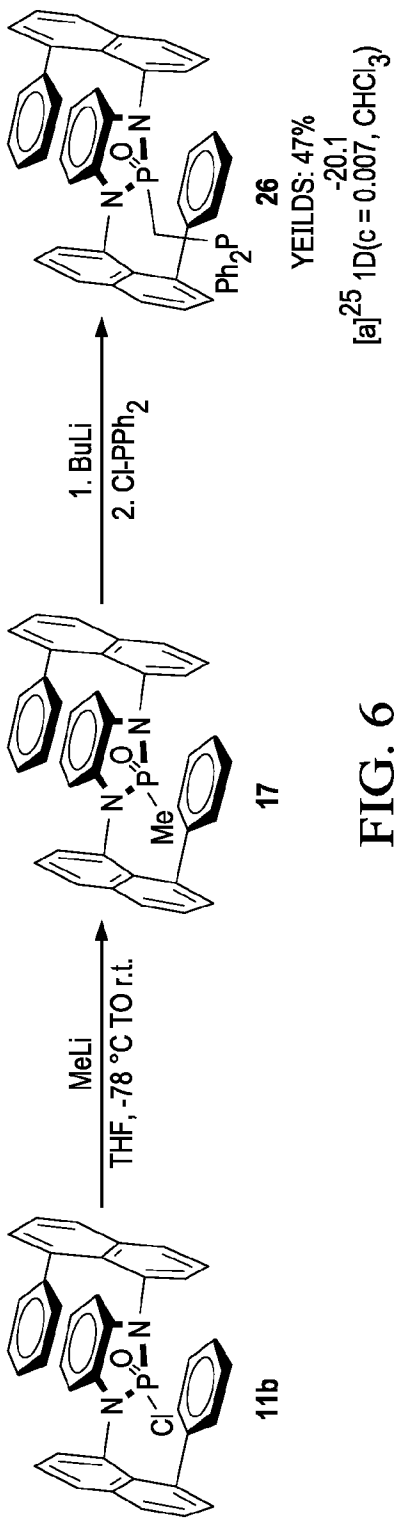

11b
MeLi
THF, -78 °C TO r.t.
17
1. BuLi
2. Cl-PPh2
26
YEILDS: 47%
-20.1
[a]25 1D(c = 0.007, CHCl3)

FIG. 6

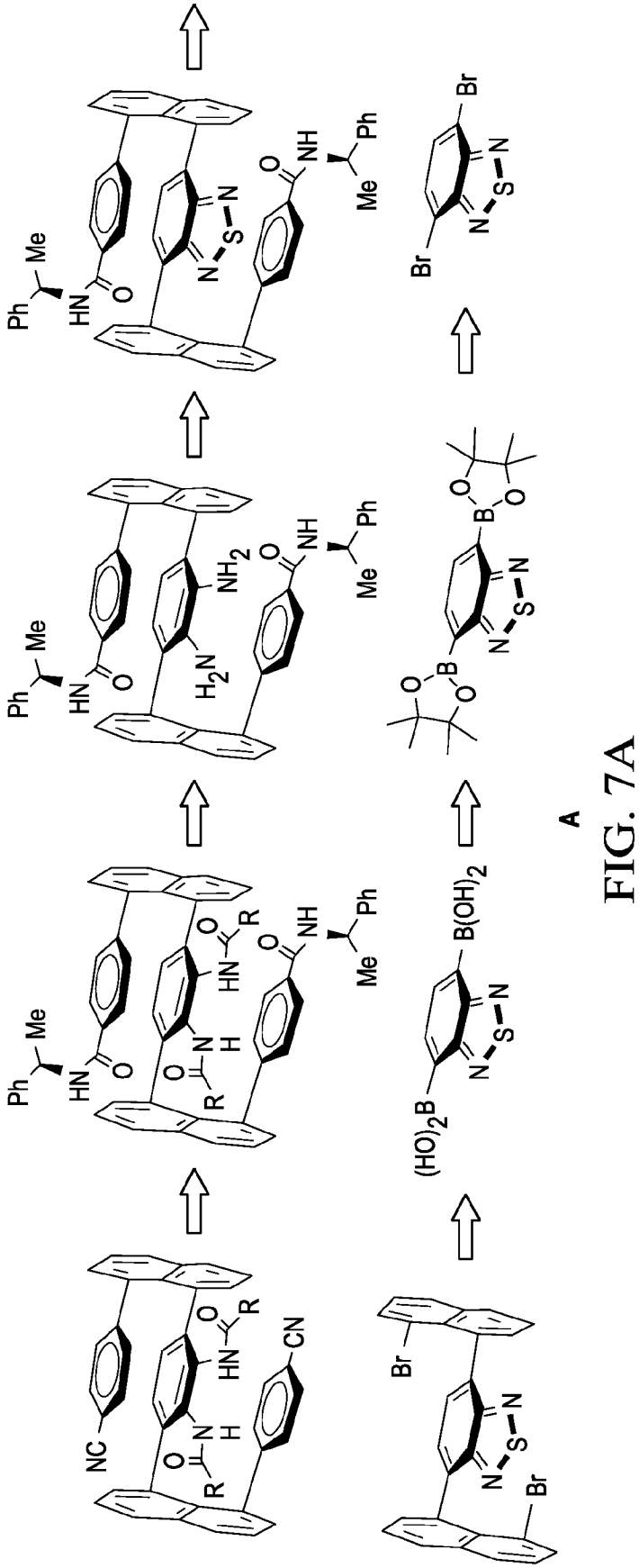
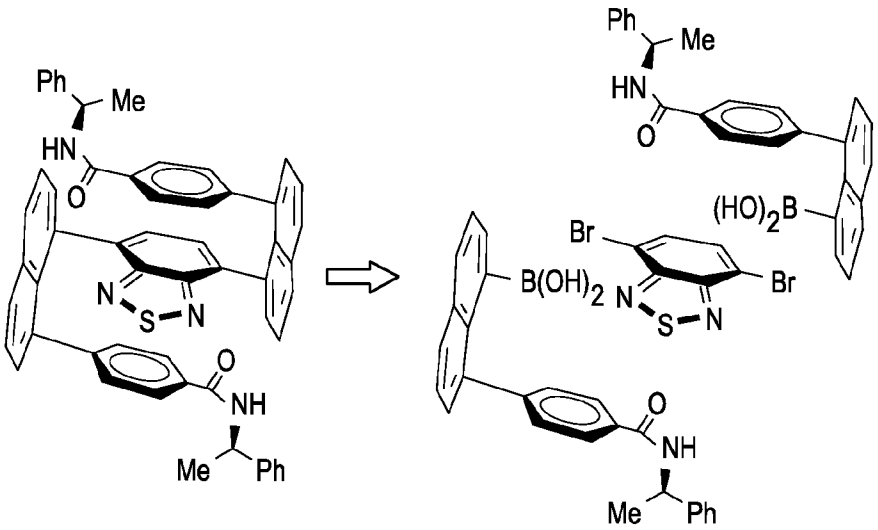
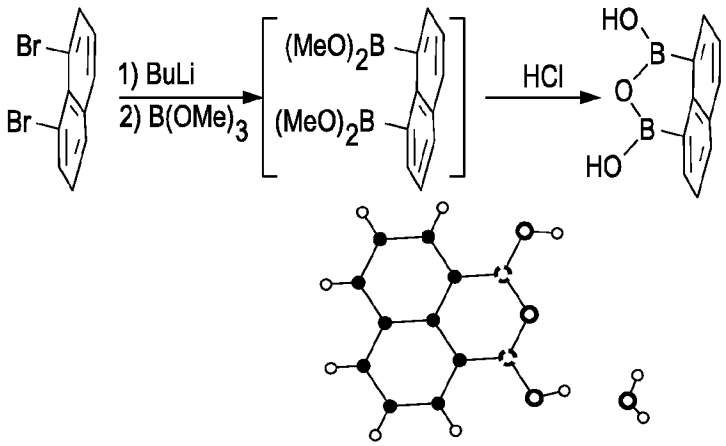


FIG. 7A



B

FIG. 7B



C

FIG. 7C

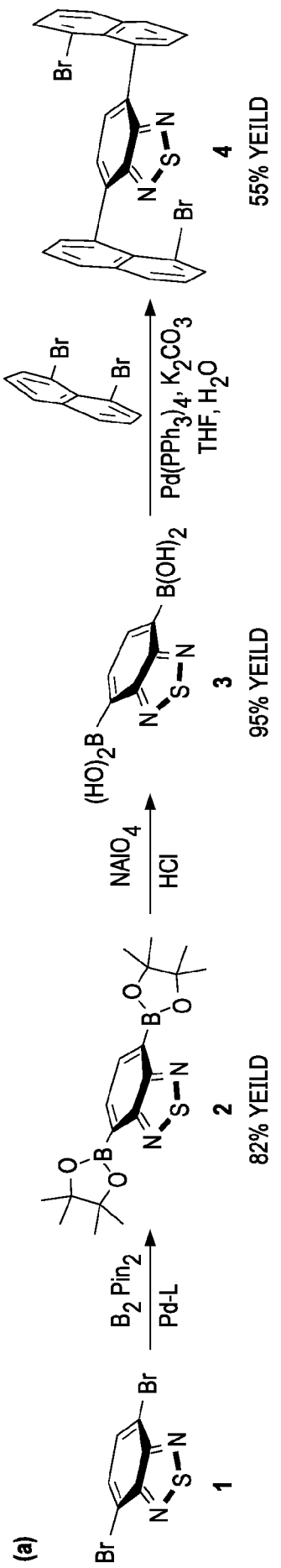

(a)
Br
Br
N
S
N
1
B2 Pin2
Pd-L
O
O
B
B
O
O
2
82% YEILD
NAIO4
HCl
(HO)2B
B(OH)2
3
95% YEILD
Pd(PPh3)4, K2CO3
THF, H2O
4
55% YEILD

FIG. 8A

(b)
HO
O
B(OH)2
5
R* — NH2
R*—NH
6
6a
67% YEILD
6b
75% YEILD
6c
79% YEILD
6d
83% YEILD
6e
67% YEILD
6f
47% YEILD
1-Naph
2-Naph
NHTs
Ph
MeO
Me
H
N
HN

FIG. 8B

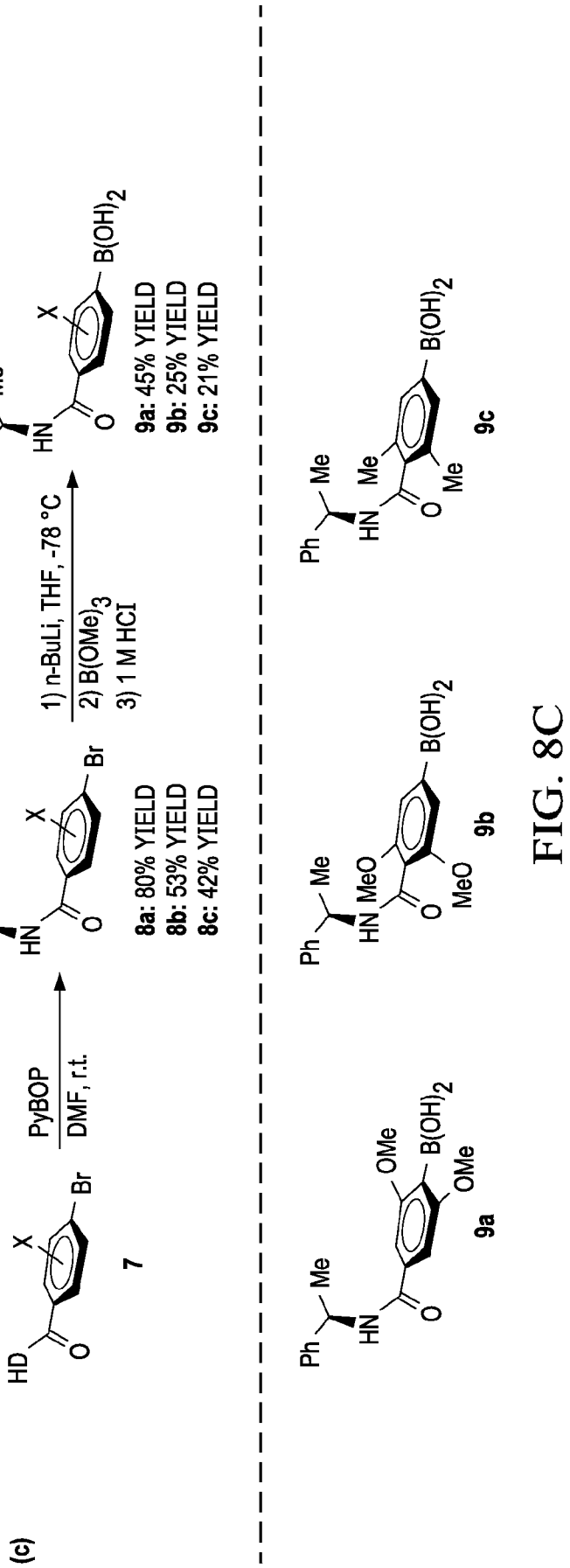

(c)
PyBOP
DMF, r.t.
1) n-BuLi, THF, -78 °C
2) B(OMe)3
3) 1 M HCl
7
8a: 80% YIELD
8b: 53% YIELD
8c: 42% YIELD
9a: 45% YIELD
9b: 25% YIELD
9c: 21% YIELD
9a
9b
9c

FIG. 8C

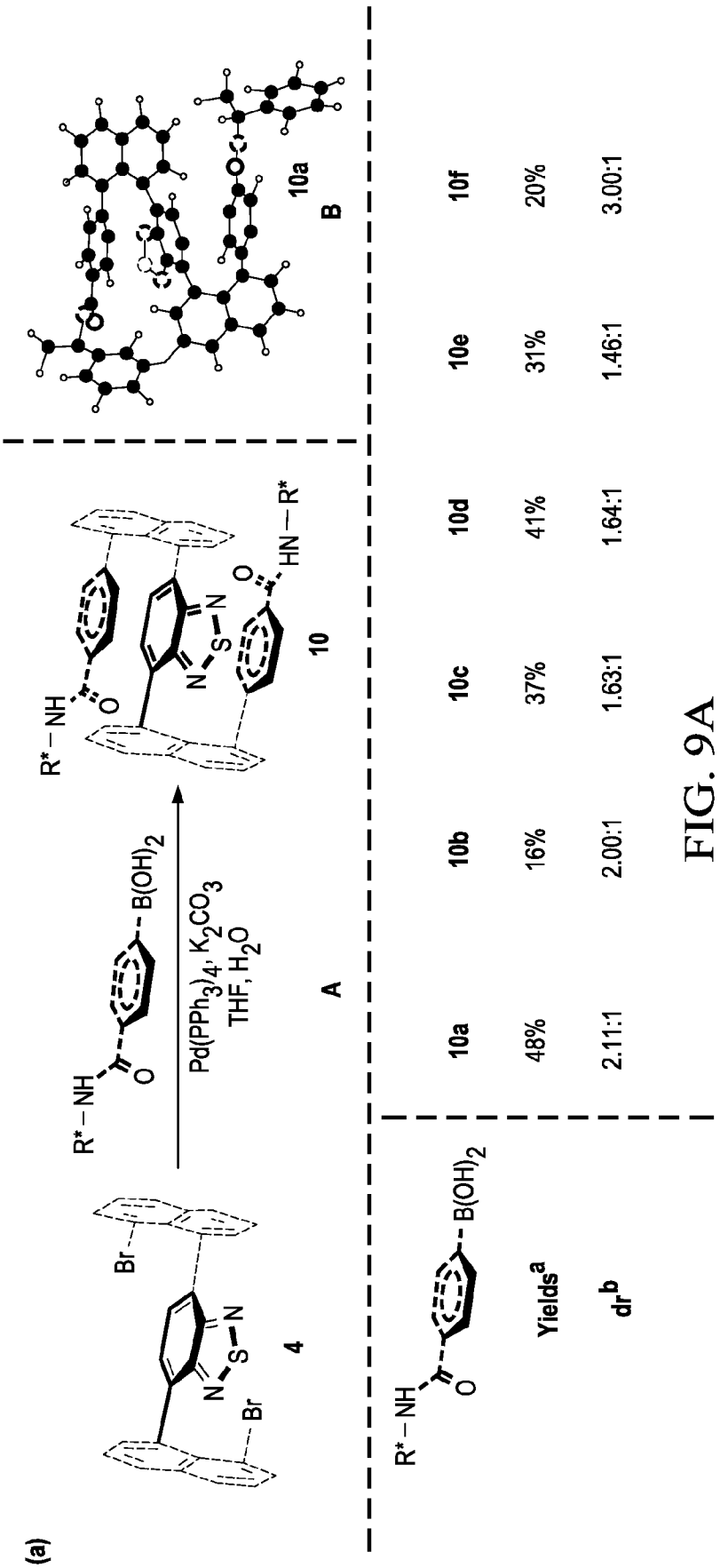

(a)
4
A
B
10
10a
Pd(PPh3)4, K2CO3
THF, H2O
B(OH)2
Br
R* – NH
HN – R*
Yields[a]
dr[b]
10a 10b 10c 10d 10e 10f
48% 16% 37% 41% 31% 20%
2.11:1 2.00:1 1.63:1 1.64:1 1.46:1 3.00:1

FIG. 9A

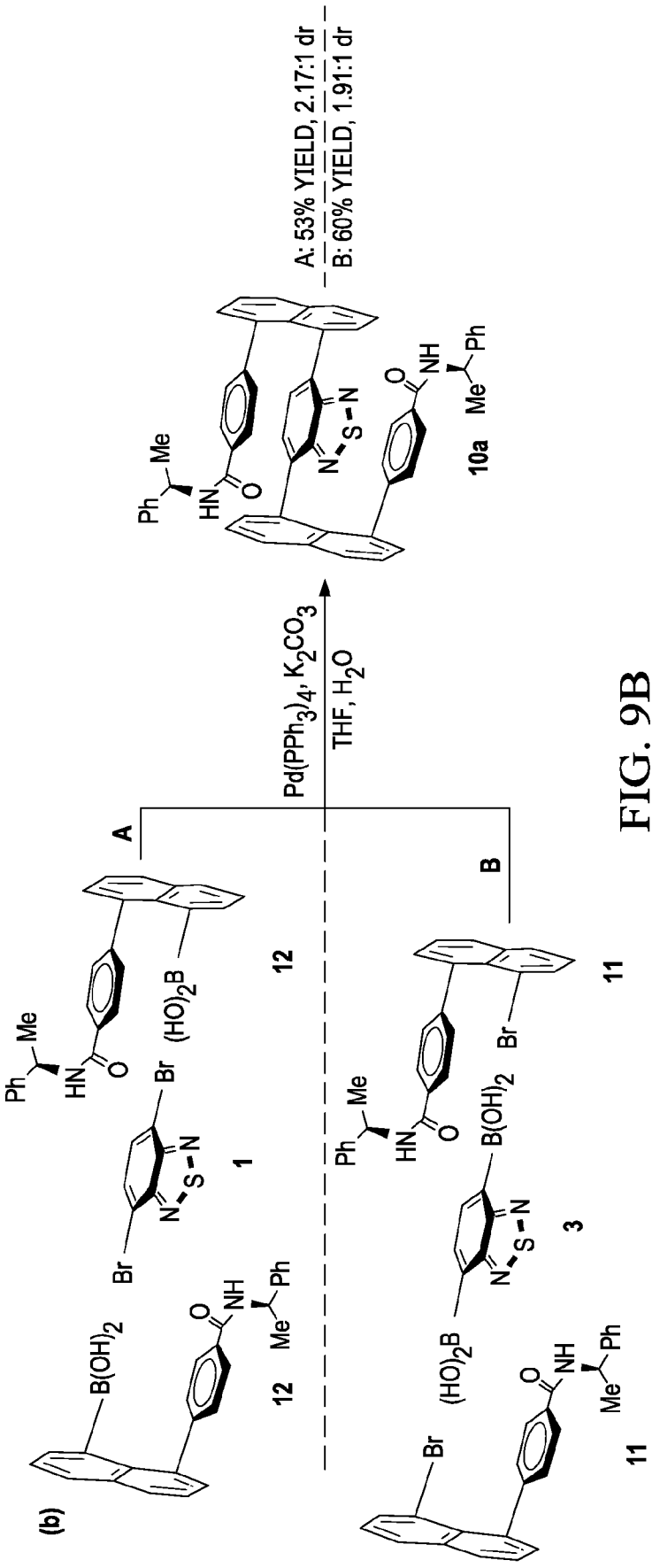

A: 53% YIELD, 2.17:1 dr
B: 60% YIELD, 1.91:1 dr
Pd(PPh3)4, K2CO3
THF, H2O
A
B
(b)
1
12
3
11
10a

FIG. 9B

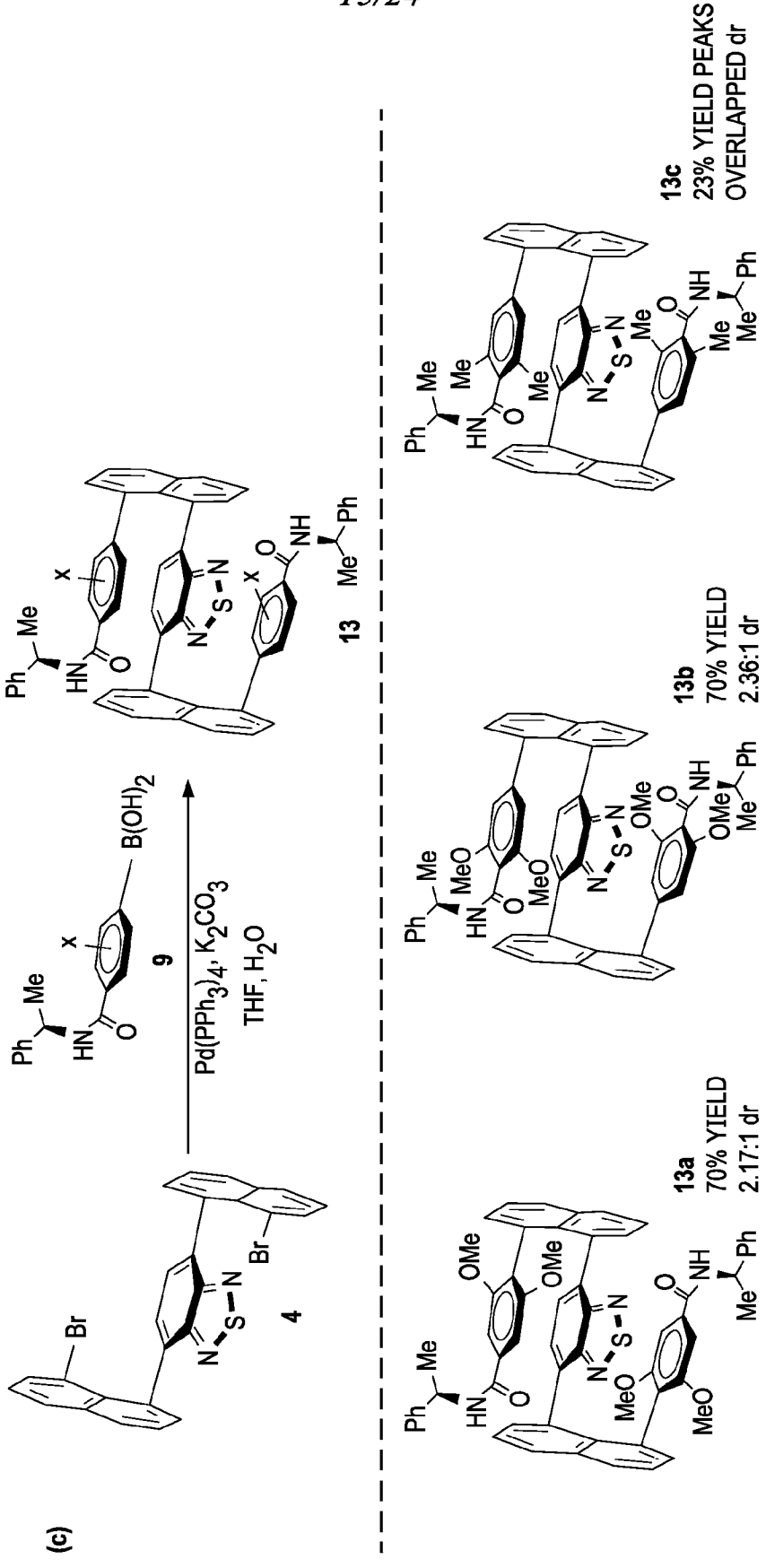

(c)
Br
4
B(OH)2
9
Pd(PPh3)4, K2CO3
THF, H2O
13
13a
70% YIELD
2.17:1 dr
13b
70% YIELD
2.36:1 dr
13c
23% YIELD PEAKS
OVERLAPPED dr

FIG. 9C

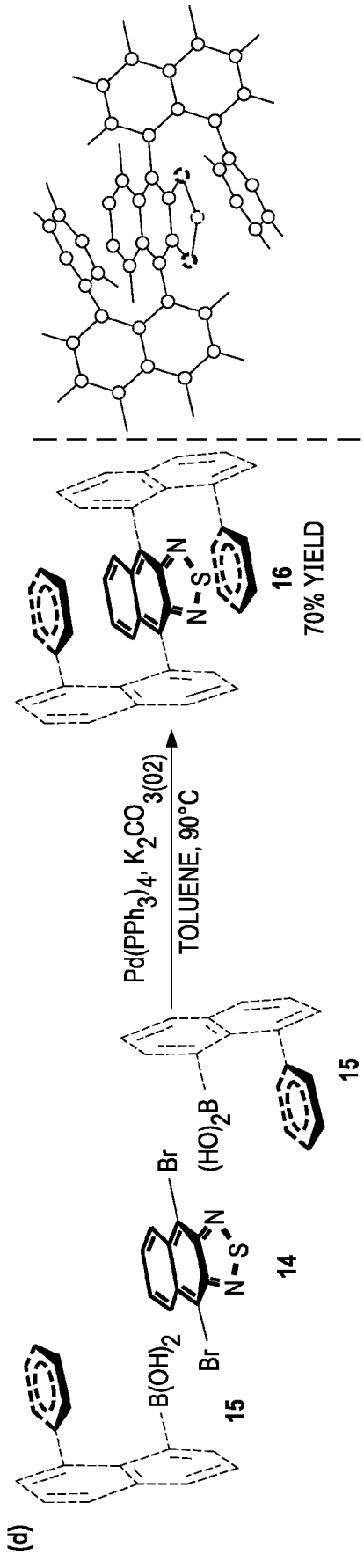

(d)
B(OH)2
15
Br
Br
N
N-S
14
(HO)2B
15
Pd(PPh3)4, K2CO3(02)
TOLUENE, 90°C
N
N-S
16
70% YIELD

FIG. 9D

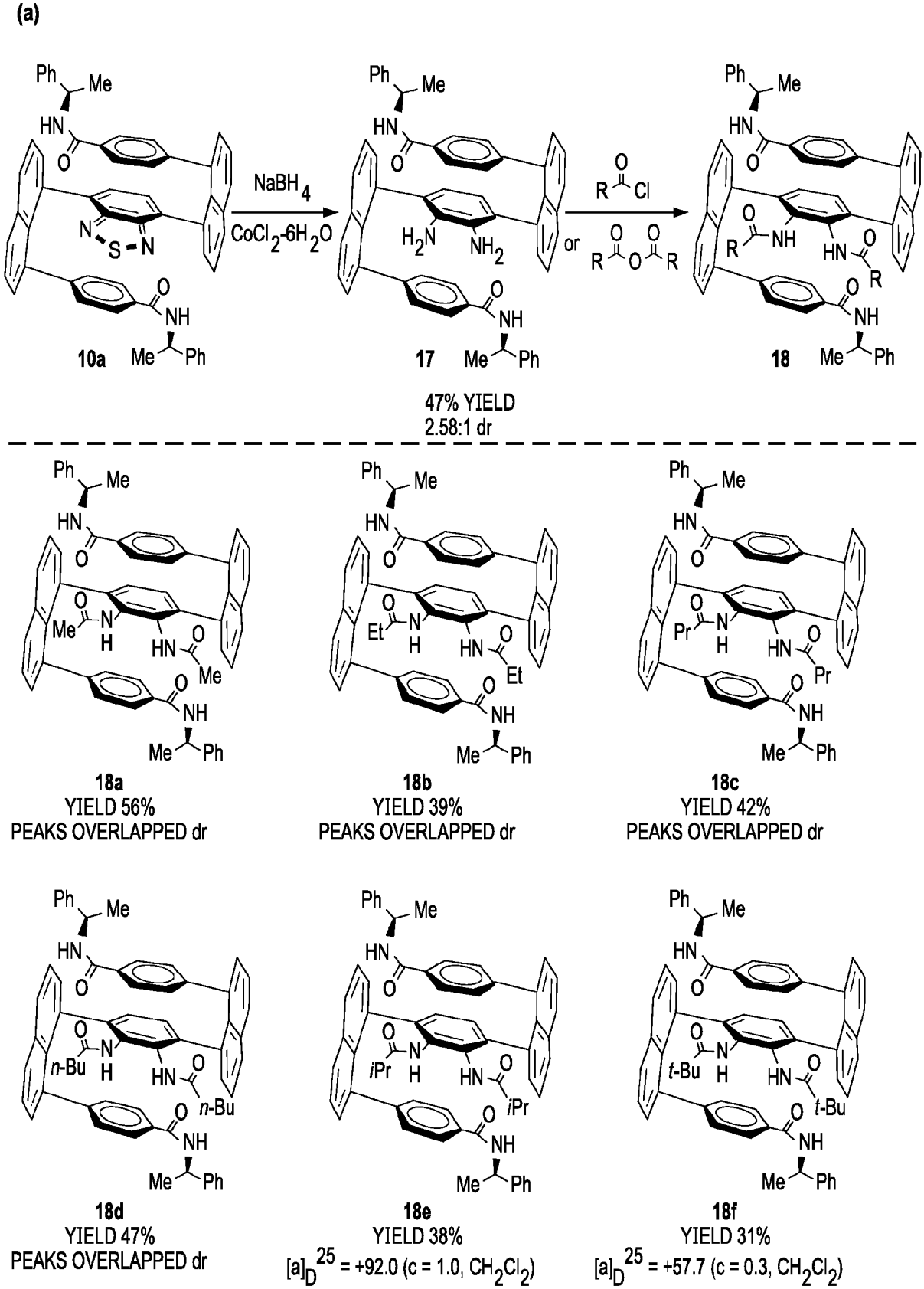

(a)
NaBH4
CoCl2-6H2O
or
10a
17
18
47% YIELD
2.58:1 dr
18a
YIELD 56%
PEAKS OVERLAPPED dr
18b
YIELD 39%
PEAKS OVERLAPPED dr
18c
YIELD 42%
PEAKS OVERLAPPED dr
18d
YIELD 47%
PEAKS OVERLAPPED dr
18e
YIELD 38%
[a]D25 = +92.0 (c = 1.0, CH2Cl2)
18f
YIELD 31%
[a]D25 = +57.7 (c = 0.3, CH2Cl2)

FIG. 10A

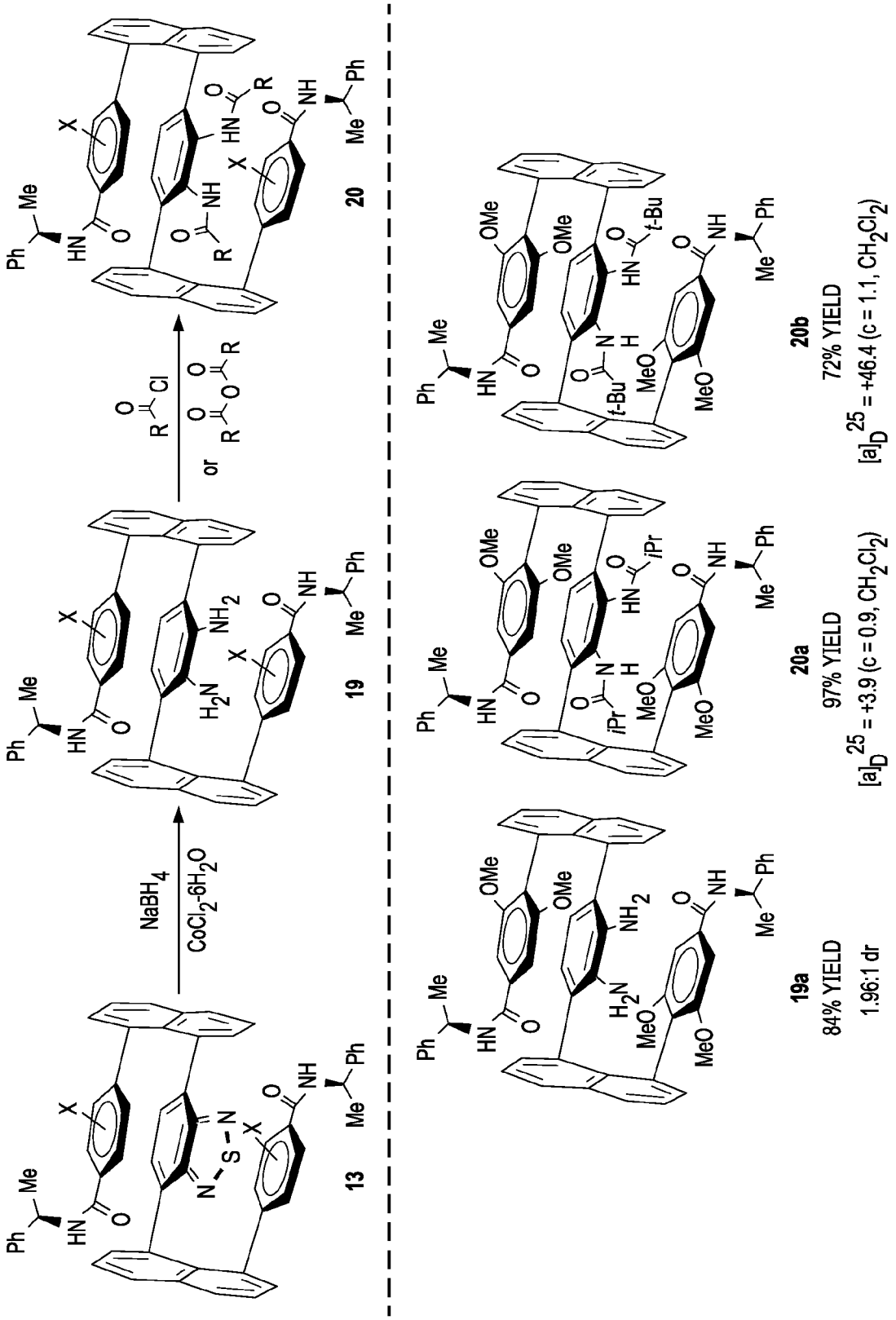

(b)
NaBH4
CoCl2-6H2O
or
13
19
20
19a
20a
20b
84% YIELD
1.96:1 dr
97% YIELD
[a]D25 = +3.9 (c = 0.9, CH2Cl2)
72% YIELD
[a]D25 = +46.4 (c = 1.1, CH2Cl2)

FIG. 10B

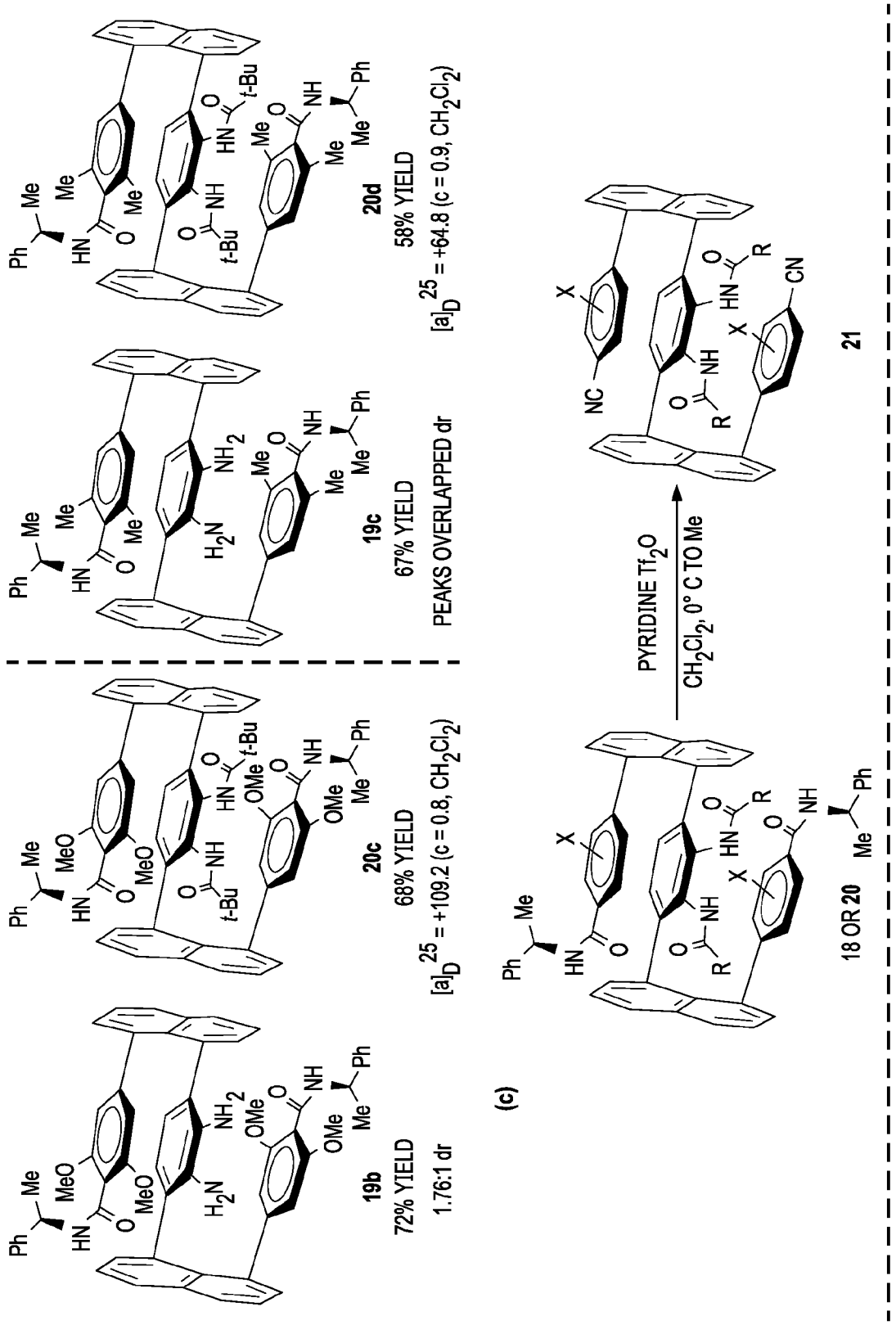
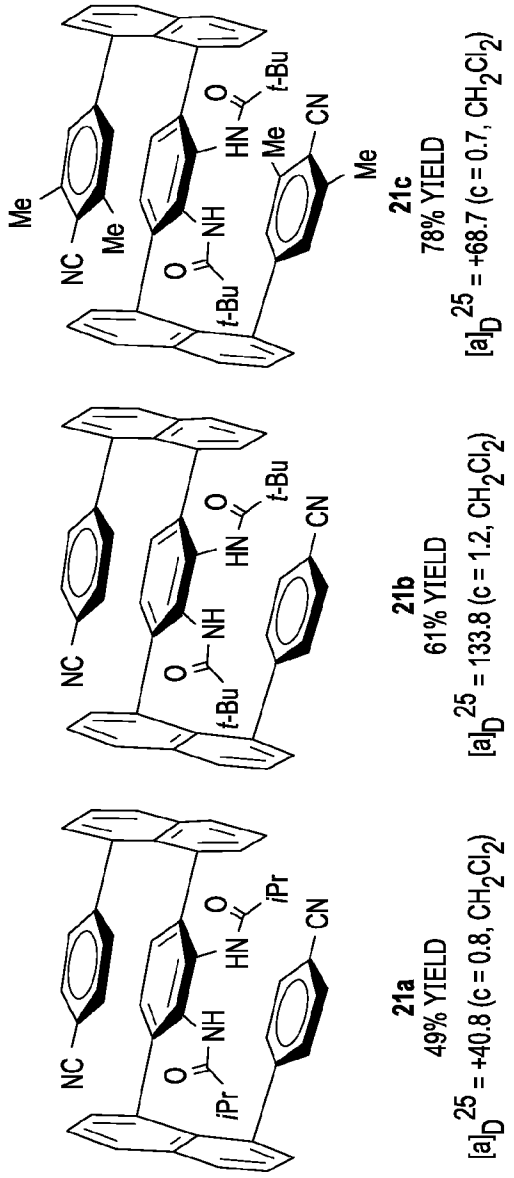


FIG. 10B
CONTINUED



21a
49% YIELD
$[a]_D^{25}$ = +40.8 (c = 0.8, CH_2Cl_2)

21b
61% YIELD
$[a]_D^{25}$ = 133.8 (c = 1.2, CH_2Cl_2)

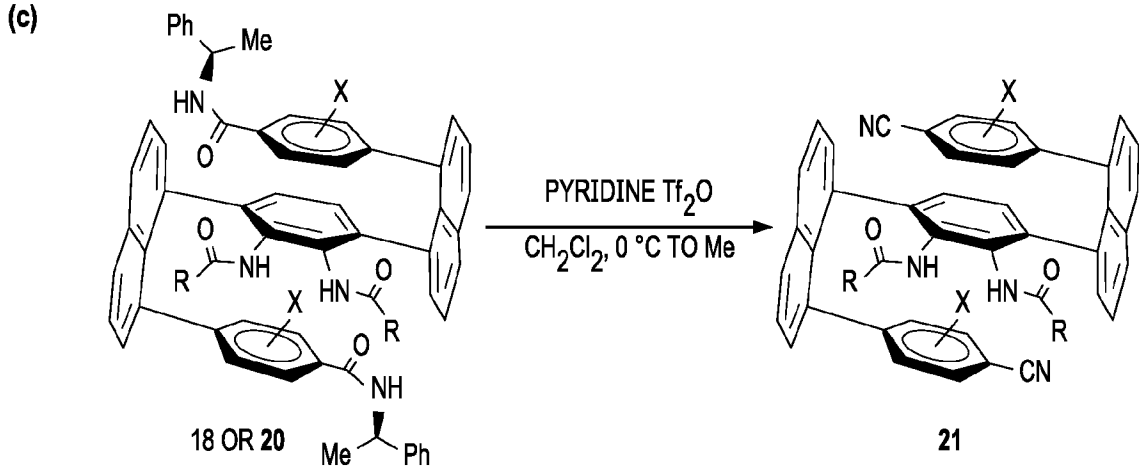
21c
78% YIELD
$[a]_D^{25}$ = +68.7 (c = 0.7, CH_2Cl_2)

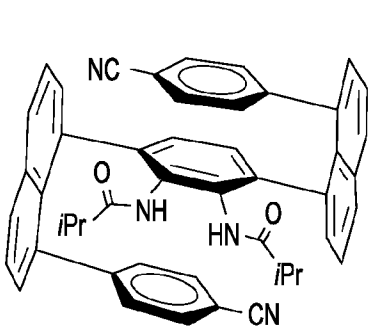
21d
80% YIELD
$[a]_D^{25}$ = +36.4 (c = 0.3, CH_2Cl_2)

21e
43% YIELD
$[a]_D^{25}$ = +51.4 (c = 0.9, CH_2Cl_2)

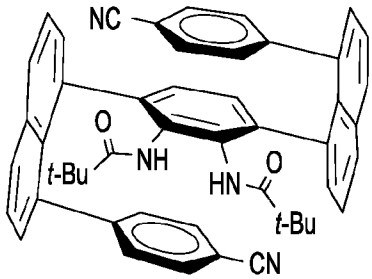
21f
81% YIELD
$[a]_D^{25}$ = +210.0 (c = 1.1, CH_2Cl_2)

FIG. 10B
CONTINUED

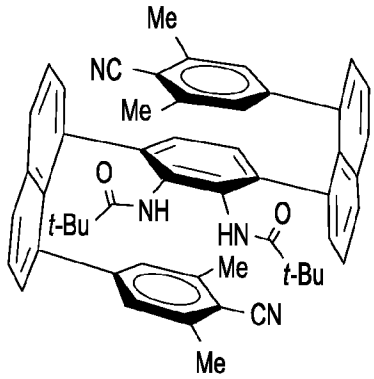




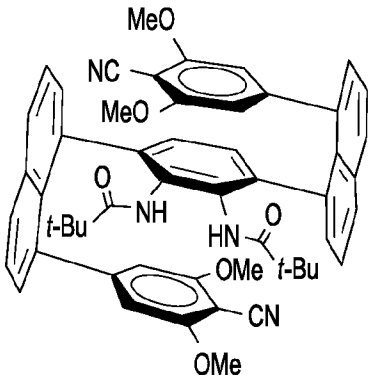
21a
49% YIELD
$[a]_D^{25}$ = +40.8 (c = 0.8, CH_2Cl_2)



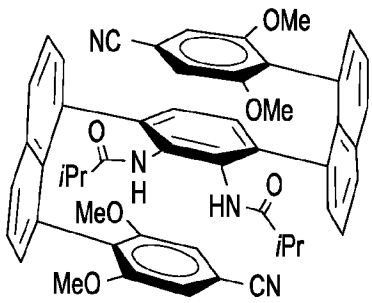
21b
61% YIELD
$[a]_D^{25}$ = 133.8 (c = 1.2, CH_2Cl_2)



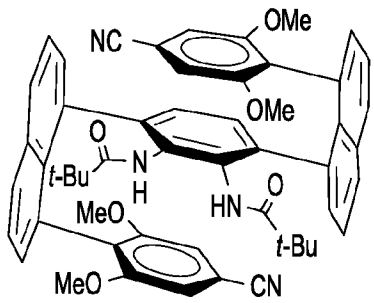
21c
78% YIELD
$[a]_D^{25}$ = +68.7 (c = 0.7, CH_2Cl_2)



21d
80% YIELD
$[a]_D^{25}$ = +36.4 (c = 0.3, CH_2Cl_2)



21e
43% YIELD
$[a]_D^{25}$ = +51.4 (c = 0.9, CH_2Cl_2)



21f
81% YIELD
$[a]_D^{25}$ = +210.0 (c = 1.1, CH_2Cl_2)

FIG. 10C

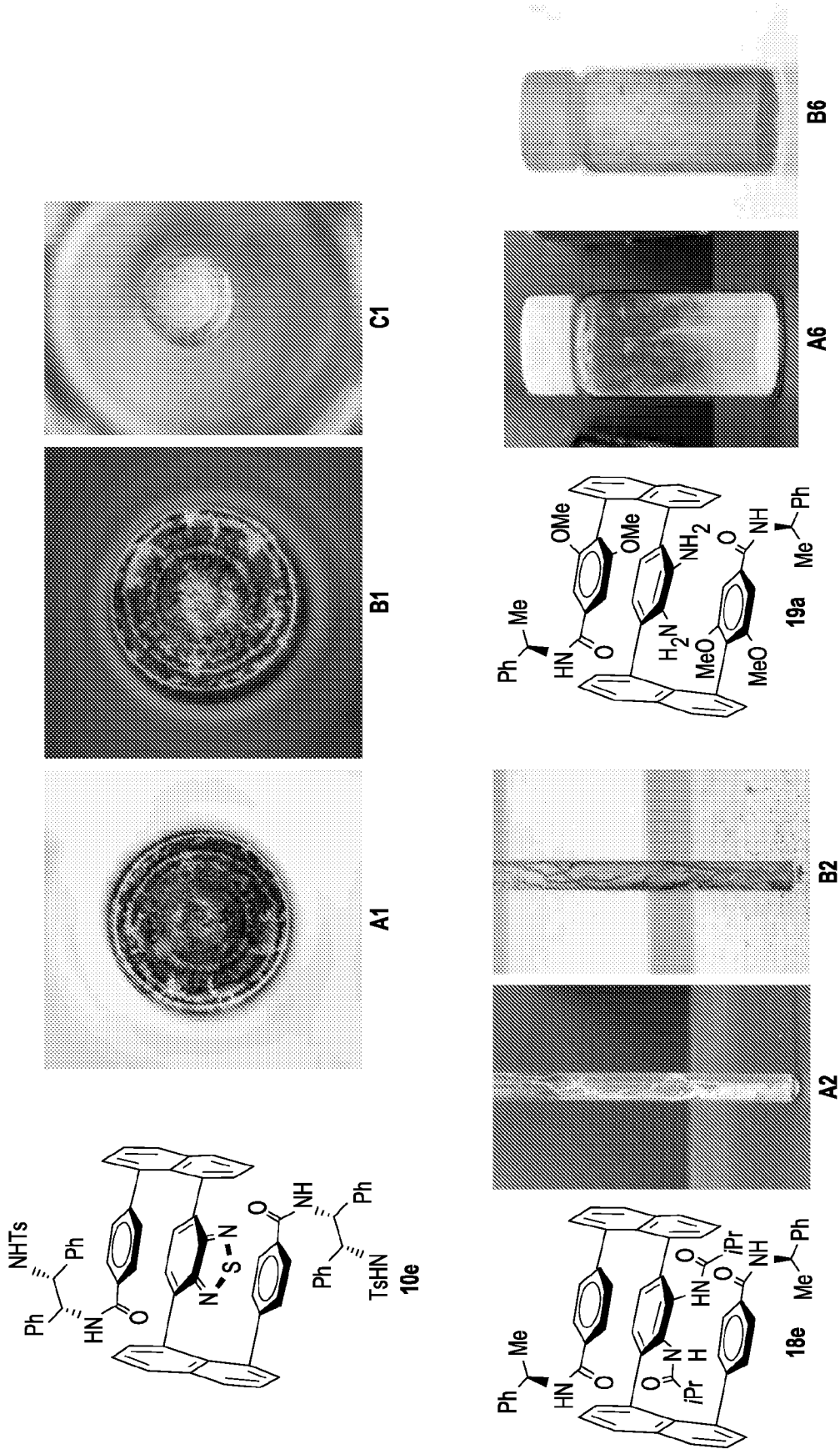


FIG. 11

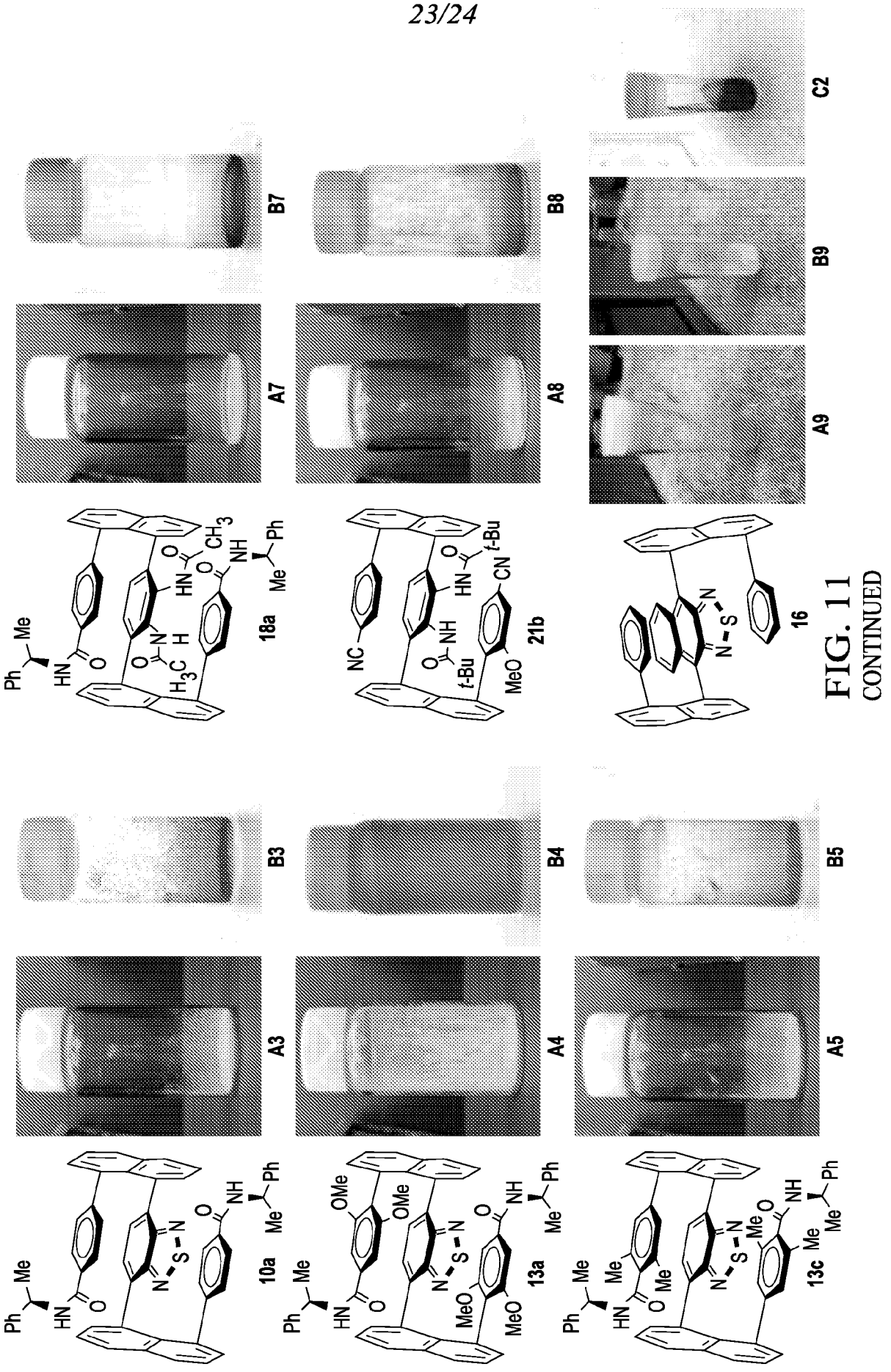


FIG. 11
CONTINUED

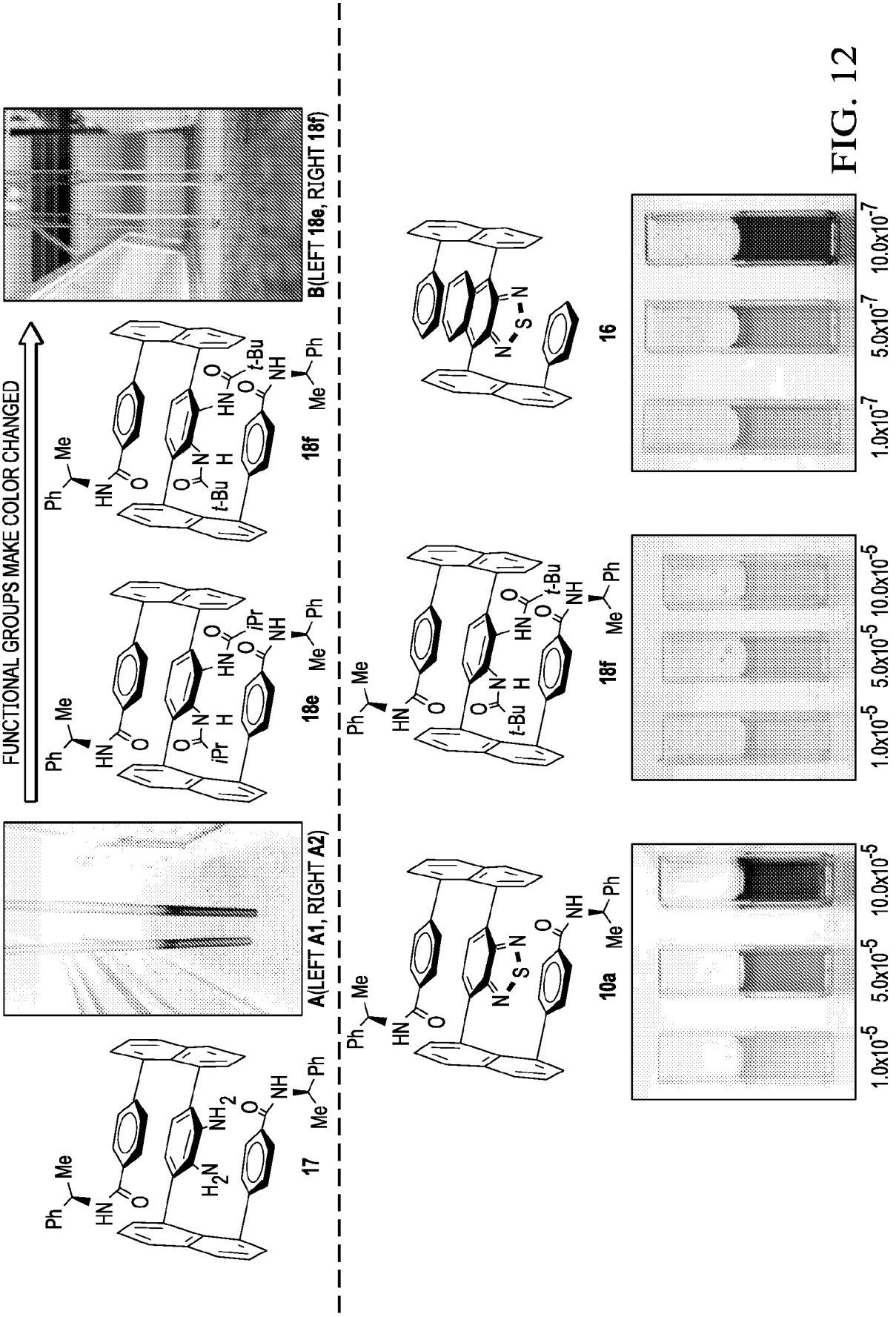

FUNCTIONAL GROUPS MAKE COLOR CHANGED
A(LEFT A1, RIGHT A2)
B(LEFT 18e, RIGHT 18f)
17
18e
18f
16
10a
1.0x10-5 5.0x10-5 10.0x10-5
1.0x10-7 5.0x10-7 10.0x10-7

FIG. 12

INTERNATIONAL SEARCH REPORT

International application No.
PCT/US 19/65657

A. CLASSIFICATION OF SUBJECT MATTER
IPC - C07F 9/36 (2020.01)
CPC - C07F 9/36

According to International Patent Classification (IPC) or to both national classification and IPC

B. FIELDS SEARCHED

Minimum documentation searched (classification system followed by classification symbols)
See Search History document

Documentation searched other than minimum documentation to the extent that such documents are included in the fields searched
See Search History document

Electronic data base consulted during the international search (name of data base and, where practicable, search terms used)
See Search History document

C. DOCUMENTS CONSIDERED TO BE RELEVANT

Category*	Citation of document, with indication, where appropriate, of the relevant passages	Relevant to claim No.
A	Lin et al. "New 3-D Chiral Framework of Indium with 1,3,5-Benzenetricarboxylate" Inorganic Chemistry. 09 December 2004 (09.12.2004) vol 44, pg. 73-76; pg. 73, abstract, pg. 75, right col, para 1, pg. 76, Scheme 1	1-40
A	US 2013/0077040 A1 (North Carolina State University) 28 March 2013 (28.03.2013); para [0011], [0021]	1-40
A	WO 2014/093723 A2 (NANJING UNIVERSITY) 19 June 2014 (19.06.2014); entire document	1-40
P, X	Wu et al. "Multilayer 3D Chirality and Its Synthetic Assembly" Research. 27 June 2019 (27.06.2019) vol 2019, pg. 1-11; entire document	1-40

☐ Further documents are listed in the continuation of Box C. ☐ See patent family annex.

* Special categories of cited documents:
"A" document defining the general state of the art which is not considered to be of particular relevance
"D" document cited by the applicant in the international application
"E" earlier application or patent but published on or after the international filing date
"L" document which may throw doubts on priority claim(s) or which is cited to establish the publication date of another citation or other special reason (as specified)
"O" document referring to an oral disclosure, use, exhibition or other means
"P" document published prior to the international filing date but later than the priority date claimed
"T" later document published after the international filing date or priority date and not in conflict with the application but cited to understand the principle or theory underlying the invention
"X" document of particular relevance; the claimed invention cannot be considered novel or cannot be considered to involve an inventive step when the document is taken alone
"Y" document of particular relevance; the claimed invention cannot be considered to involve an inventive step when the document is combined with one or more other such documents, such combination being obvious to a person skilled in the art
"&" document member of the same patent family

Date of the actual completion of the international search	Date of mailing of the international search report
18 February 2020	09 MAR 2020
Name and mailing address of the ISA/US Mail Stop PCT, Attn: ISA/US, Commissioner for Patents P.O. Box 1450, Alexandria, Virginia 22313-1450 Facsimile No. 571-273-8300	Authorized officer Lee Young Telephone No. PCT Helpdesk: 571-272-4300